Brief Overview of Severe Weather Forecasting

ATM 401–Synoptic Meteorology II
Spring 2010

Lance Bosart, Tom Galarneau, Jr., Heather Archambault, and Nick Metz

Ingredients Needed for Severe Wx

- **Lift, instability, moisture**
  - **Lift:** Surface boundary (front) or disturbance
  - **Instability:** Warm at surface/cold aloft
  - **Moisture:** Warm, humid boundary layer

- **Wind shear**
  - **Speed shear:** Winds increase with height
  - **Directional shear:** Winds change direction with height (Ideal: SE near surface, SW at midlevels, NW at upper levels)
  - **High wind events:** High speed shear
  - **Tornadoes:** High speed and directional shear

Severe Thunderstorm Formation

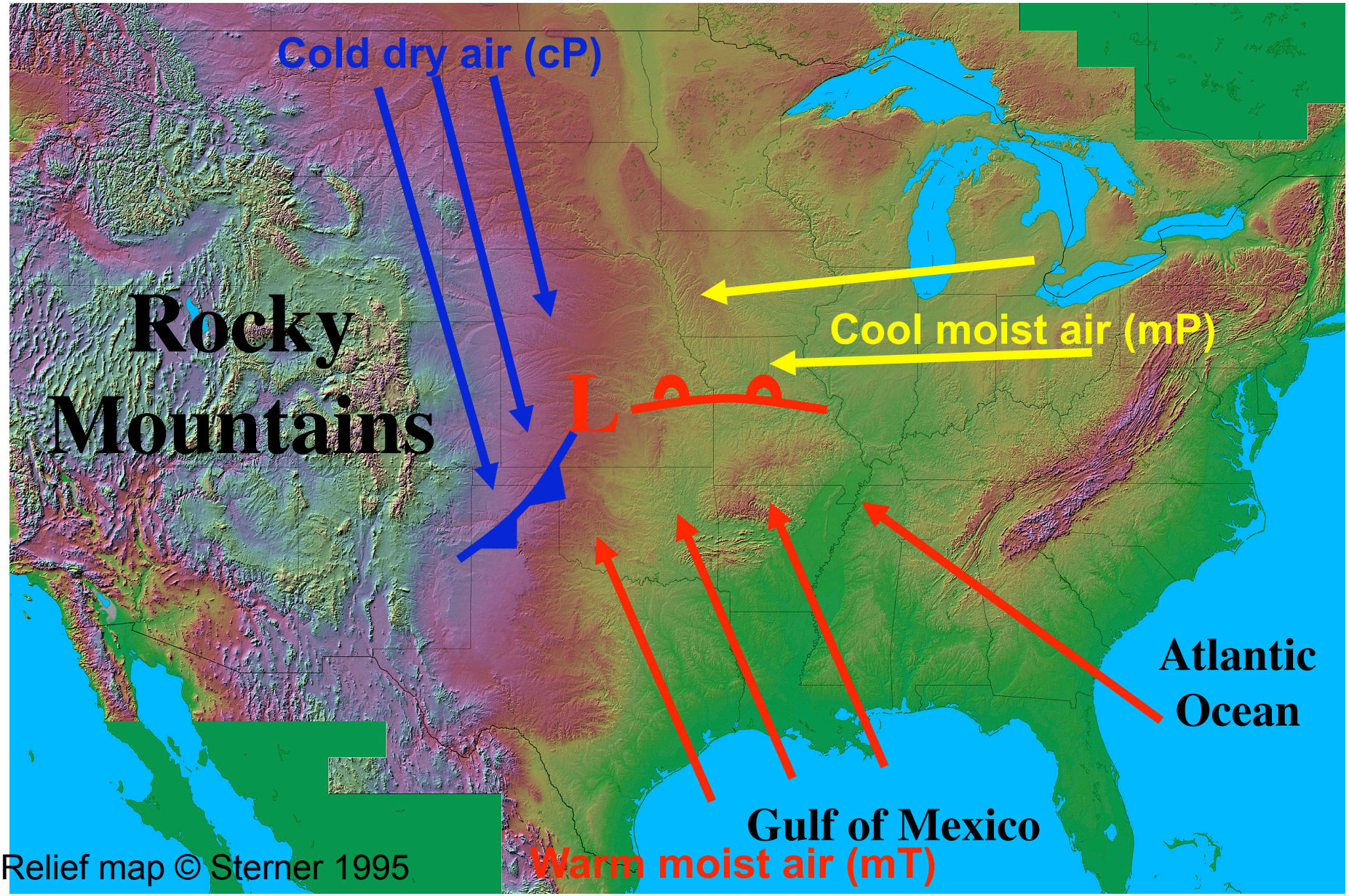

Severe Thunderstorm Formation

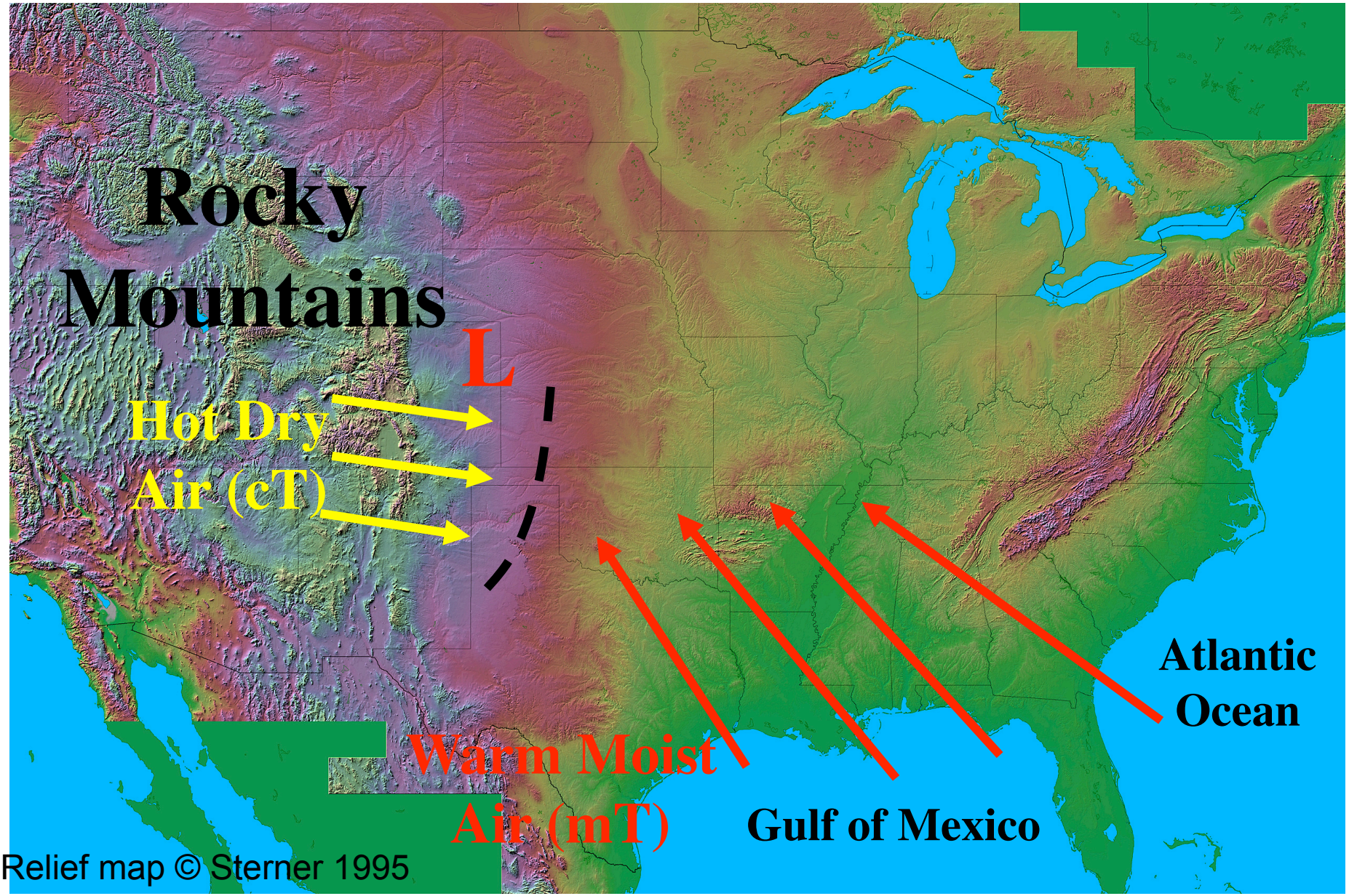

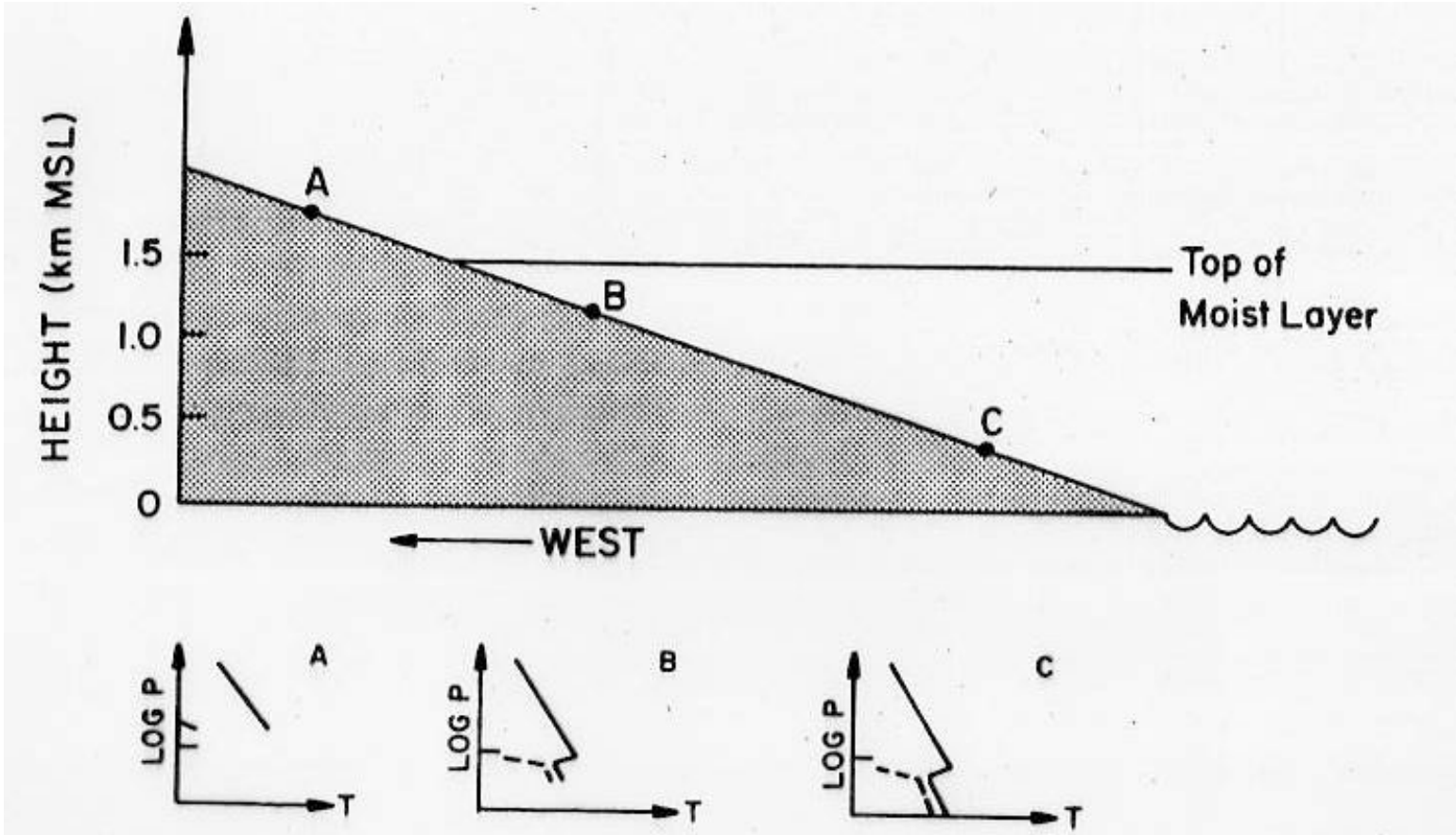

Figure 2.43 Schematic vertical cross section of the dryline and its relationship to topography. Idealized soundings (temperature, solid lines; dew point, dashed lines) at points A, B, C (bottom) represent the conditions west, just east, and far east of the dryline.

Bluestein 1993

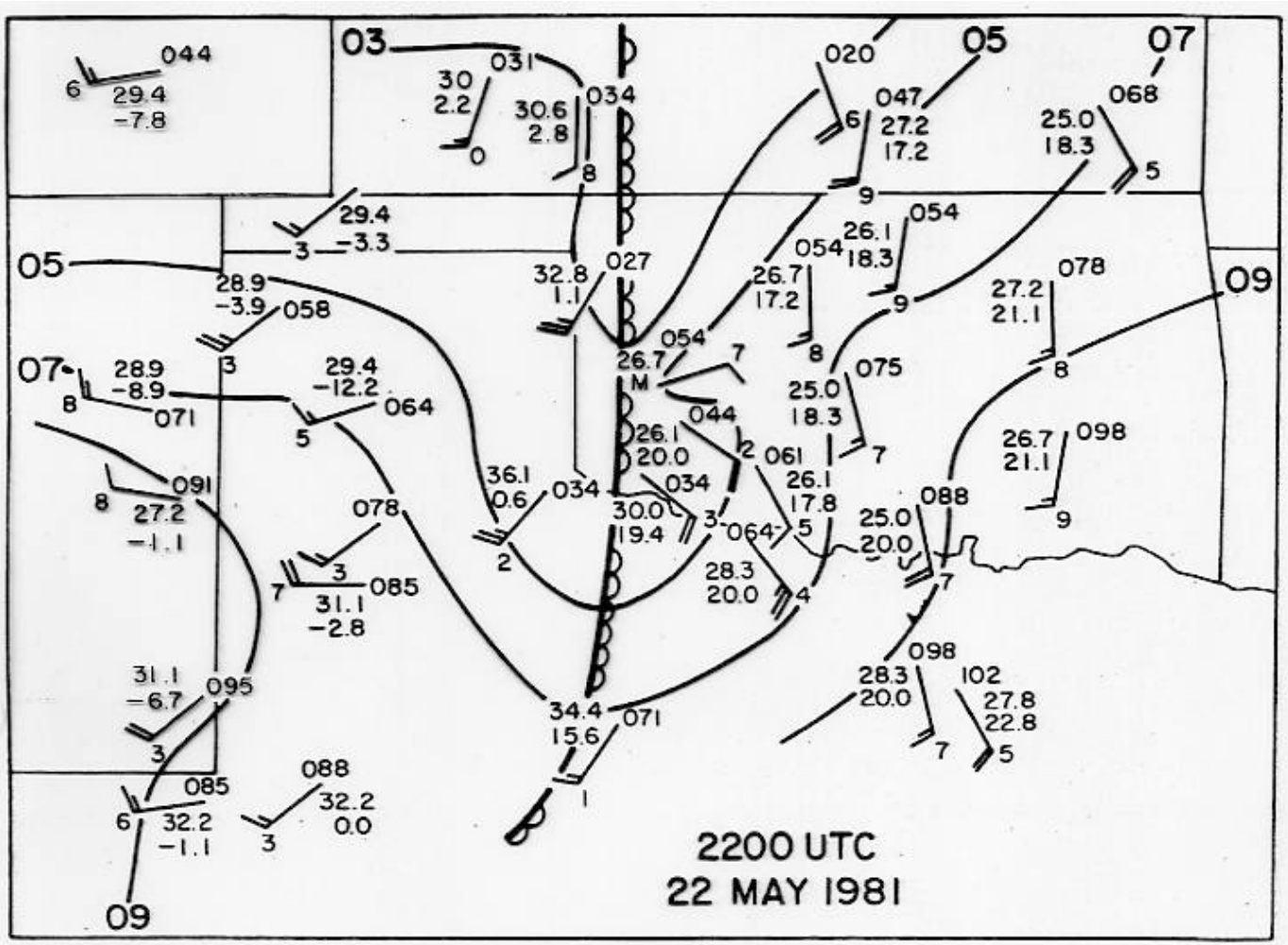

Figure 2.38 Surface analysis in Oklahoma, Texas, and Kansas of a dryline (scalloped line) under "quiescent" conditions at 2200 UTC, May 22, 1981. Altimeter setting (solid lines) in mb without the leading 10; temperature and dew point plotted in °C; altimeter setting plotted in tens of mb, without the leading 10; whole barb = 5 m s^{-1}; half barb = 2.5 m s^{-1}. At the time of this analysis tornadic storms were occurring just east of the dryline in western Oklahoma. Winds east of the dryline are generally from the south and southeast, while winds west of the dryline are from the southwest and west. Dew points east of the dryline are around 20°C; dew points west of the dryline are near and below 0°C.

Bluestein 1993

Examples of Surface Boundaries

1700 UTC 8 April 2008

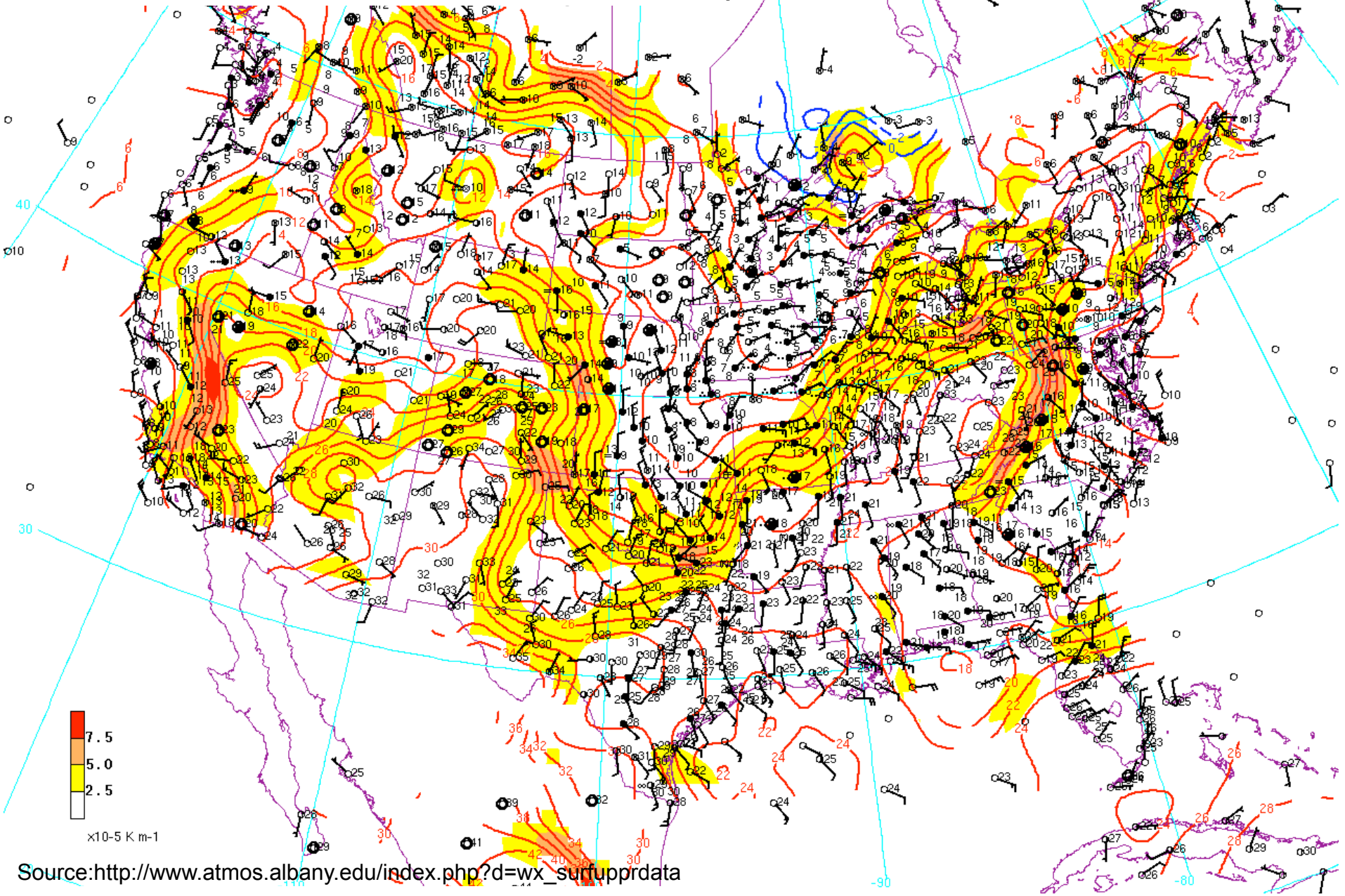

Source:http://www.atmos.albany.edu/index.php?d=wx_surfupprdata

Surface θ (°C) and and θ gradient (× K 100 km^{-1})

C; x10-5 K m-1)

Examples of Surface Boundaries

1700 UTC 8 April 2008

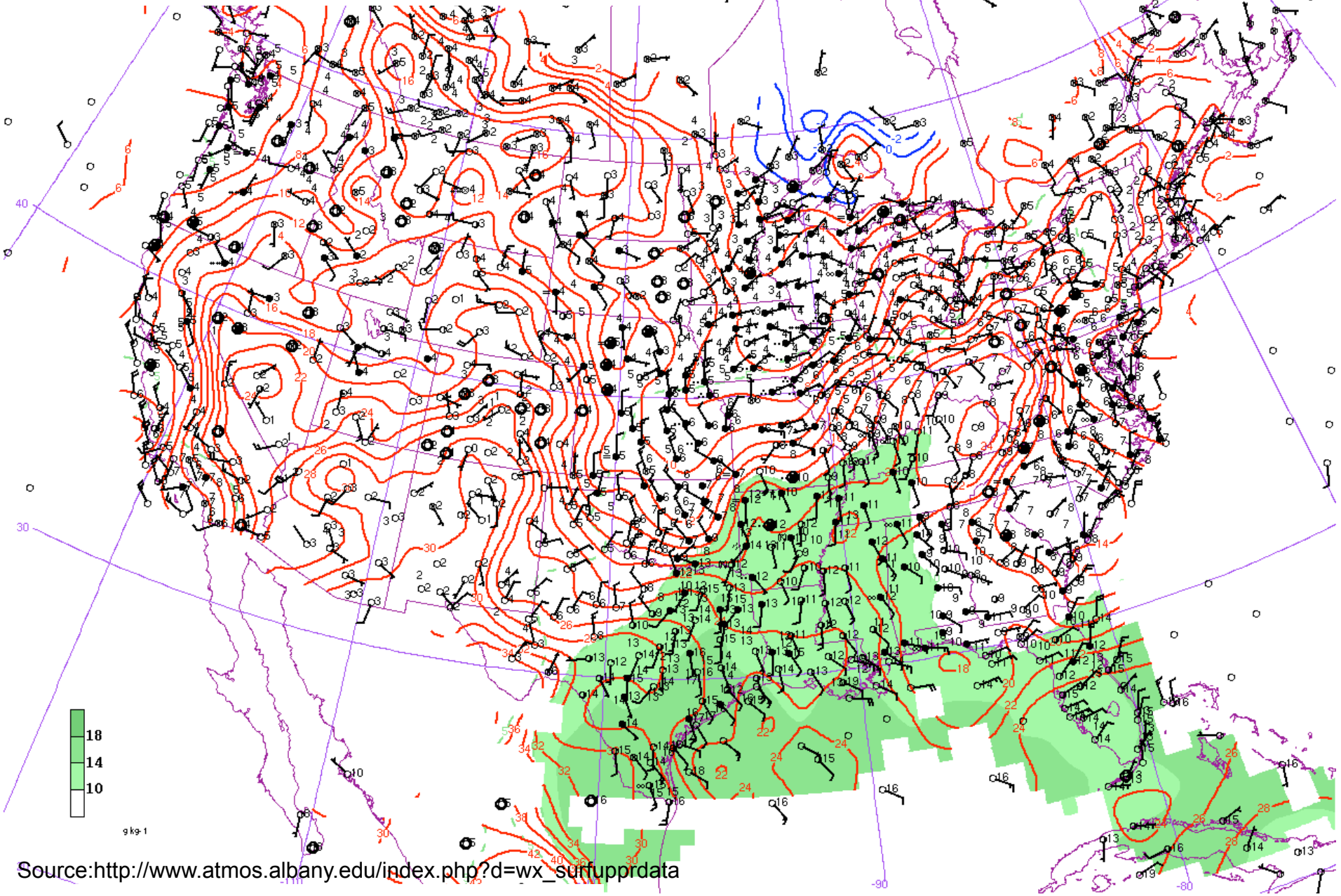

Source:http://www.atmos.albany.edu/index.php?d=wx_surfupprdata

Surface θ (°C) and mixing ratio (g kg^{-1})

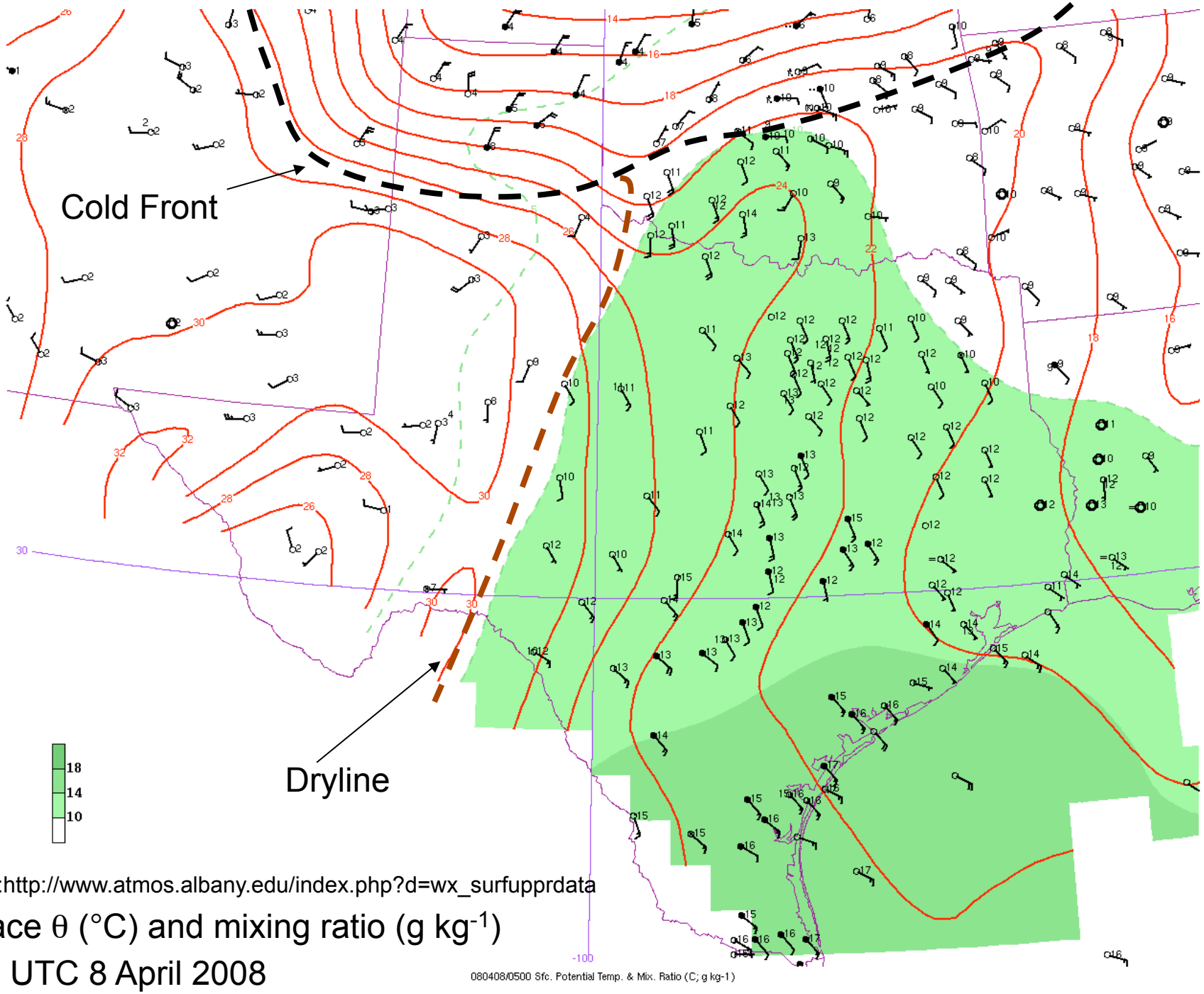

Source:http://www.atmos.albany.edu/index.php?d=wx_surfupprdata

Surface θ (°C) and mixing ratio (g kg^{-1})

0500 UTC 8 April 2008

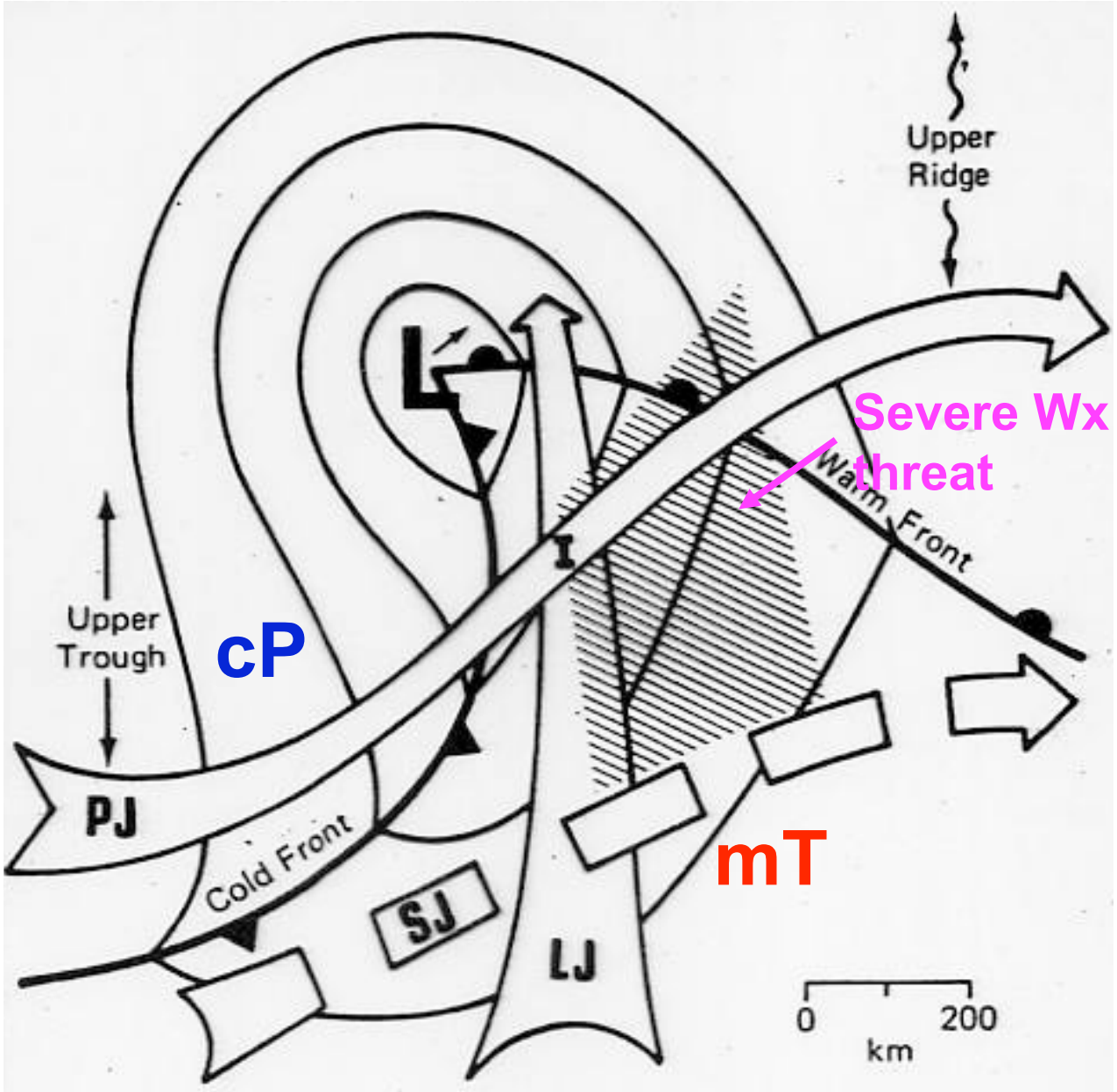

- ***Lift*** **provided by cold front and upper trough.**
- ***Moisture*** **advected from south in warm sector.**
- ***Instability*** **from heating in warm sector.**

Source: Barnes and Newton (1983)

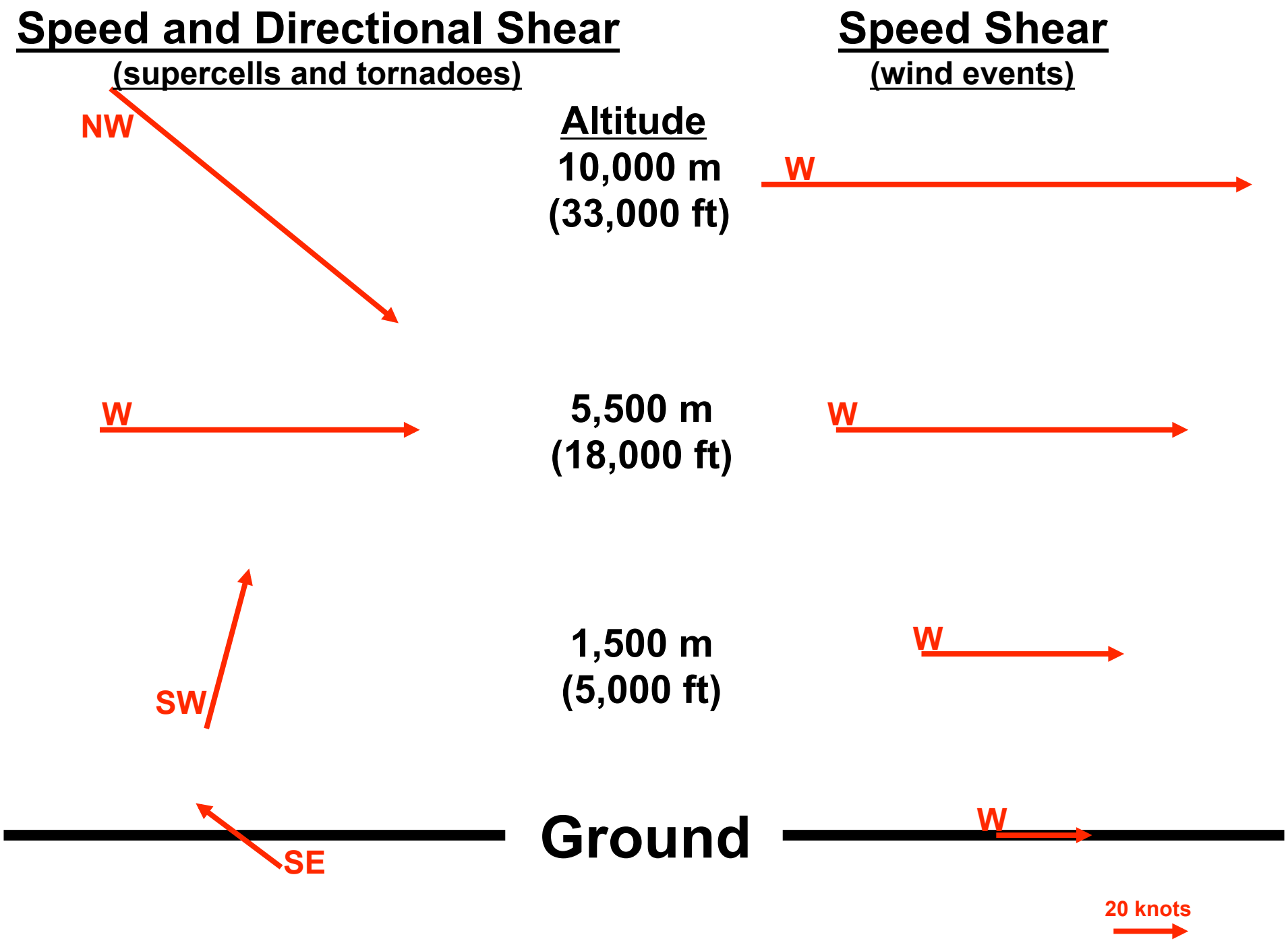
Speed and Directional Shear
(supercells and tornadoes)
Speed Shear
(wind events)
Altitude
10,000 m
(33,000 ft)
NW
W
W
5,500 m
(18,000 ft)
W
SW
1,500 m
(5,000 ft)
W
Ground
SE
W
20 knots

Storm Structure

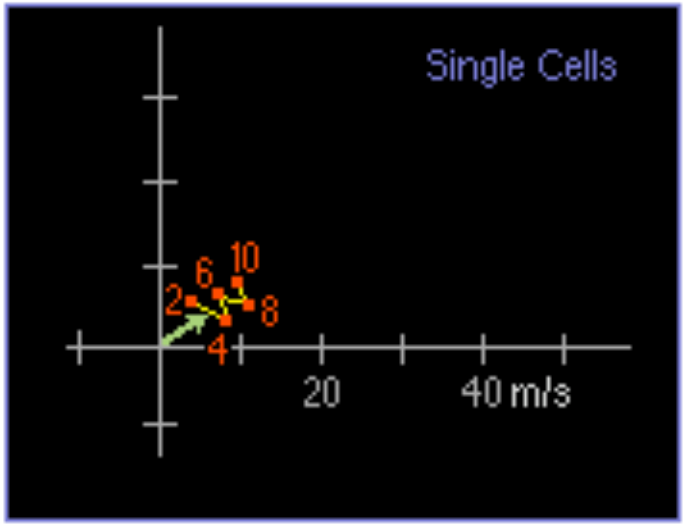

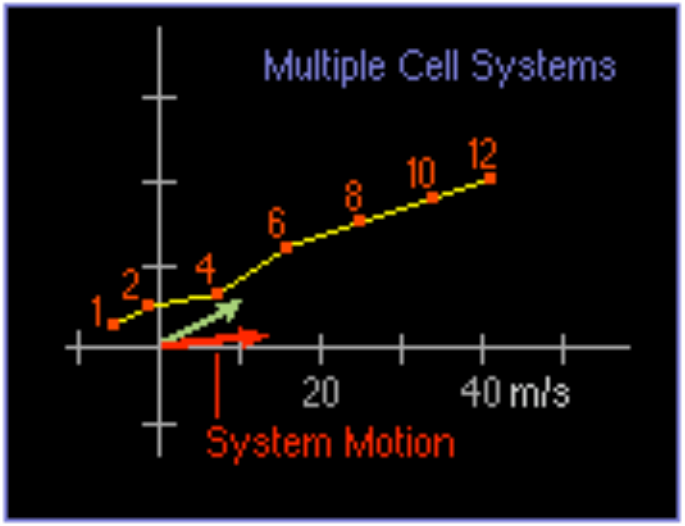

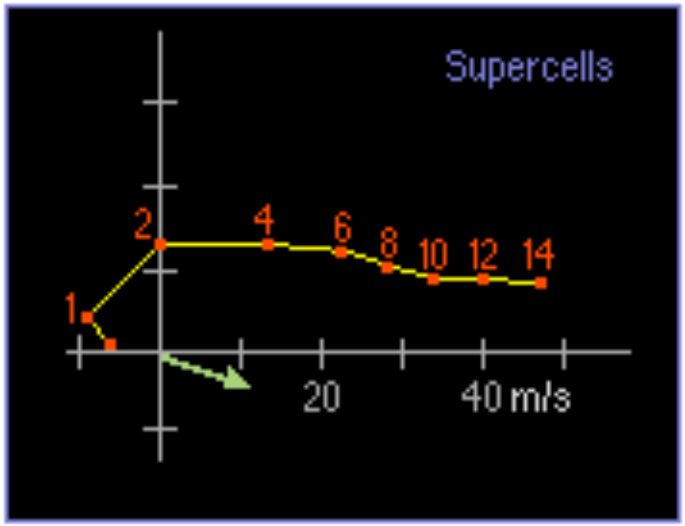

Green Arrow = Cell Motion

Chisholm and Renick, 1972

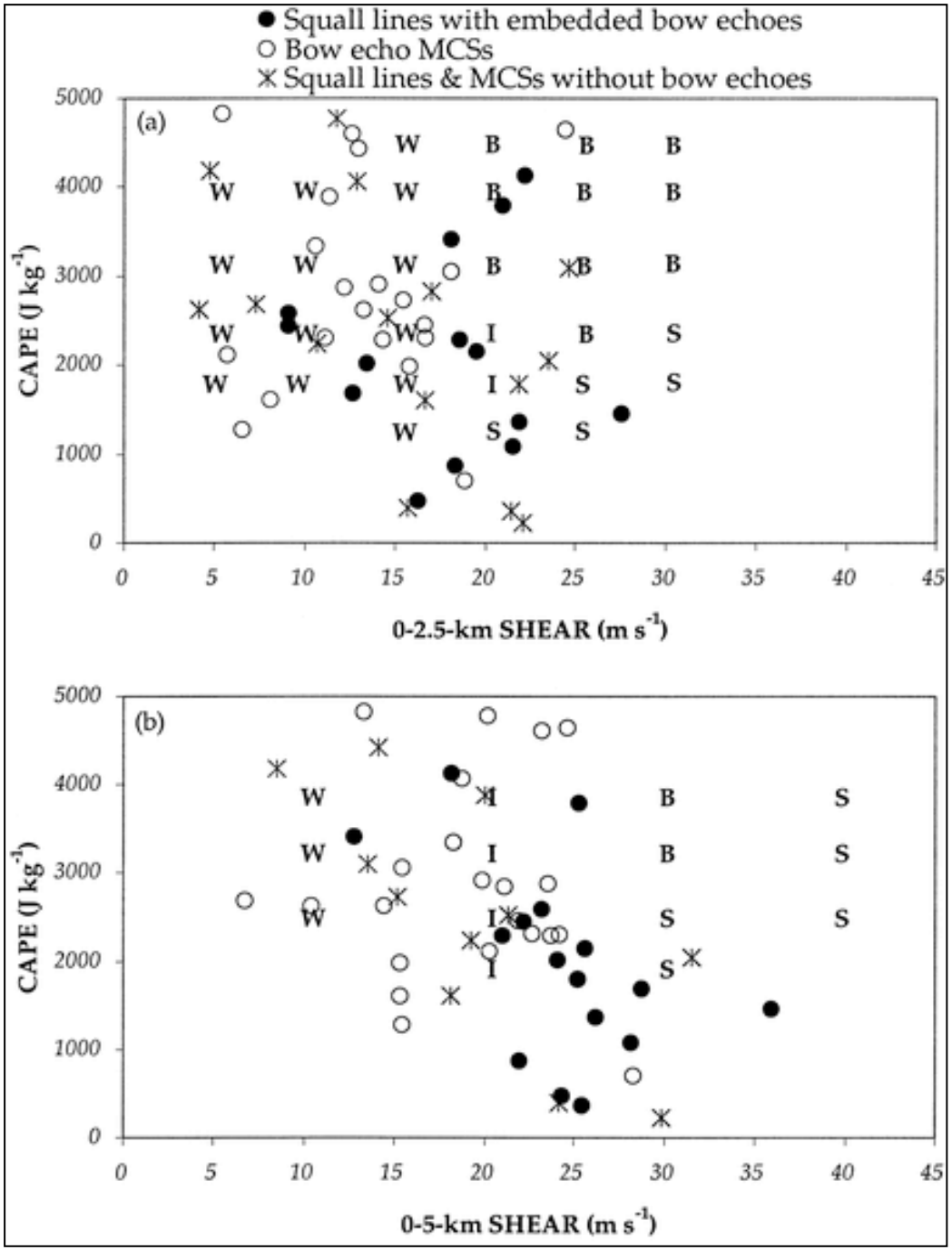

- **CAPE/shear phase space governs the type of convective organization**

- **W: weakly organized (ordinary)**
- **B: bow echoes**
- **I: intermediate between weak updrafts and bow echoes**
- **S: supercells**

- **Letters are from idealized simulations while shapes are from actual observations**

Sources: Weisman (1993); Coniglio et al. (2004)

Ordinary Cells

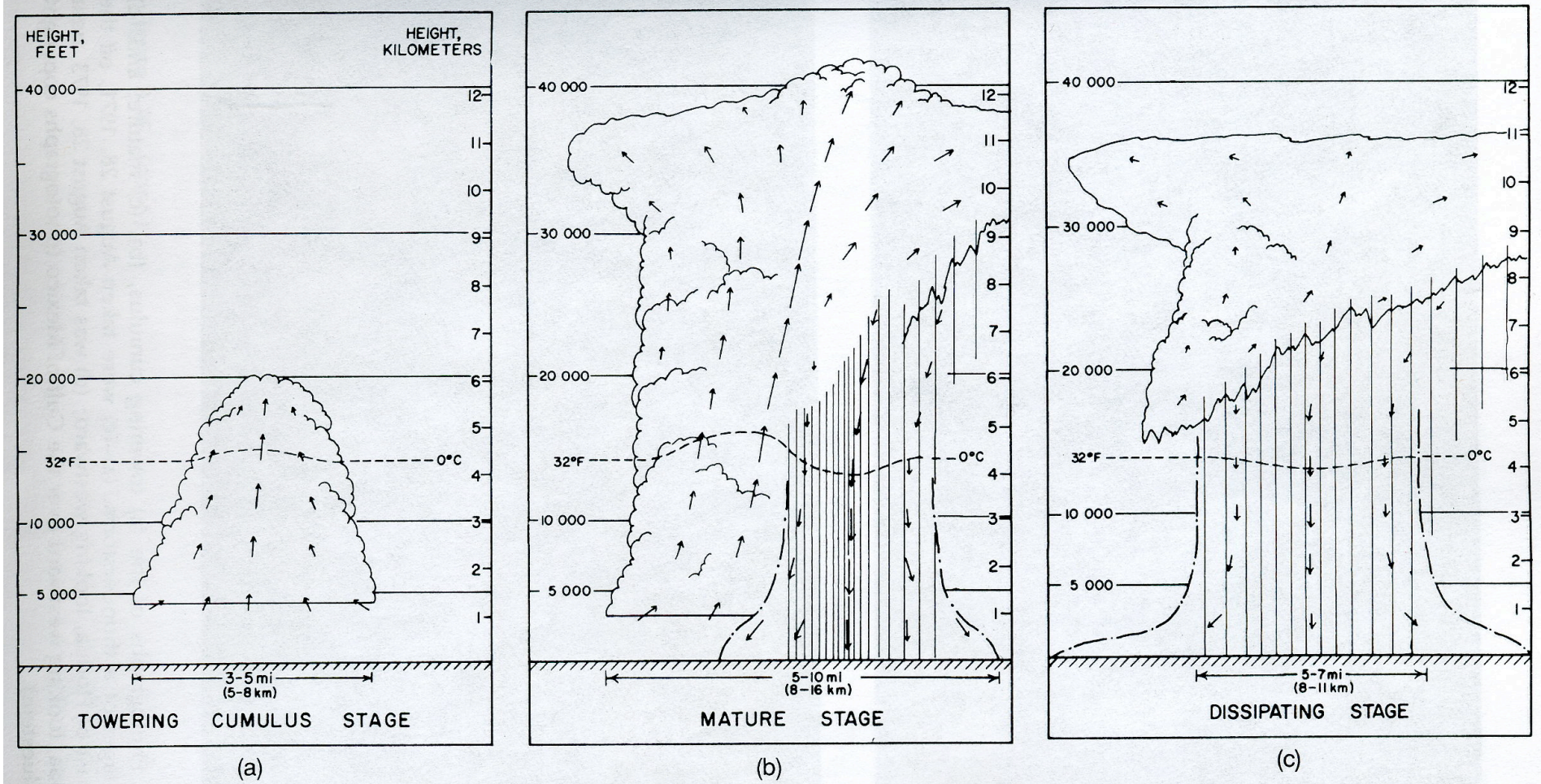

Figure 3.15 The Byers–Braham model of the three stages in the life of a thunderstorm: (a) towering cumulus stage, (b) mature stage, and (c) dissipating stage. Arrows indicate the sense of air motion (from Doswell, 1985).

Bluestein (1993)

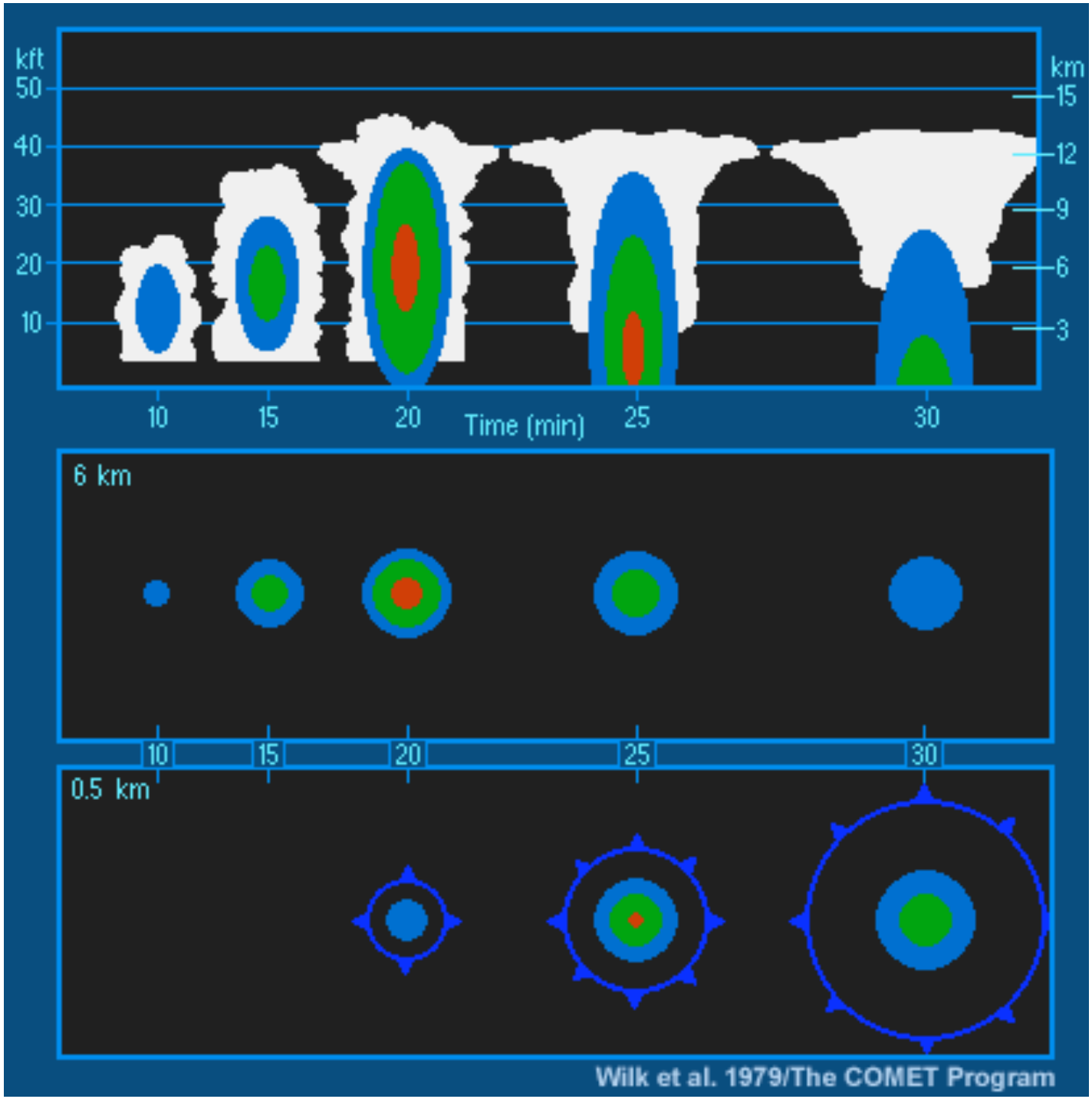
kft
50
40
30
20
10
km
15
12
9
6
3
10
15
20
Time (min)
25
30
6 km
10
15
20
25
30
0.5 km
Wilk et al. 1979/The COMET Program

Multicell Storms

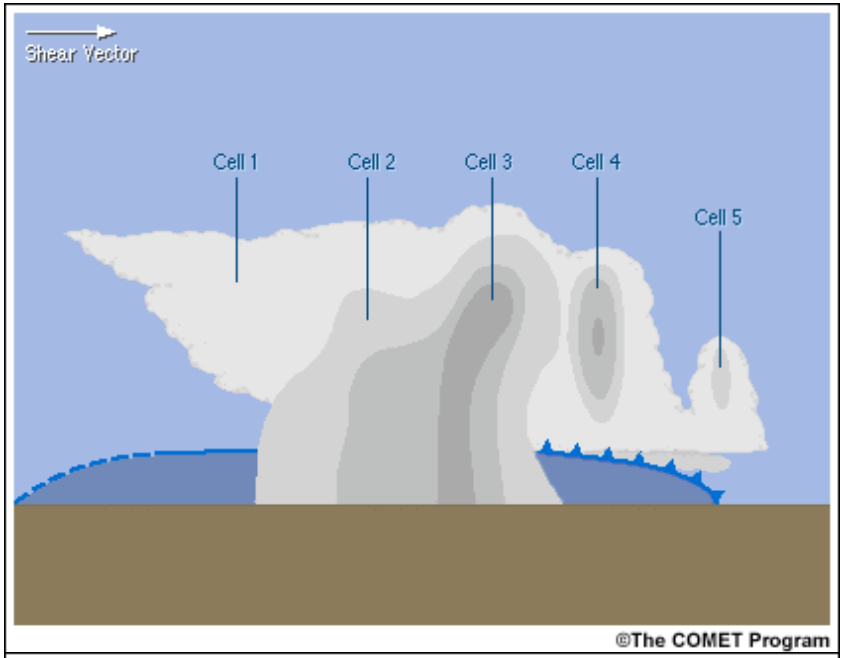

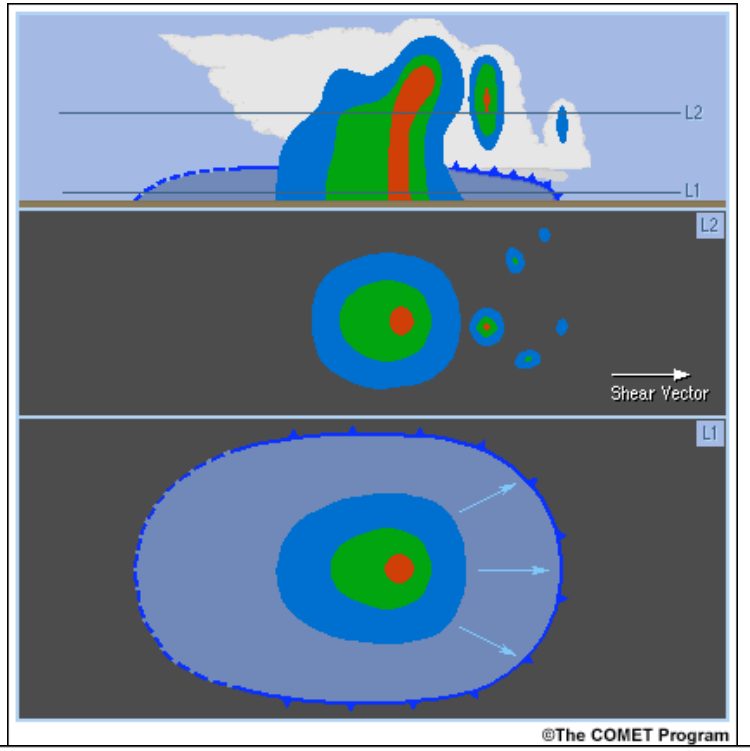

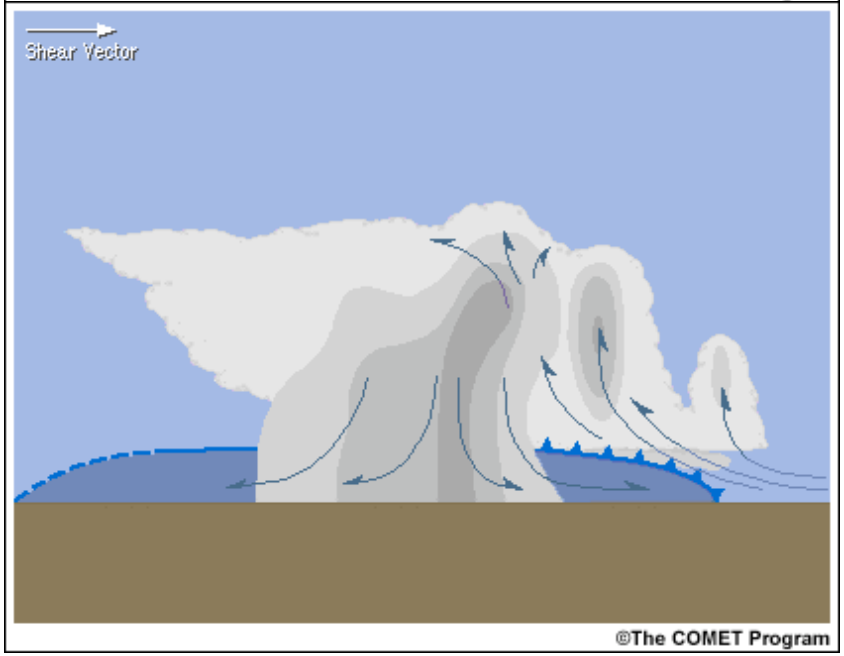

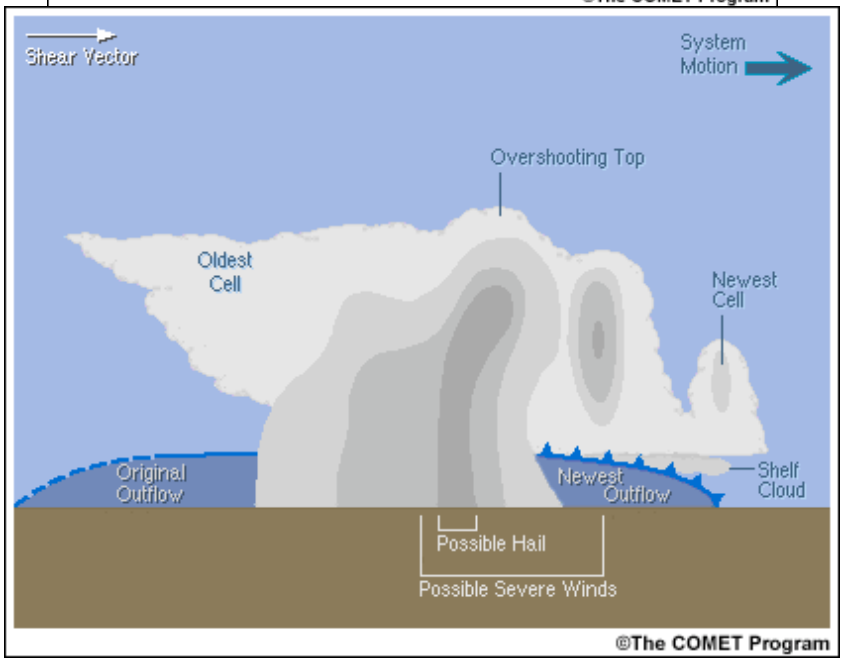

Bow echo structure

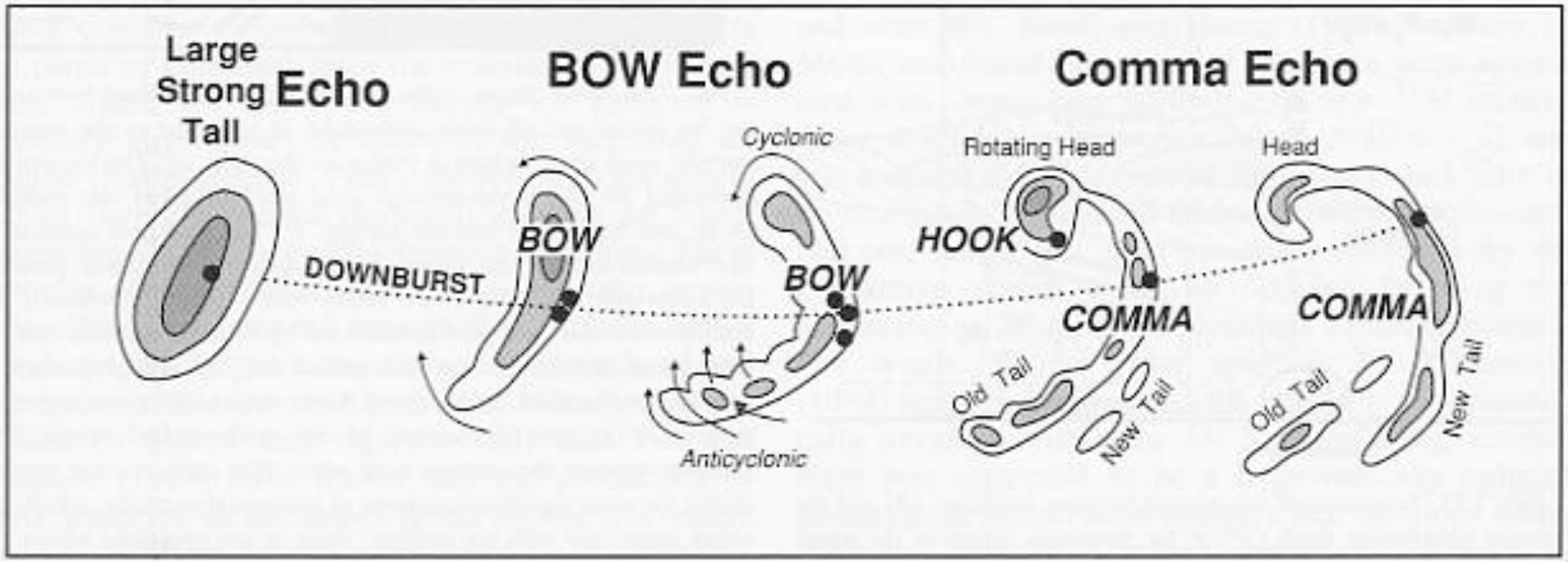

FIG. 7.37. A typical morphology of radar echoes associated with bow echoes that produce strong and extensive downbursts. Black dots indicate possible location of tornadoes. Based on a figure from Fujita (1978).

Wakimoto 2001

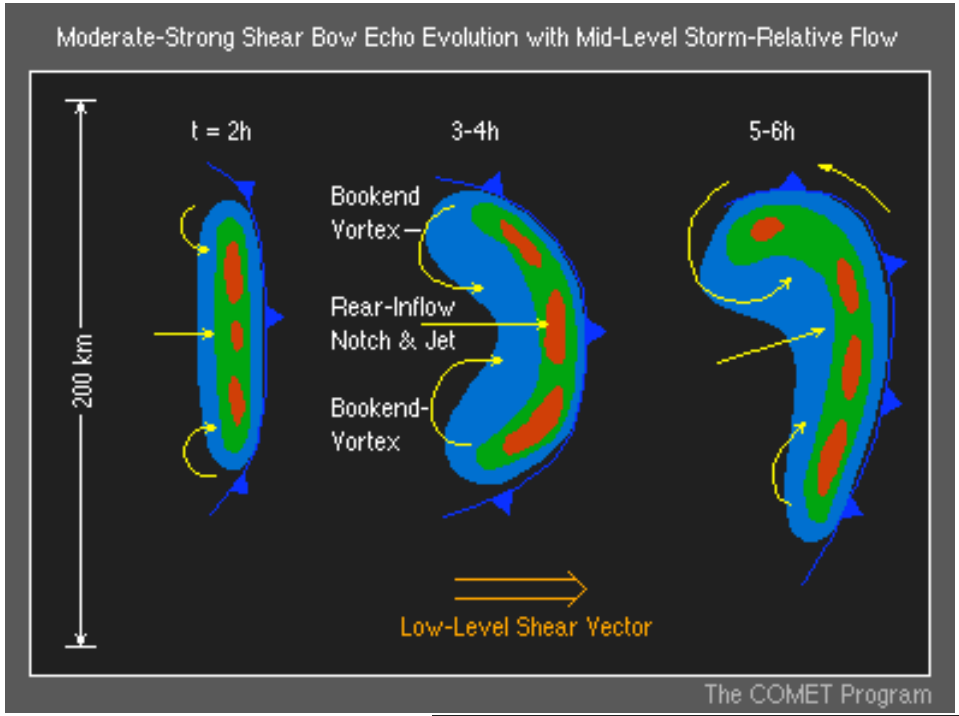
Moderate-Strong Shear Bow Echo Evolution with Mid-Level Storm-Relative Flow
t = 2h
3-4h
5-6h
Bookend
Vortex
Rear-Inflow
Notch & Jet
Bookend-
Vortex
200 km
Low-Level Shear Vector
The COMET Program

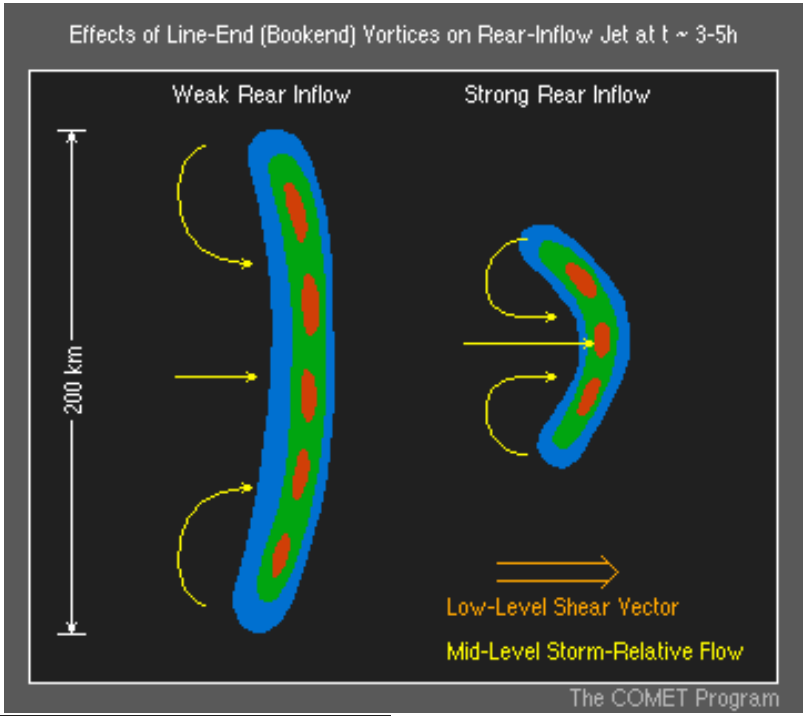
Effects of Line-End (Bookend) Vortices on Rear-Inflow Jet at t ~ 3-5h
Weak Rear Inflow
Strong Rear Inflow
200 km
Low-Level Shear Vector
Mid-Level Storm-Relative Flow
The COMET Program

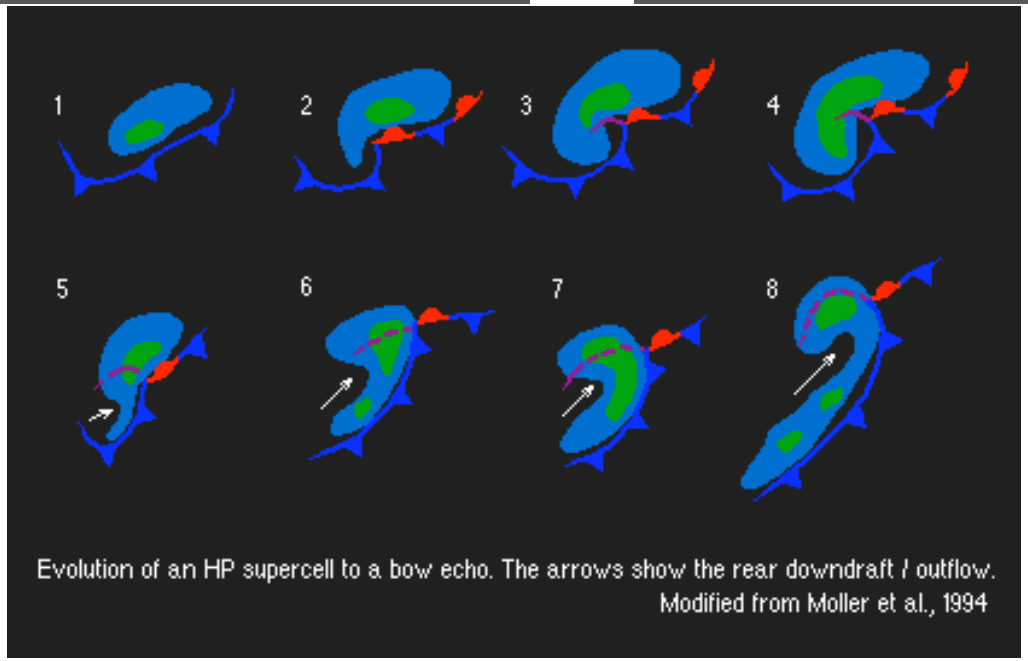
1
2
3
4
5
6
7
8
Evolution of an HP supercell to a bow echo. The arrows show the rear downdraft / outflow.
Modified from Moller et al., 1994

2D Horizontal Vorticity Equation

$$\frac{d\eta}{dt} = -\frac{\partial B}{\partial x}$$

where η (Horizontal Vorticity) $= \partial u/\partial z - \partial w/\partial x$

Courtesy: M. Weisman

Bluestein (1993)

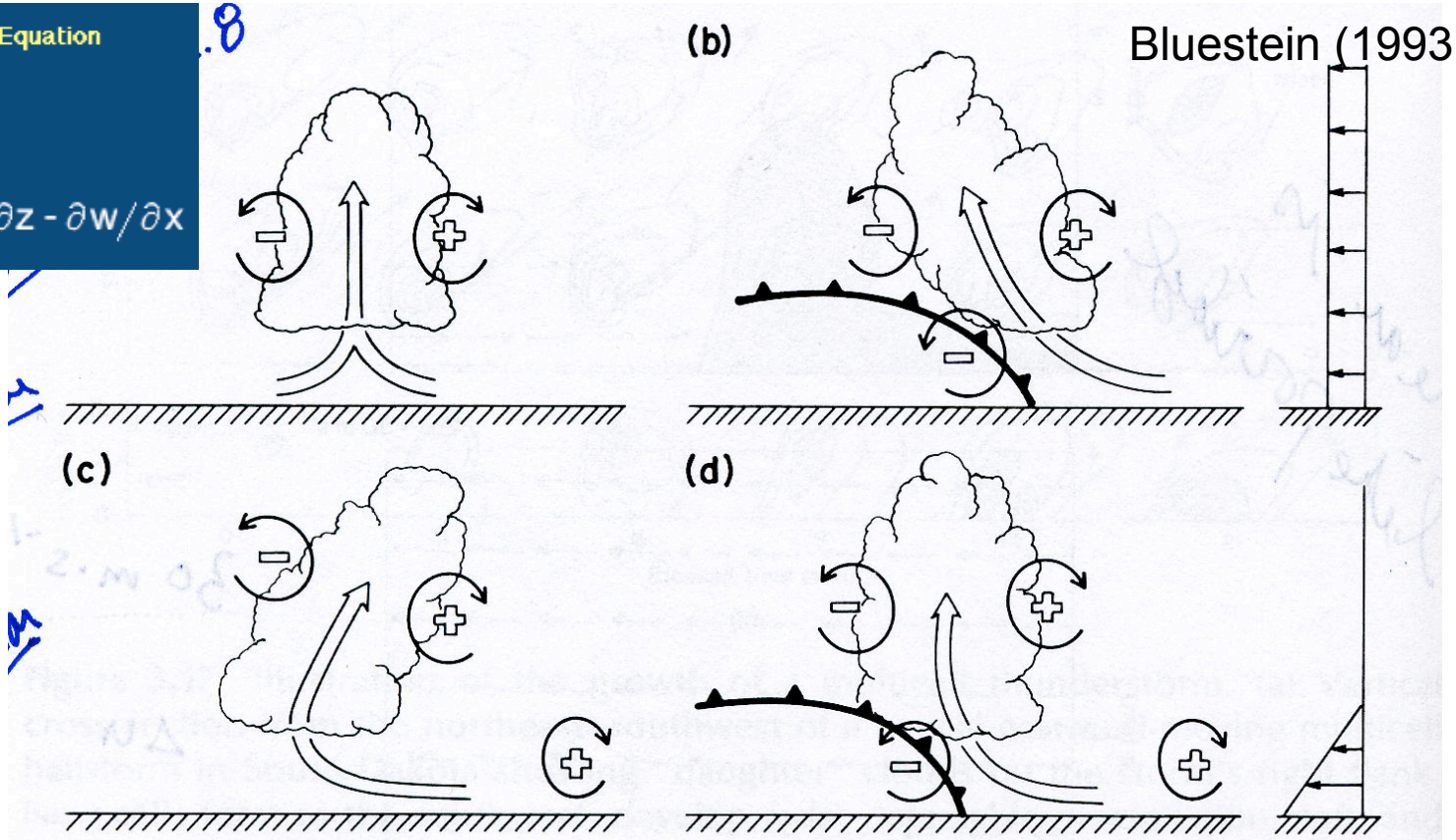

Figure 3.19 Schematic diagram showing how a buoyant updraft may be influenced by vertical wind shear and/or a cold pool. (a) With no vertical wind shear and no cold pool, the axis of the updraft (thick arrow) produced by the thermally created, symmetric vorticity (sense of rotation indicated by thin arrows and plus and minus signs) distribution is vertical. (b) With a cold pool (underneath cold-front symbol) and no shear, the distribution is biased by the negative vorticity of the underlying cold pool and causes the updraft to lean as shown. (c) With shear and no cold pool, the distribution is biased toward positive vorticity, and this causes the updraft to lean as shown. (d) With both a cold pool and shear, the two effects may negate each other, and allow an erect updraft. Environmental wind profile indicated at the right for (a) and (b) (top) and for (c) and (d) (bottom) (from Rotunno et al., 1988). (Courtesy of the American Meteorological Society)

RKW Theory

Rotunno et al. (JAS, 1988)

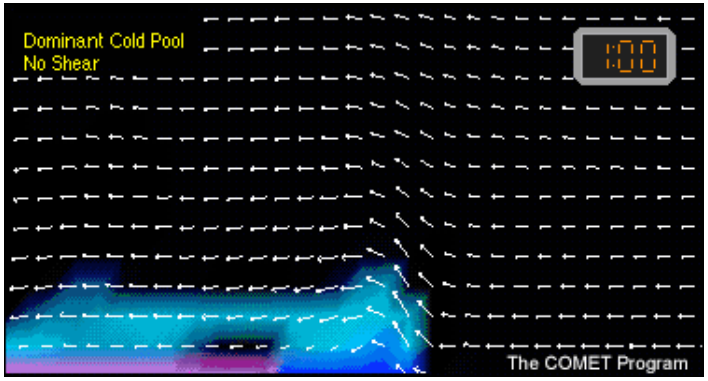

$C/\Delta u > 1$

"Optimal" condition for cold pool lifting

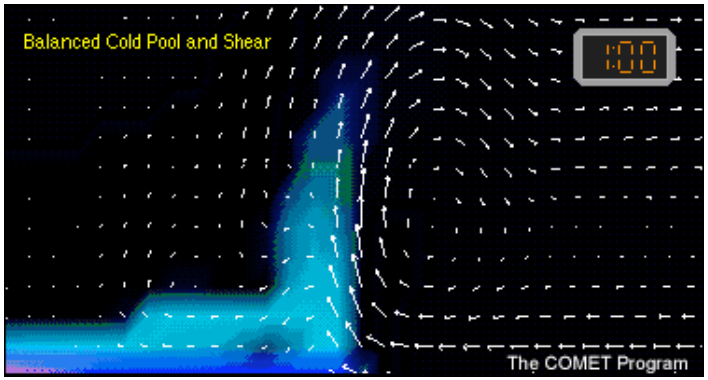

$C/\Delta u = 1$

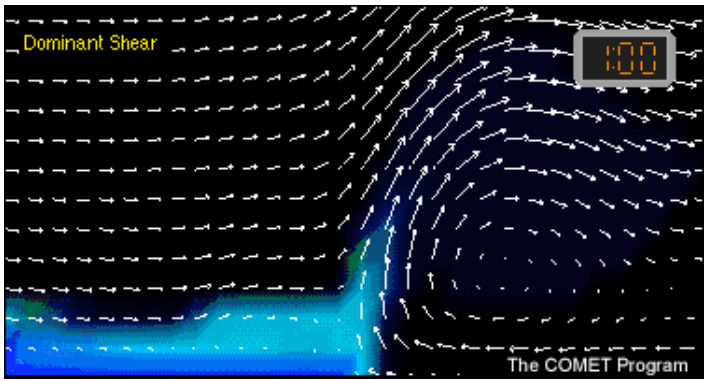

$C/\Delta u < 1$

2D Horizontal Vorticity Equation

$$\frac{d\eta}{dt} = -\frac{\partial B}{\partial x}$$

where η (Horizontal Vorticity) $= \partial u/\partial z - \partial w/\partial x$

Courtesy: M. Weisman

Derechos

Extremely intense bow echoes that produce swaths of significant wind damage

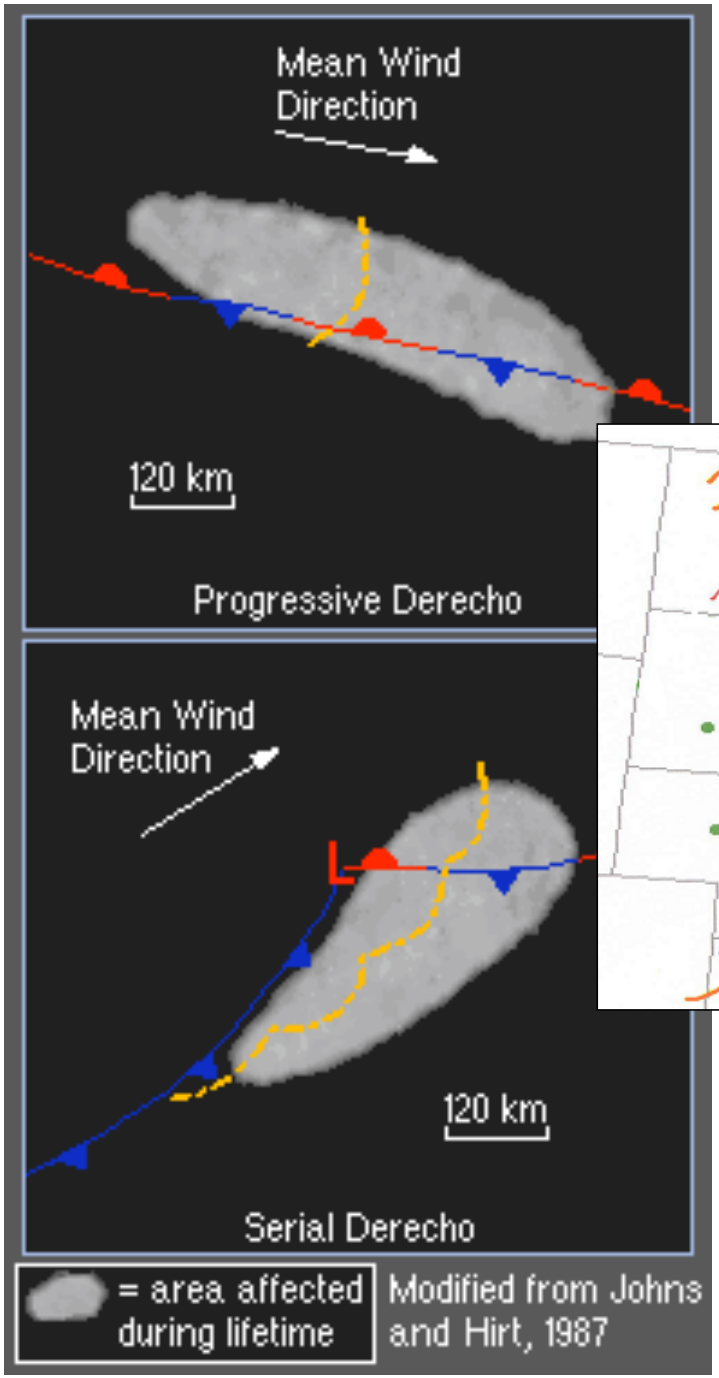

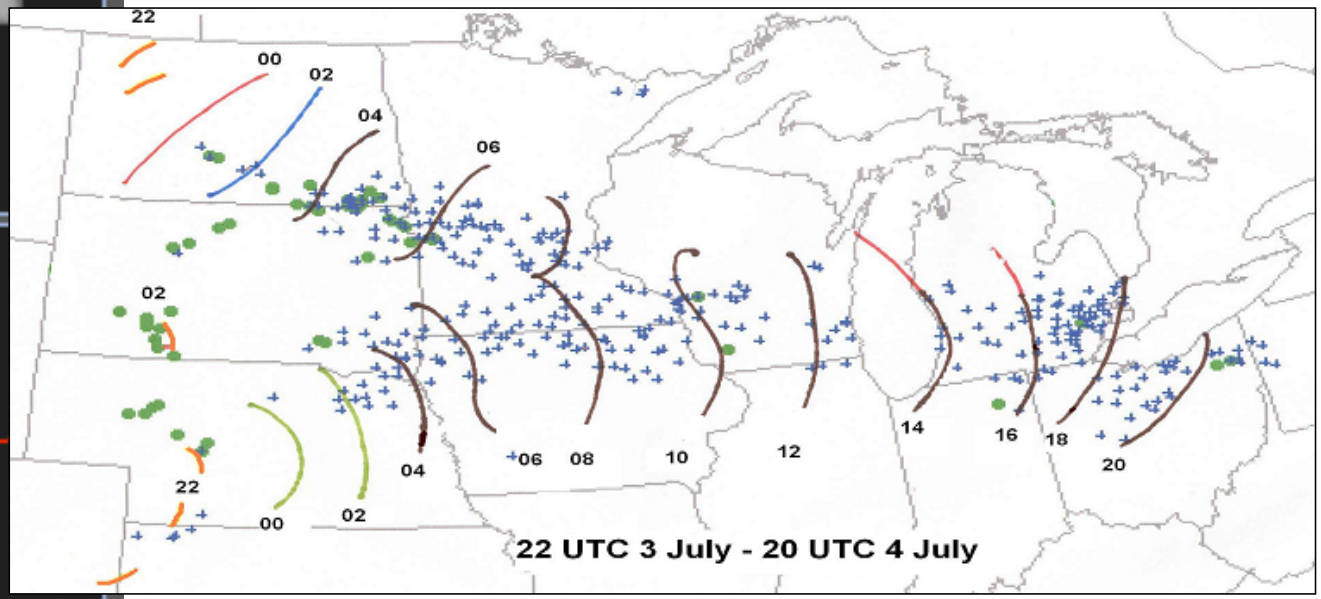

3-4 July 2003 progressive derecho

Example of Bow Echo/Derecho Courtesy NWS Albany, NY

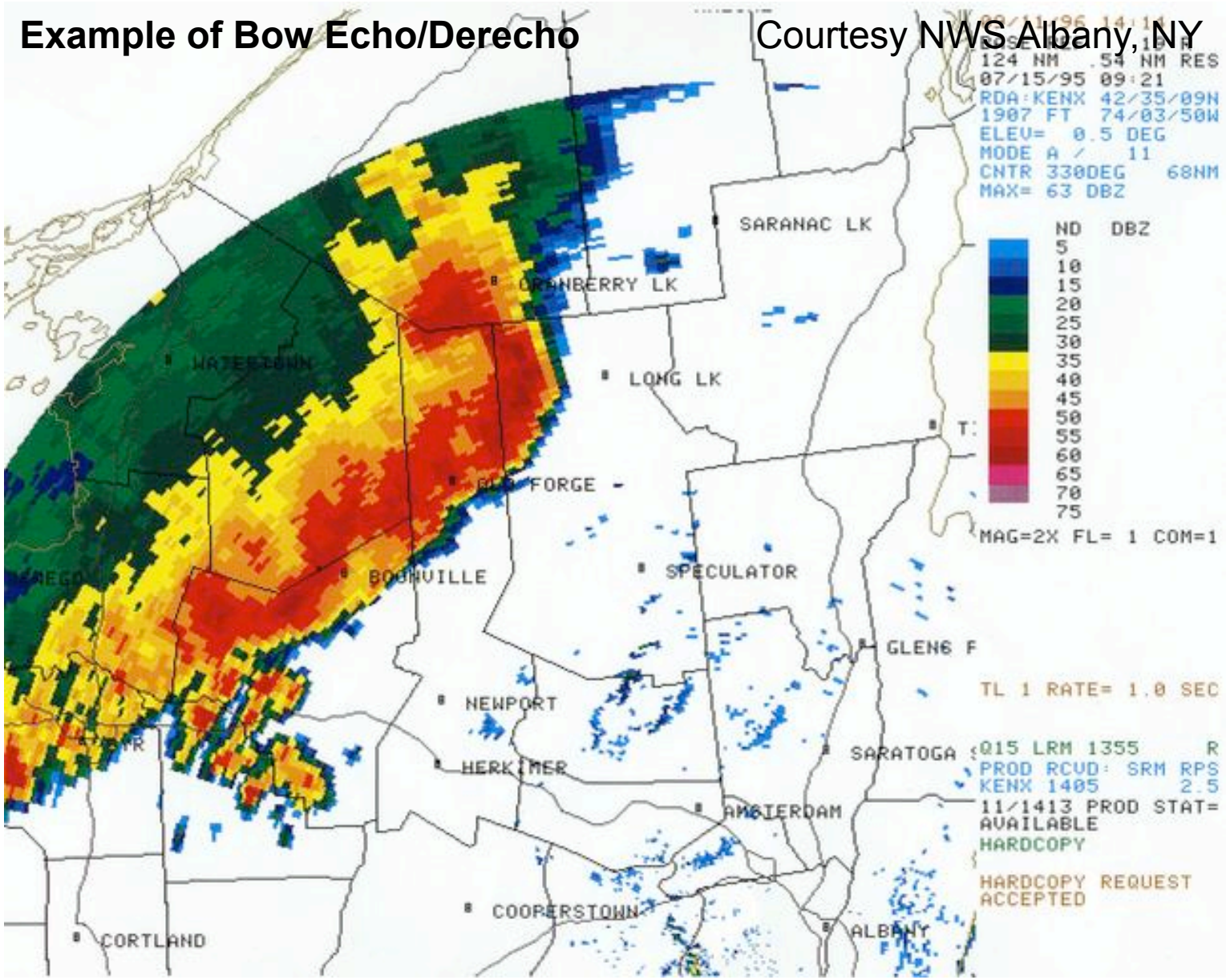

15 July 1995 5:21 a.m. EDT

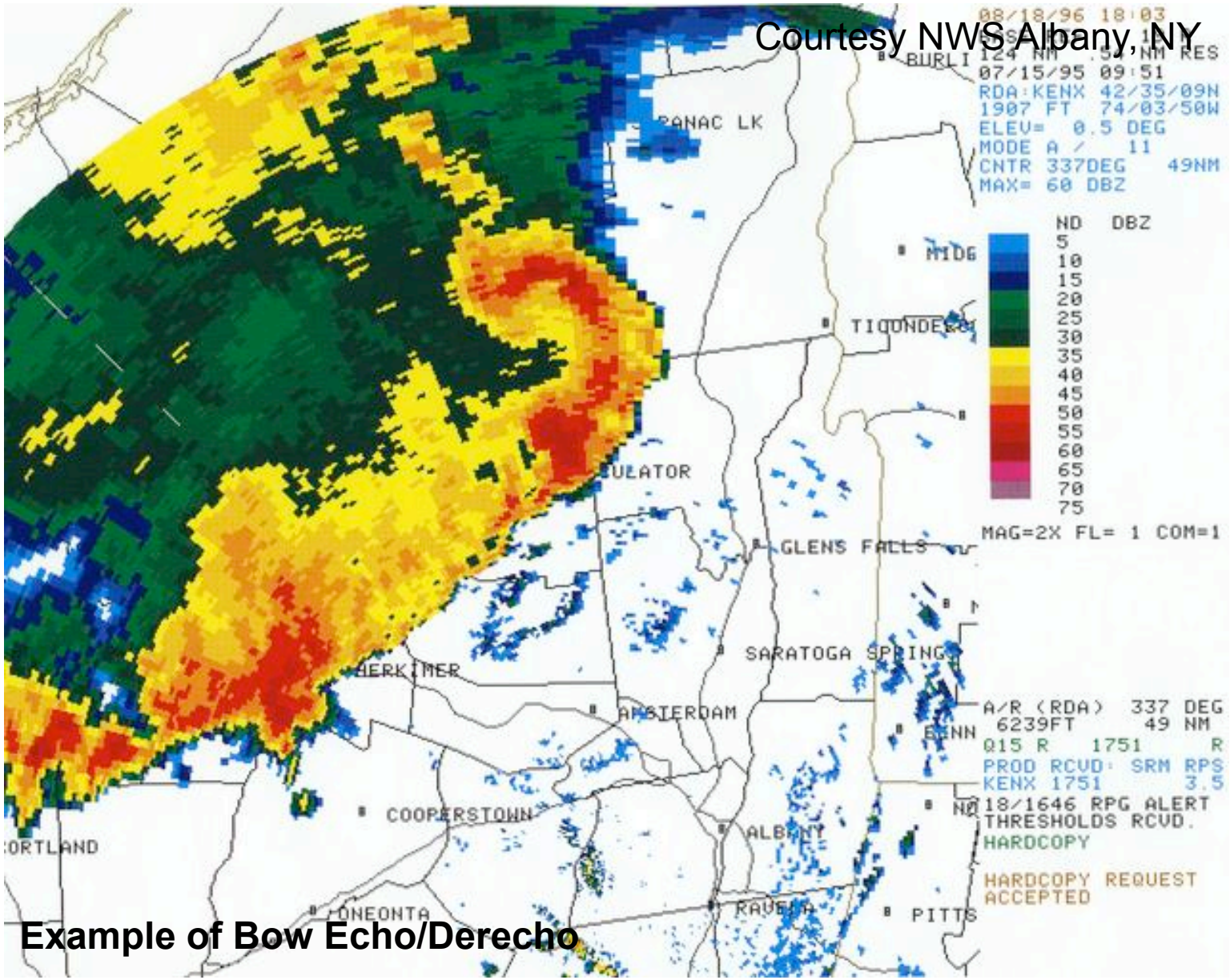

Example of Bow Echo/Derecho

15 July 1995 5:51 a.m. EDT

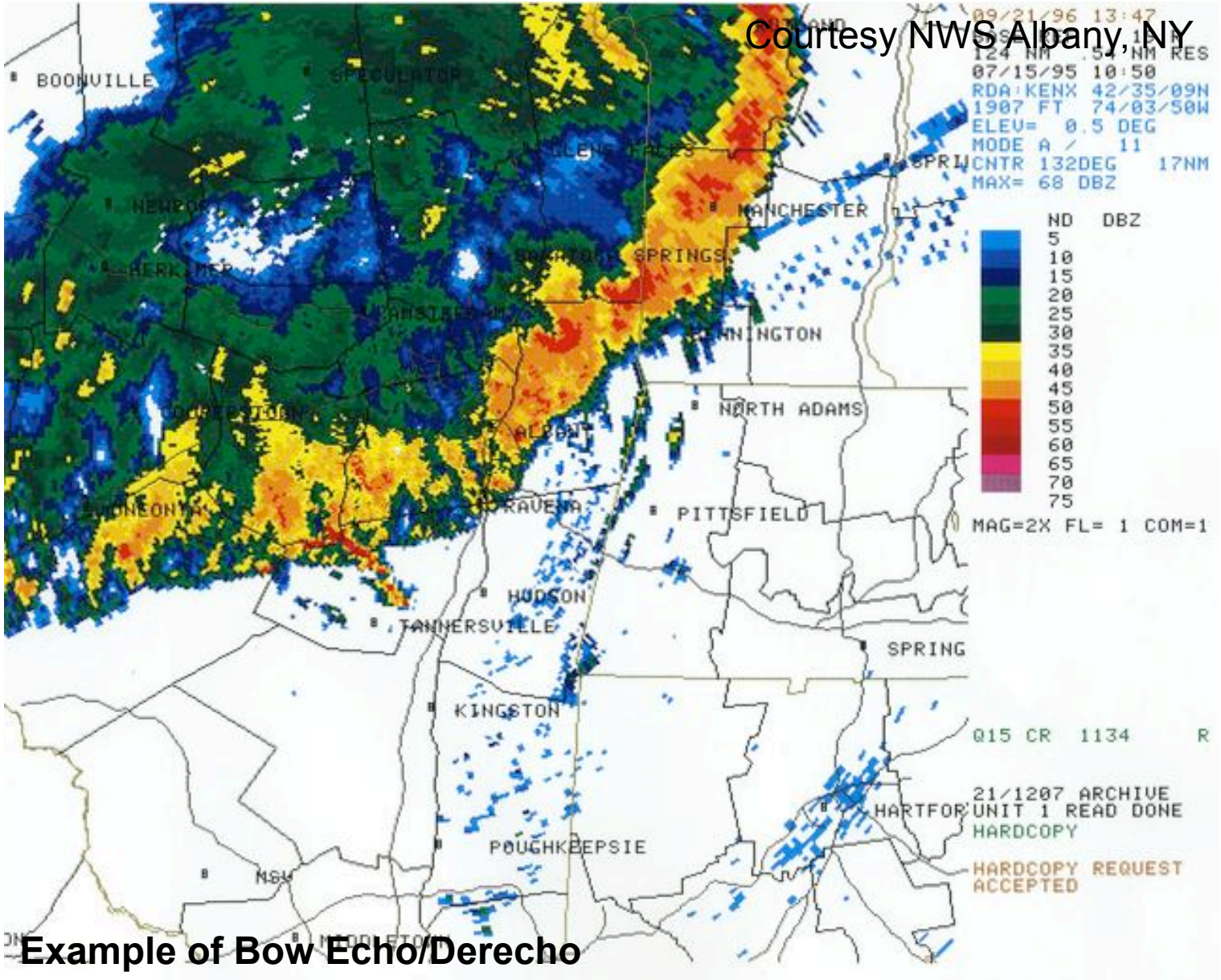

Example of Bow Echo/Derecho

15 July 1995 6:50 a.m. EDT

High Wind Events Climatology and Physical Processes

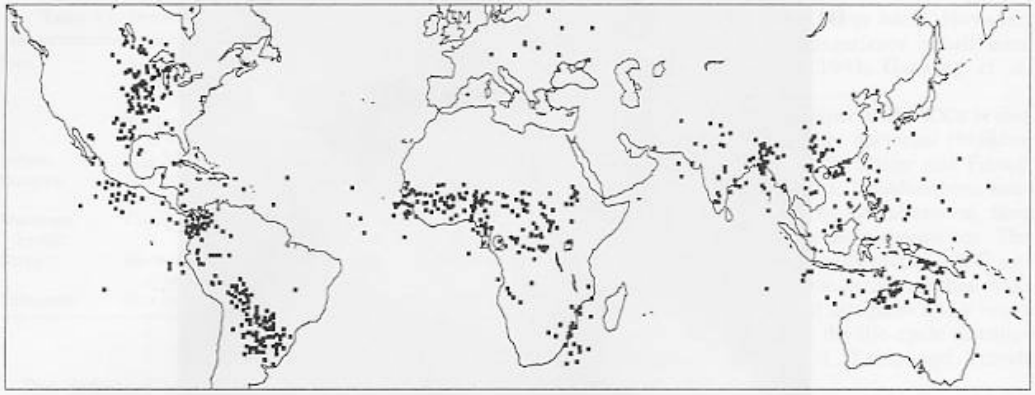

FIG. 9.2. Locations of MCCs based upon 1–3-yr regional samples of satellite imagery (from Laing and Fritsch 1997). Locations are shown for the time of maximum extent of the cold-cloud shield. Additional data concerning the samples are given in the appendix.

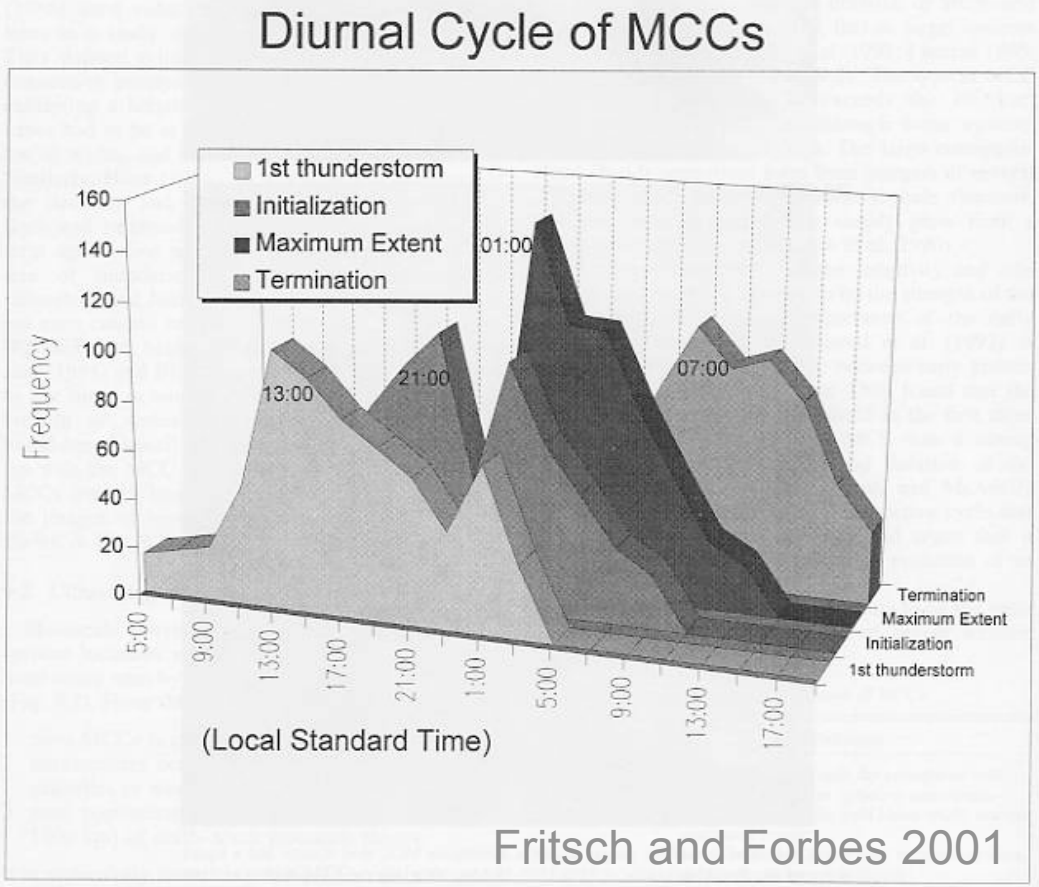

FIG. 9.3. Distribution of the times of occurrence of stages in MCC life cycle. From the global distribution of Laing and Fritsch (1997).

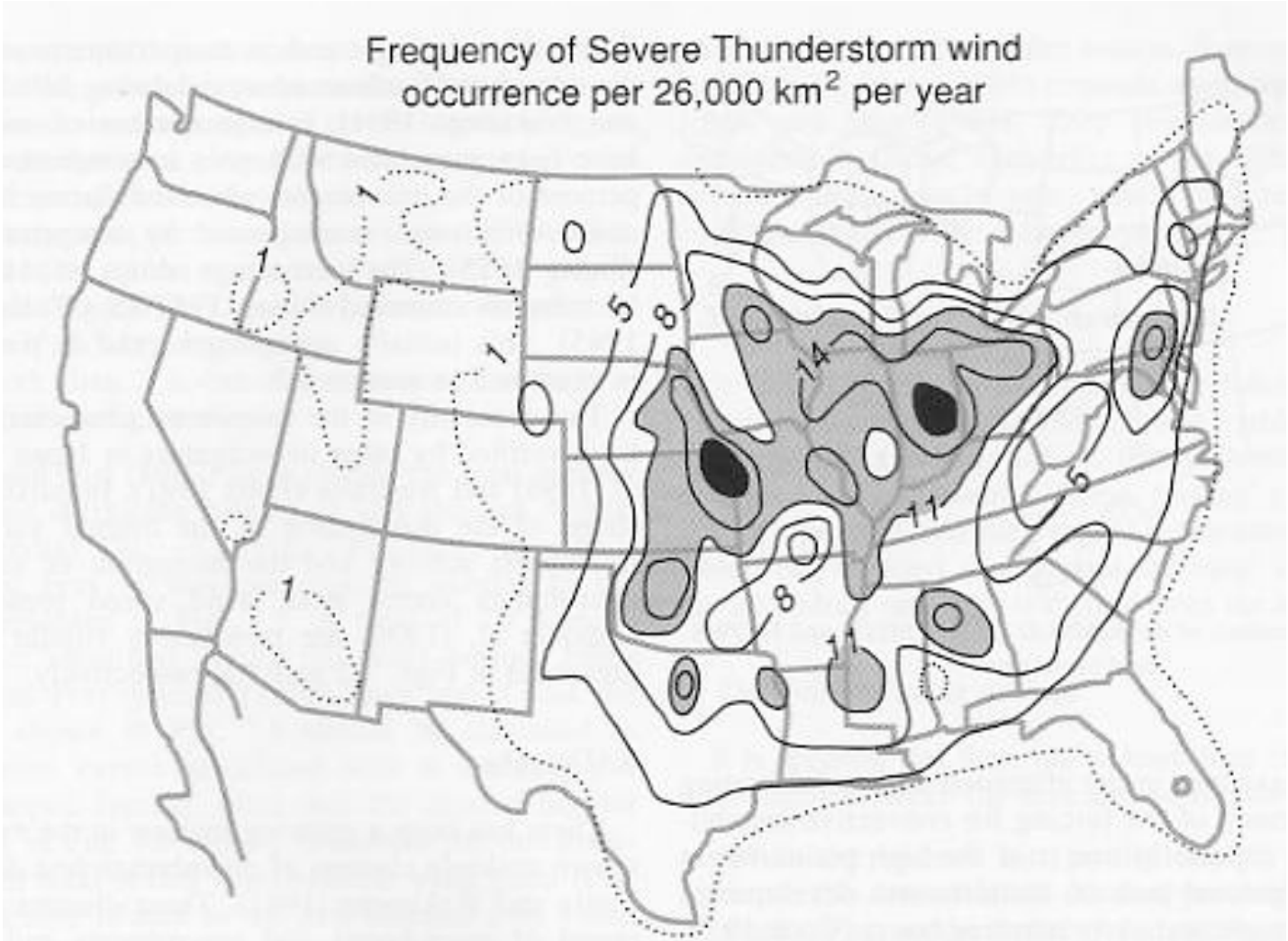

FIG. 7.3. Frequency of any severe thunderstorm wind occurrence per 26 000 km^2 per year. Dashed black lines are isopleths of one. Values greater than 11 and 17 are shaded gray and black, respectively. Based on a figure from Kelly et al. (1985).

Wakimoto 2001

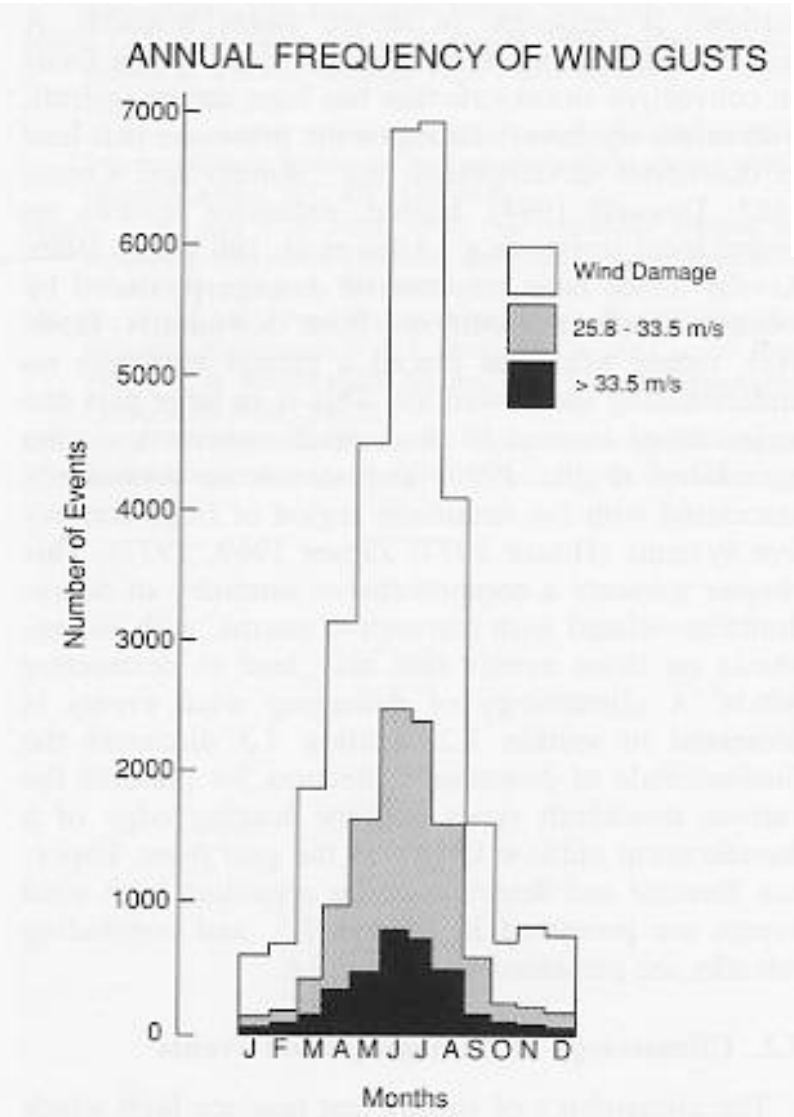

FIG. 7.1. Monthly distribution of occurrences of thunderstorm-related wind damage. Based on a figure from Kelly et al. (1985).

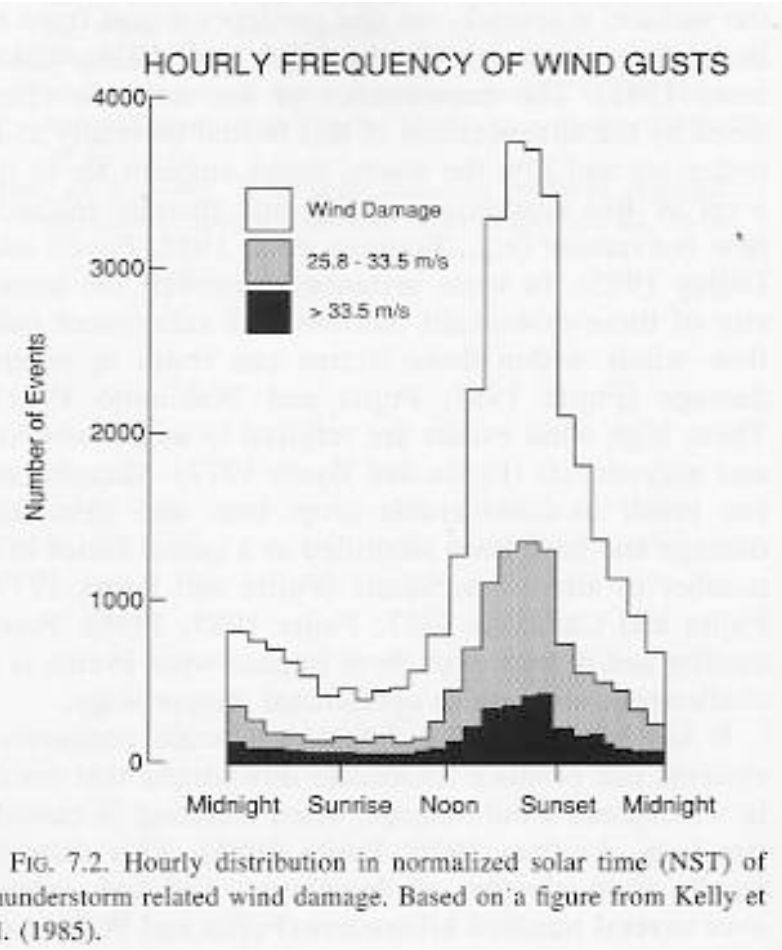

FIG. 7.2. Hourly distribution in normalized solar time (NST) of thunderstorm related wind damage. Based on a figure from Kelly et al. (1985).

Wakimoto 2001

Microburst structure

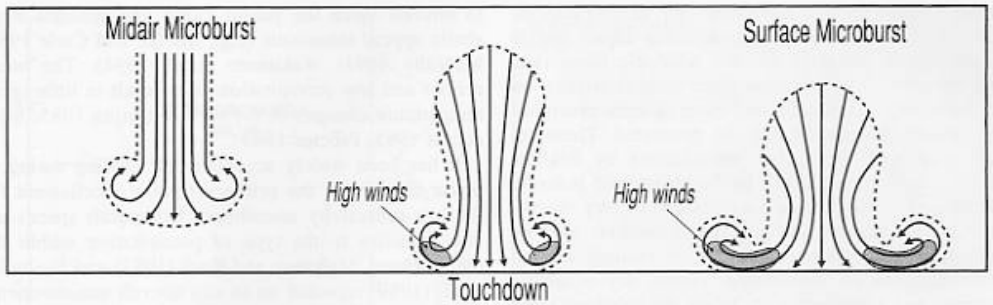

FIG. 7.13. Conceptual model of a microburst hypothesized to explain ground-damage patterns. Three stages of development are shown. A midair microburst may or may not descend to the surface. If it does, the outburst winds develop immediately after its touchdown. Based on a figure from Fujita (1985).

sphere varies with height. While rotation does not appear to enhance microburst downdraft speeds, it will be shown in section 7.5 that it can be used as a useful precursor for detecting microbursts.

Results from a variety of studies (e.g., Wilson et al. 1984; Fujita 1985; Wakimoto 1985; Mielke and Carle 1987; Hjelmfelt et al. 1989; Proctor 1989; Roberts and Wilson 1989; Wolfson et al. 1990) reveal that microburst winds are associated with a continuum of rain rates that range from heavy thunderstorm precipitation to virga shafts either from altocumuli or from clouds that have been referred to as shallow high-based cumulonimbi (Brown et al. 1982). Fujita (1985) and Wakimoto (1985) subdivided microbursts into dry/low-reflectivity and wet/high-reflectivity microbursts. The following definitions are used to describe these two phenomena (Fujita and Wakimoto 1981; Wilson et al. 1984; Fujita 1985).

Dry/low-reflectivity microburst: A microburst associated with <0.25 mm of rain or a radar echo <35 dBZ in intensity.

Wet/high-reflectivity microburst: A microburst associated with >0.25 mm of rain or a radar echo >35 dBZ in intensity.

(i) Low-reflectivity or dry microbursts

Numerical calculations (Hookings 1965; Kamburova and Ludlam 1966; Harris 1977; Srivastava 1985, 1987; Proctor 1989) have shown the sensitivity of downdraft intensity as a function of drop size, rain

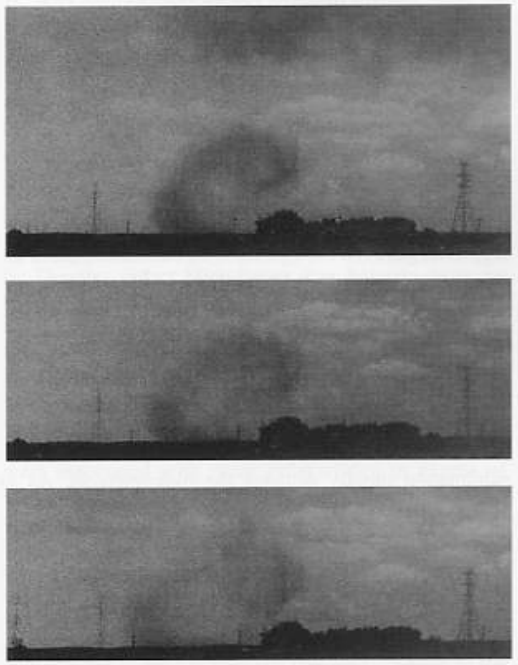

FIG. 7.14. A sequence of photographs showing a curl of dust behind the leading edge of a microburst outflow on 15 Jul 1982. Photos taken by B. Waranauskas (from Fujita 1985).

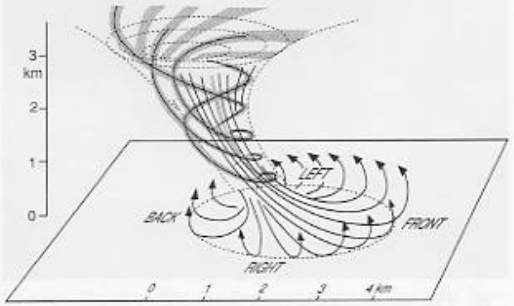

FIG. 7.15. Three-dimensional visualization of a microburst. Based on a figure from Fujita (1985).

Wakimoto 2001

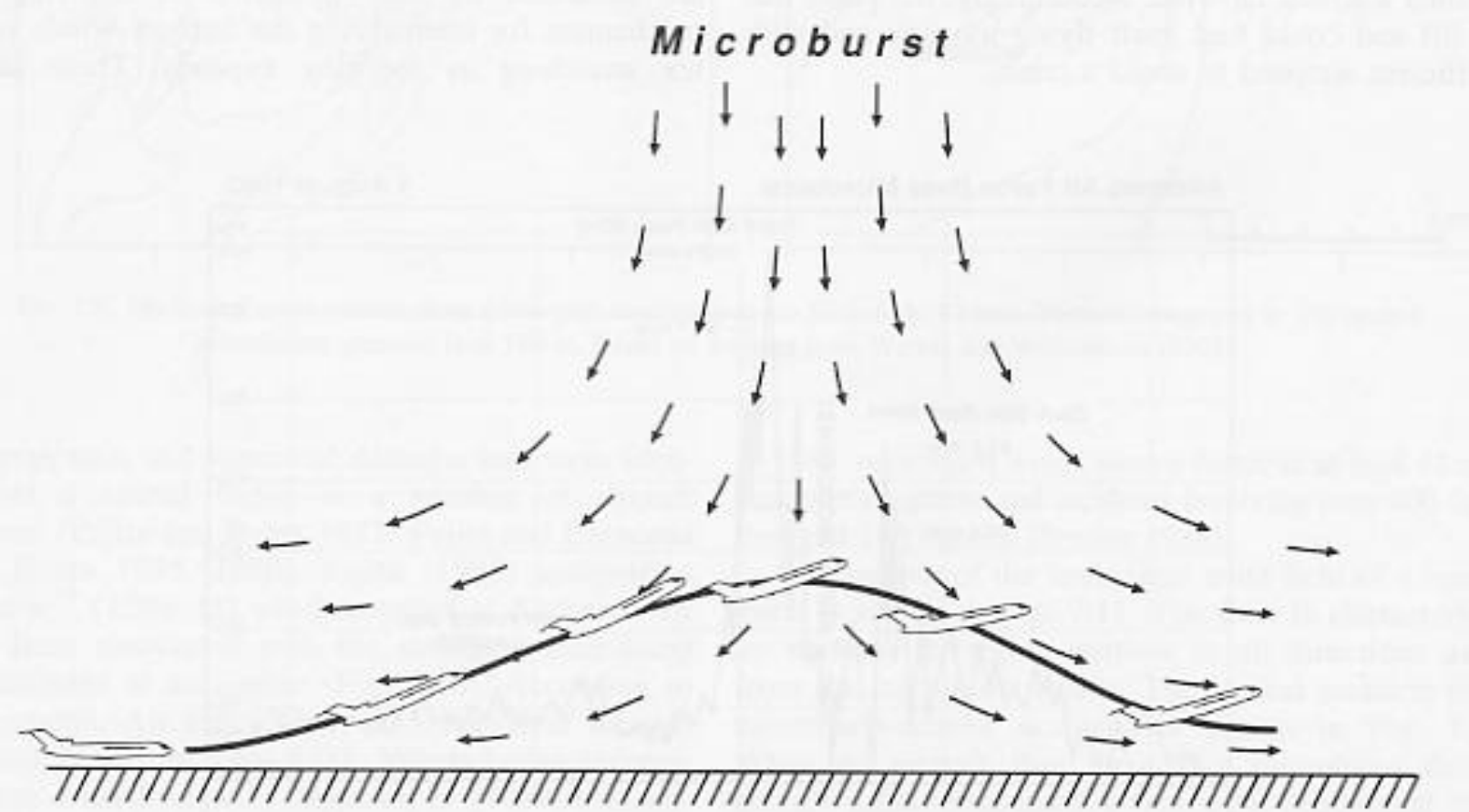

FIG. 7.12. Schematic diagram illustrating the impact of a microburst on aircraft performance during takeoff. The airplane first encounters a headwind and first experiences added lift. This is followed in short succession by a decreasing headwind component, a downdraft, and finally a strong tailwind, which may lead to an impact with the ground. Composite drawing based on numerous studies of aircraft accidents by Fujita and Caracena (1977), Fujita and Byers (1977), and Fujita (1978, 1985, 1986).

http://severewx.atmos.uiuc.edu/21/online.21.1.html

Wakimoto 2001

Supercell Structure

Supercell Structure

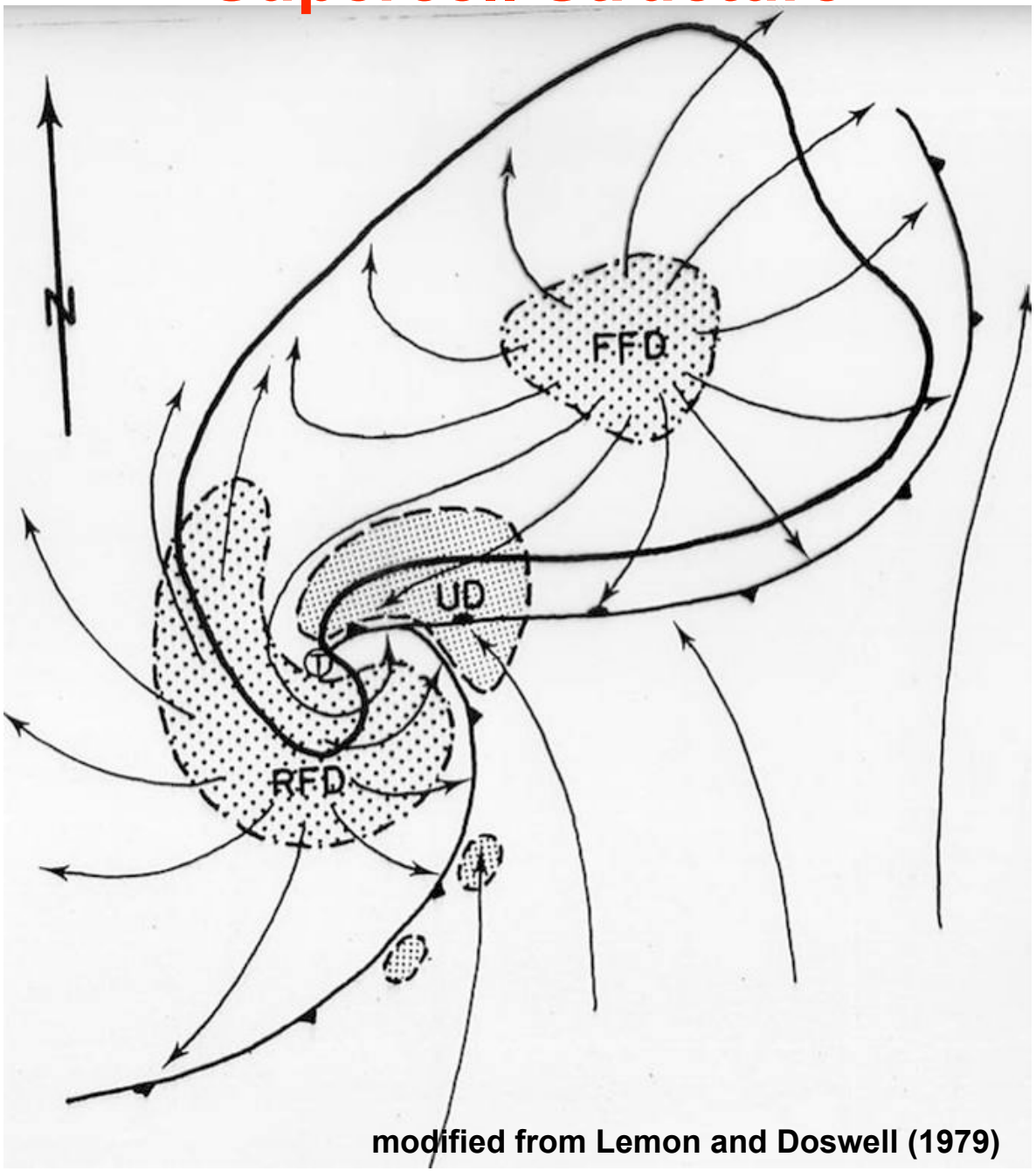

modified from Lemon and Doswell (1979)

Supercell Structure

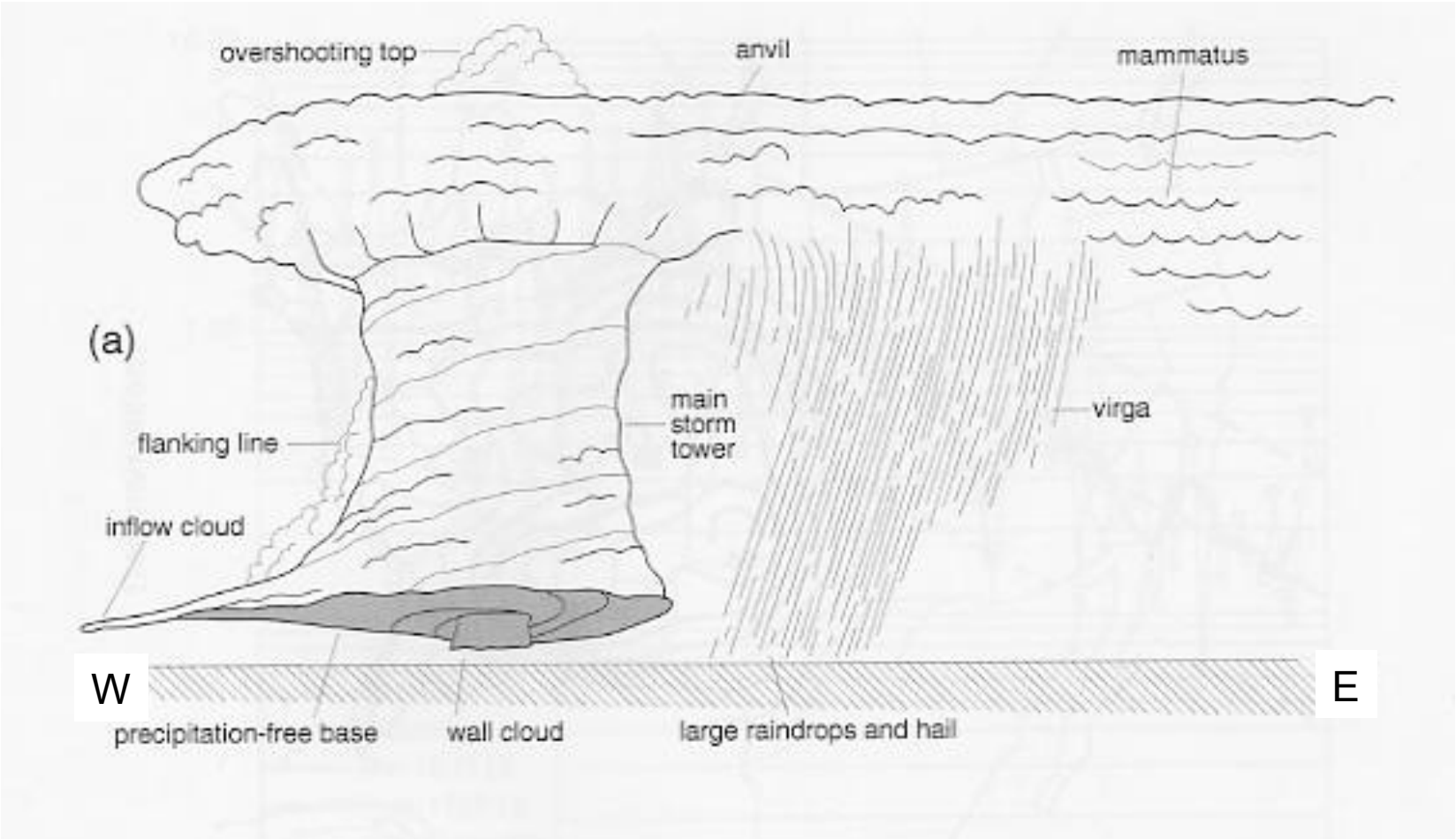

Davies-Jones et al. 2001

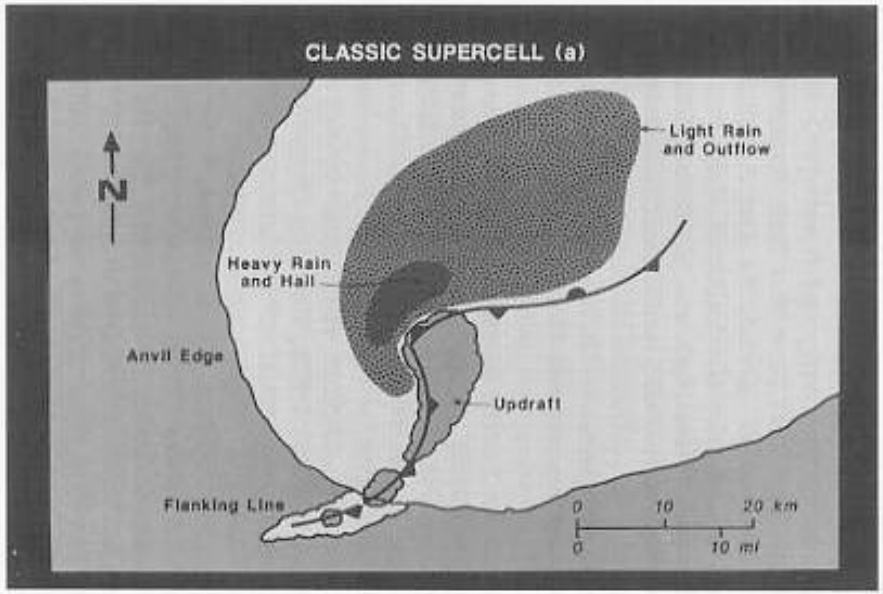

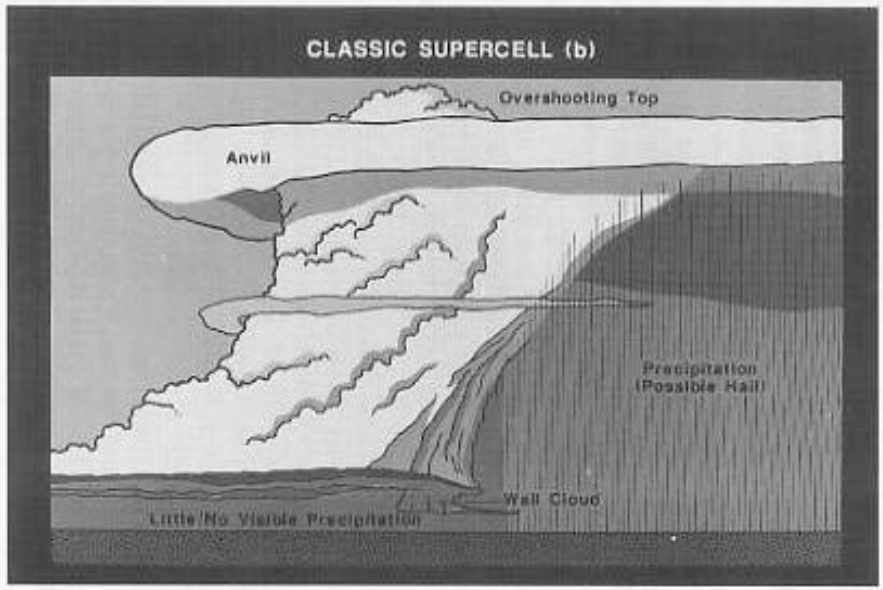

FIG 11.5. Schematics for a classic supercell showing (a) a plan view from above, and (b) an idealized view of the storm by a surface observer to the storm's east (from Moller et al. 1994).

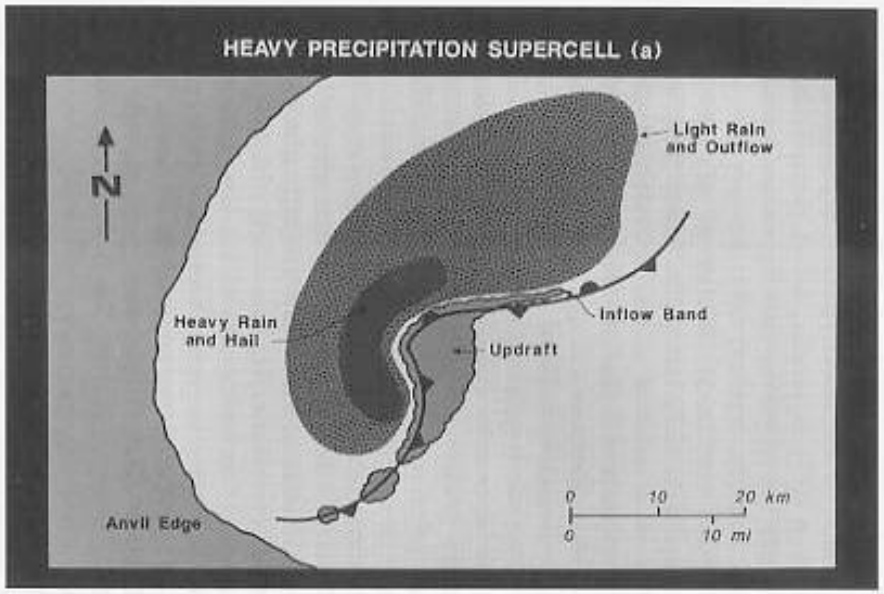

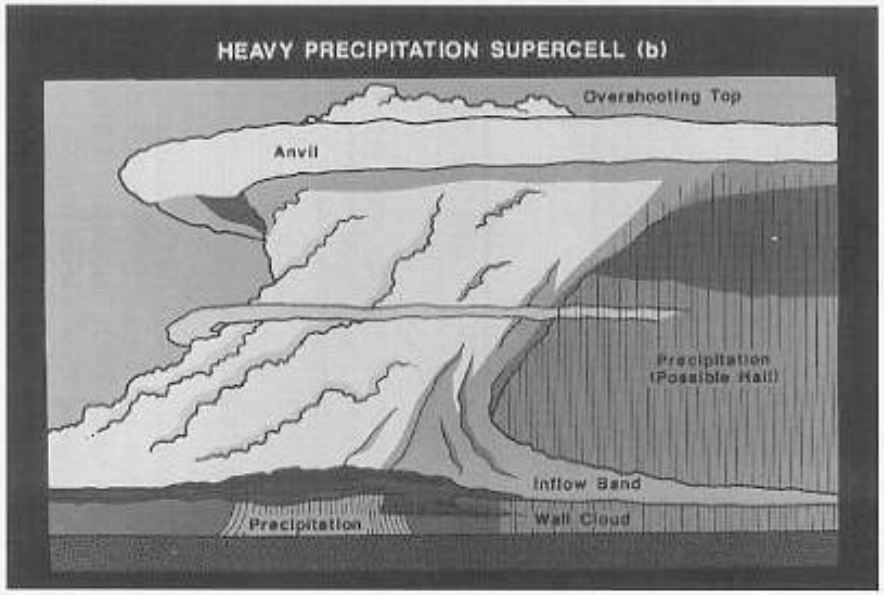

FIG 11.6. Same as in Figs. 11.5a,b except for a heavy- (or high-) precipitation supercell (from Moller et al. 1994).

Moller 2001

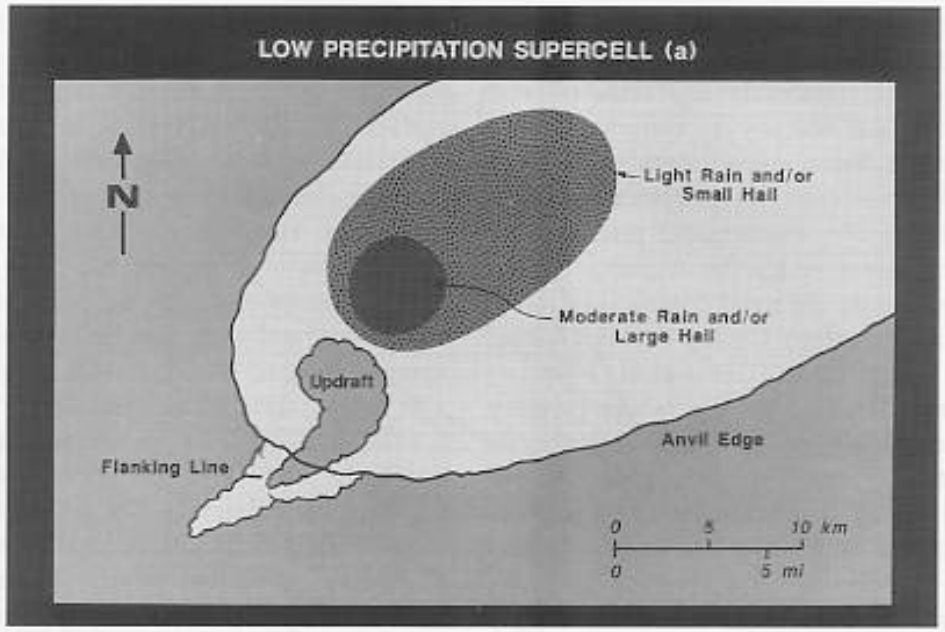

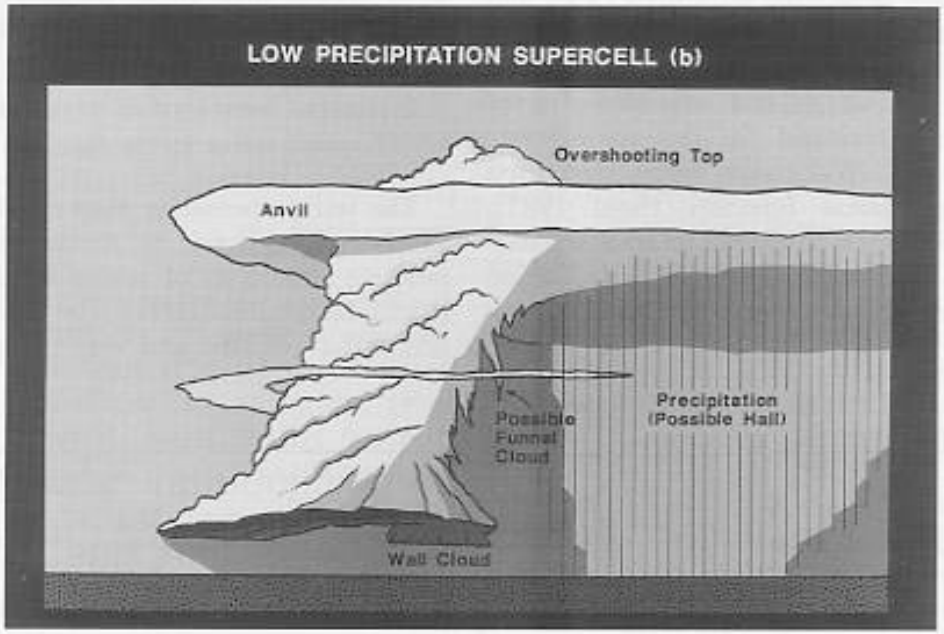

FIG 11.7. Same as in Figs. 11.5a,b except for a low-precipitation supercell (from Moller et al. 1994).

Moller 2001

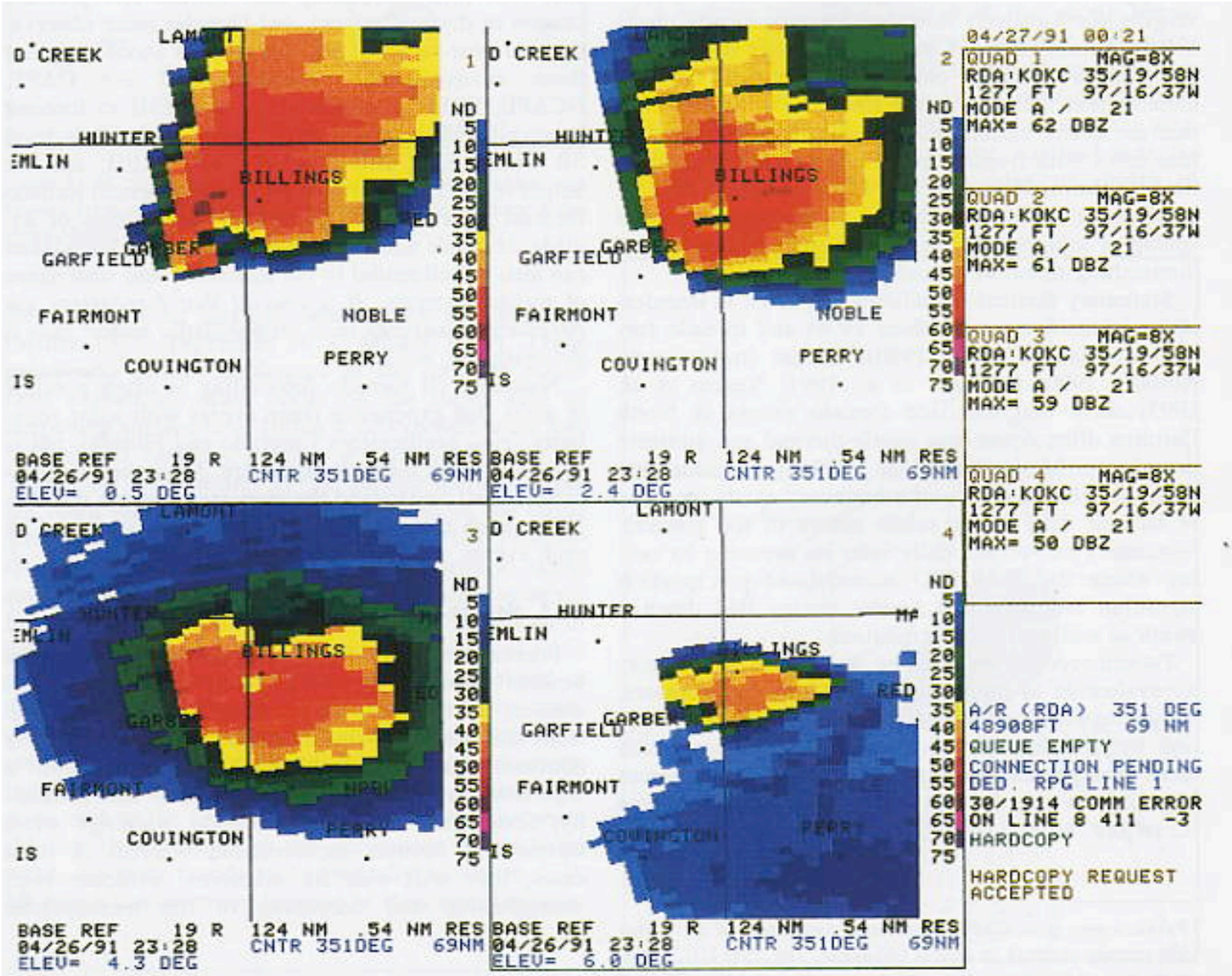

FIG 11.20. (a) WSR-88D reflectivity of 26 Apr 1991 Red Rock, OK, tornadic storm showing low-level (0.5° elevation) hook echo in upper left panel, midlevel bounded weak echo region (BWER) and echo overhang in upper right panel (2.4°) and lower left panel (4.3°), and storm top displaced above the BWER and overhang in lower right panel (6.0°).

http://severewx.atmos.uiuc.edu/18/050399.reflectivity.html

Moller 2001

Bluestein (1993)

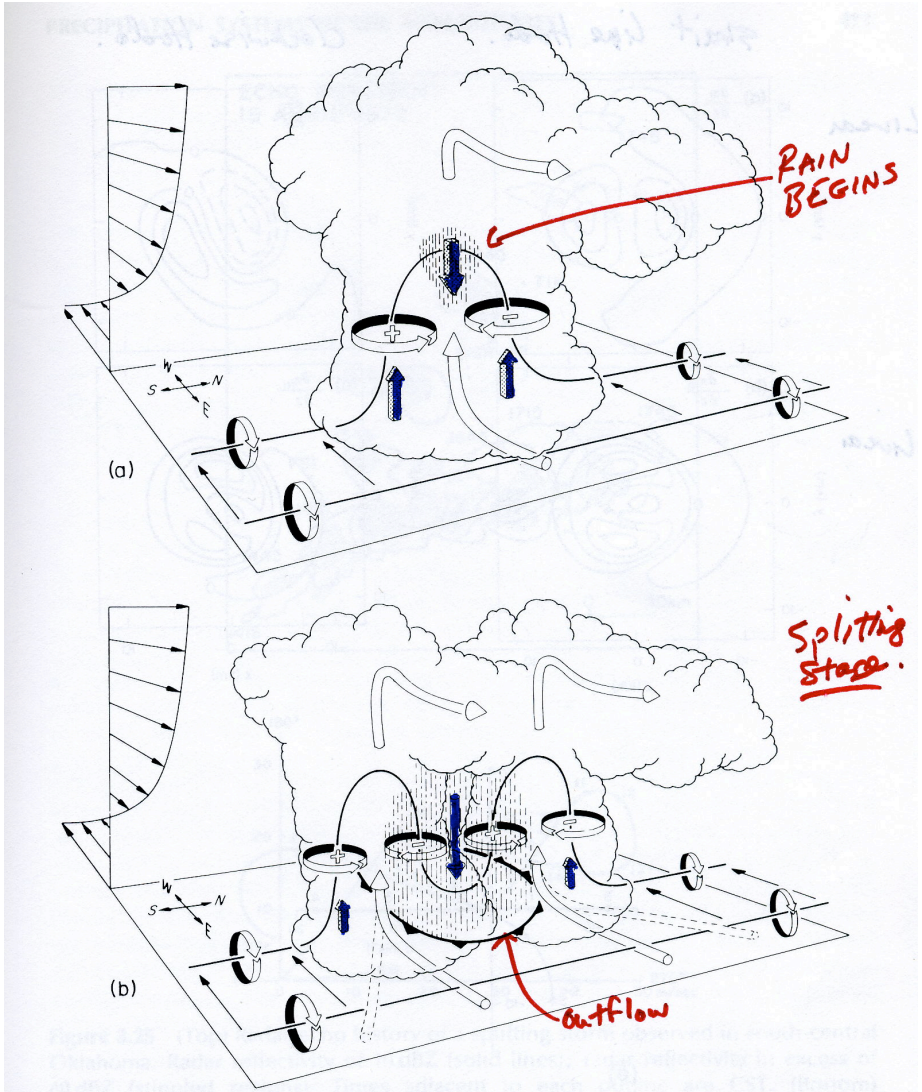

Figure 3.23 Schematic diagram depicting how a typical vortex line (streamline of three-dimensional vorticity vector) contained within (westerly) environmental shear is deformed as it interacts with a convective cell (viewed from the southeast). Direction of cloud-relative airflow (cylindrical arrows); vortex lines (solid lines), with the sense of rotation indicated by circular arrows; the forcing influences that promote new updraft and downdraft growth (shaded arrows); regions of precipitation (vertical dashed lines). (a) Initial stage: Vortex line loops into the vertical as it is swept into the updraft. (b) Splitting stage: Downdraft forming between the splitting updraft cells tilts vortex line downward, producing two vortex pairs. Boundary of the cold air spreading out beneath the storm (cold-front symbol at the surface) (from Klemp, 1987; adapted from Rotunno, 1981). (Courtesy of the American Meteorological Society)

Bluestein (1993)

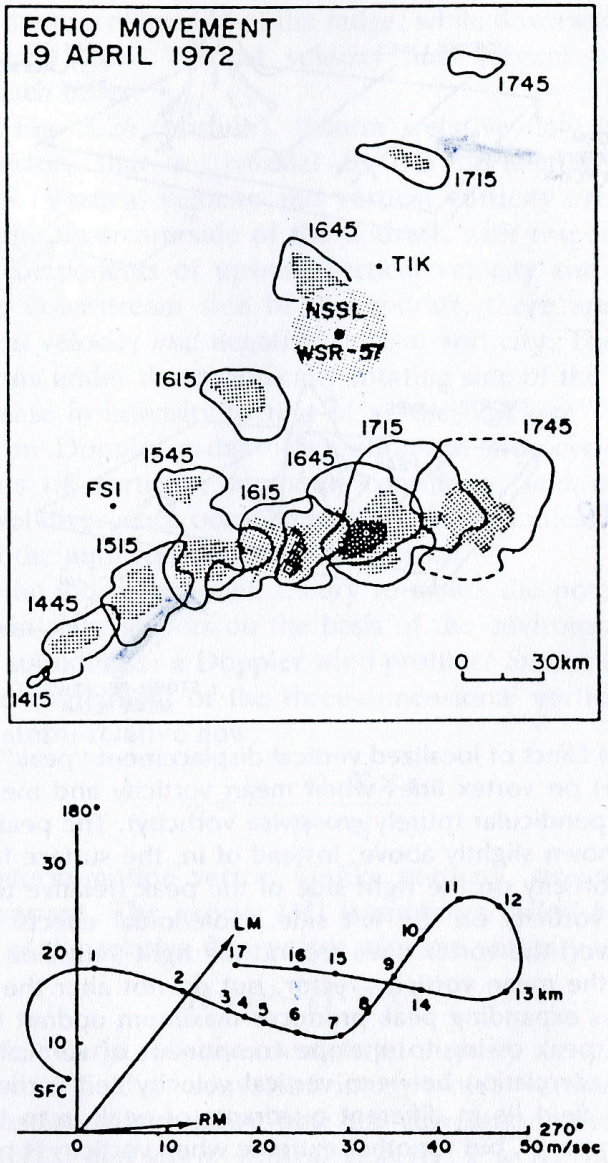

Figure 3.25 (Top) Radar-echo history of a splitting storm observed in south-central Oklahoma. Radar reflectivity of 10 dBZ (solid lines); radar reflectivity in excess of 40 dBZ (stippled regions). Times adjacent to each outline are CST. (Bottom) Hodograph representative of the storm's environment. Heights in km AGL. Motion of the right-moving (RM) and left-moving (LM) cells (from Weisman and Klemp, 1986; adapted from Burgess, 1974). (Courtesy of the American Meteorological Society)

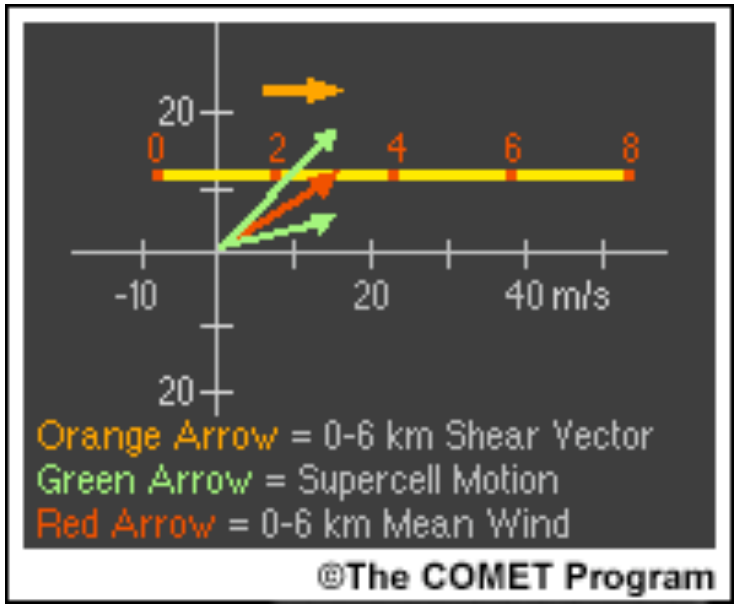
20
0
2
4
6
8
-10
20
40 m/s
20
Orange Arrow = 0-6 km Shear Vector
Green Arrow = Supercell Motion
Red Arrow = 0-6 km Mean Wind
©The COMET Program

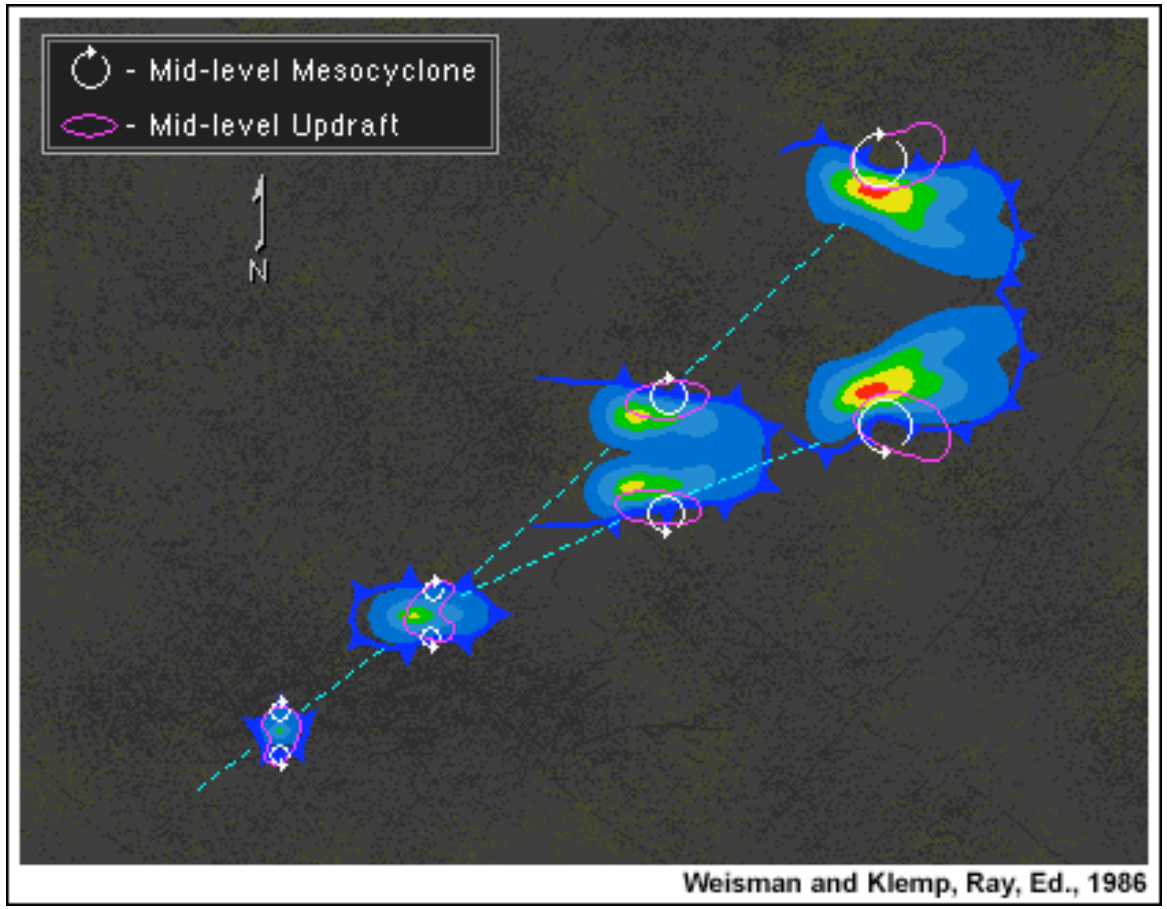
- Mid-level Mesocyclone
- Mid-level Updraft
N
Weisman and Klemp, Ray, Ed., 1986

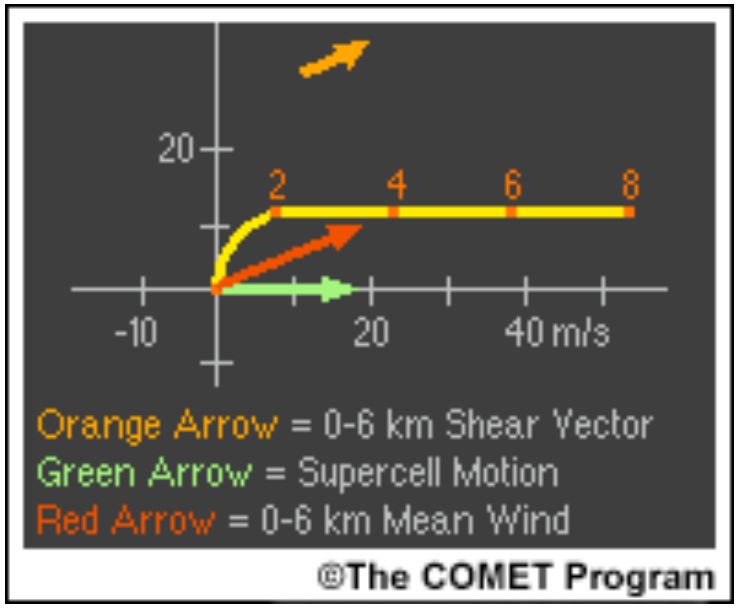
20
2
4
6
8
-10
20
40 m/s
Orange Arrow = 0-6 km Shear Vector
Green Arrow = Supercell Motion
Red Arrow = 0-6 km Mean Wind
©The COMET Program

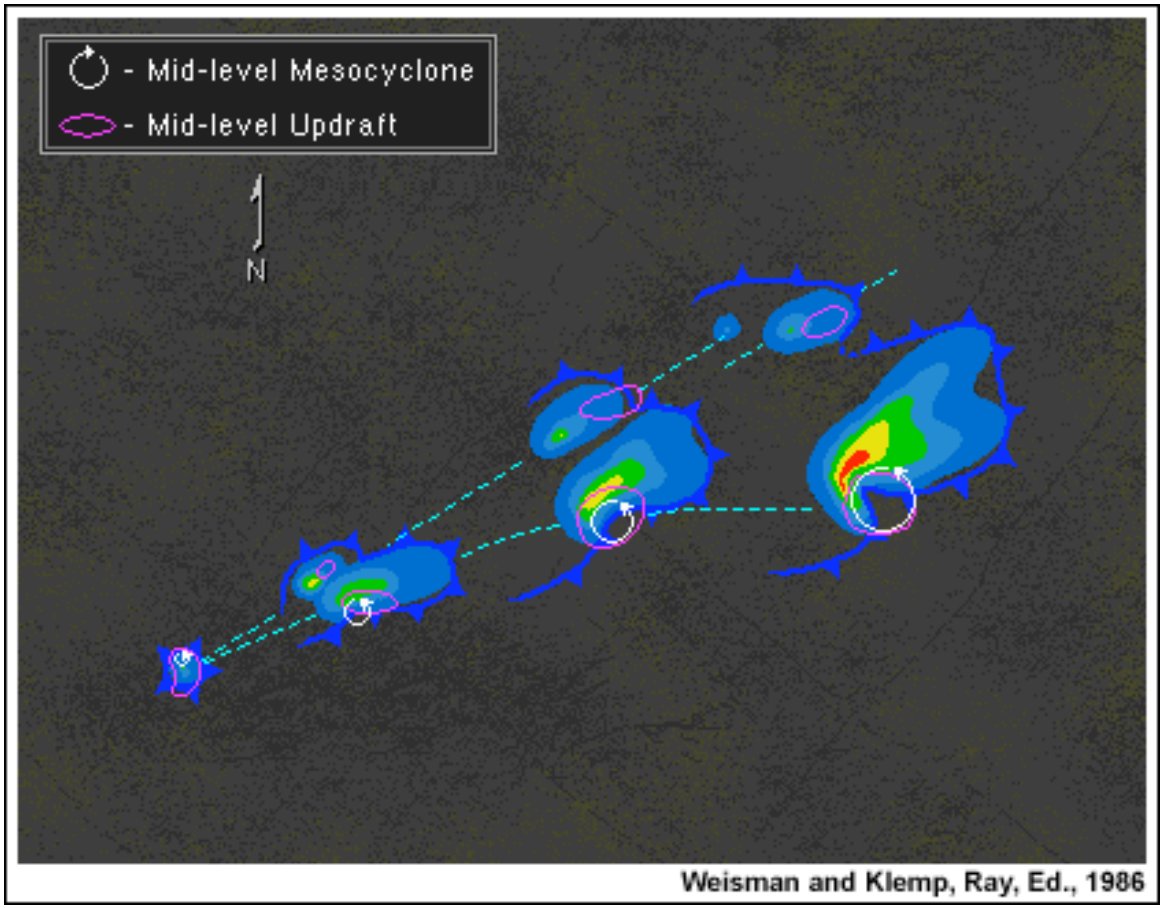
- Mid-level Mesocyclone
- Mid-level Updraft
N
Weisman and Klemp, Ray, Ed., 1986

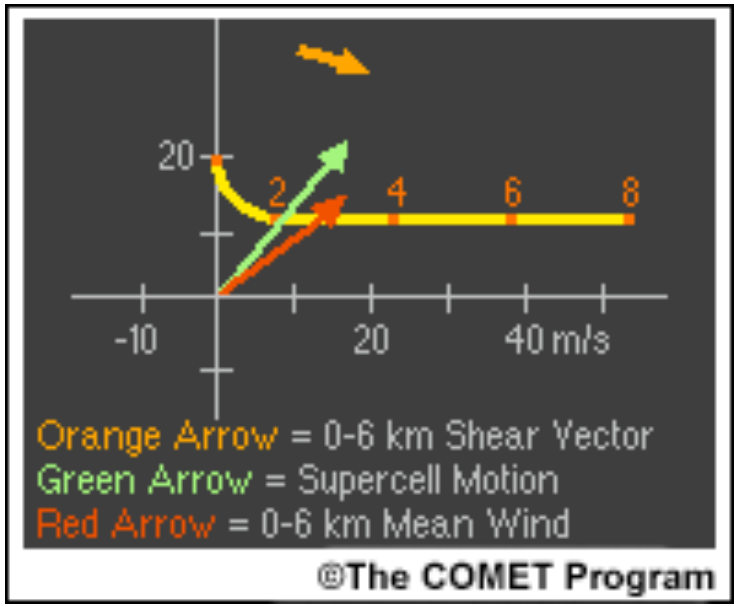
20
2
4
6
8
-10
20
40 m/s
Orange Arrow = 0-6 km Shear Vector
Green Arrow = Supercell Motion
Red Arrow = 0-6 km Mean Wind
©The COMET Program

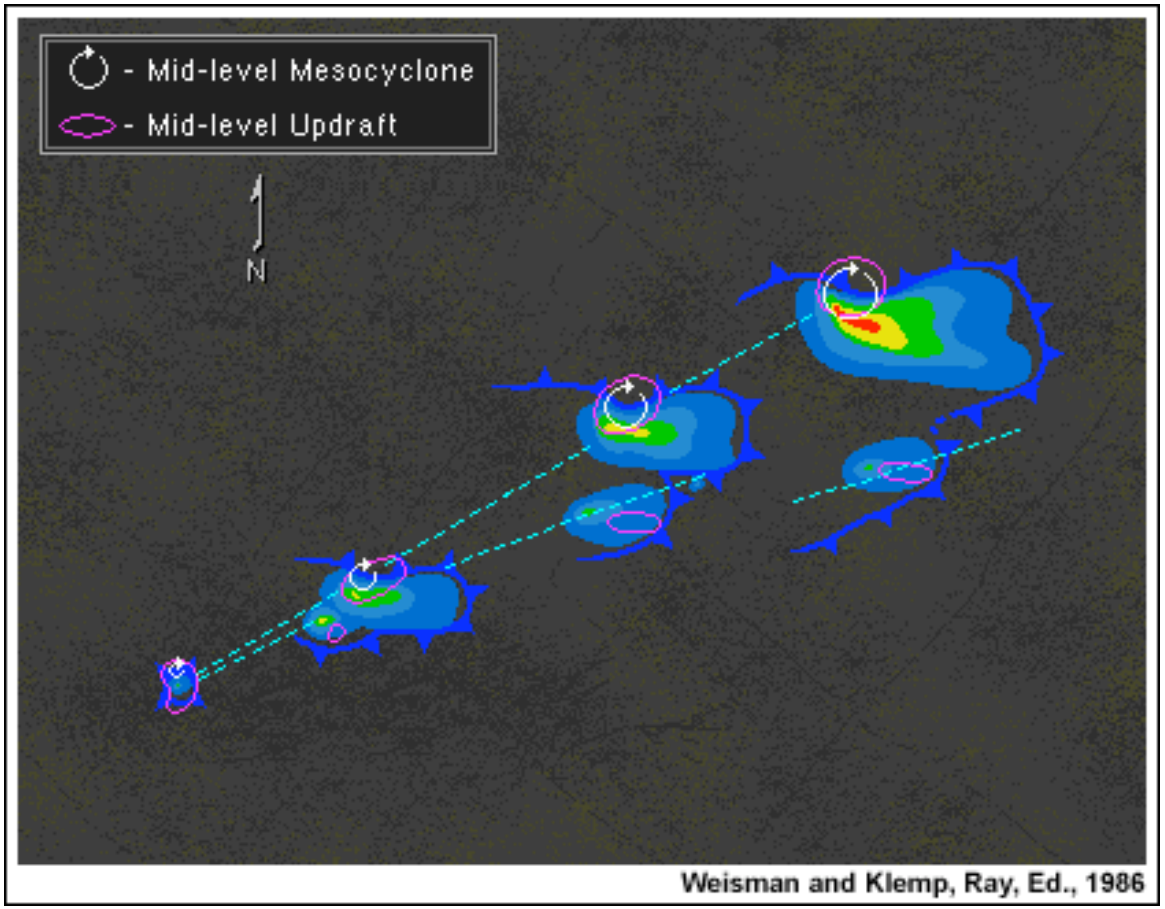
- Mid-level Mesocyclone
- Mid-level Updraft
N
Weisman and Klemp, Ray, Ed., 1986

Tornado Climatology

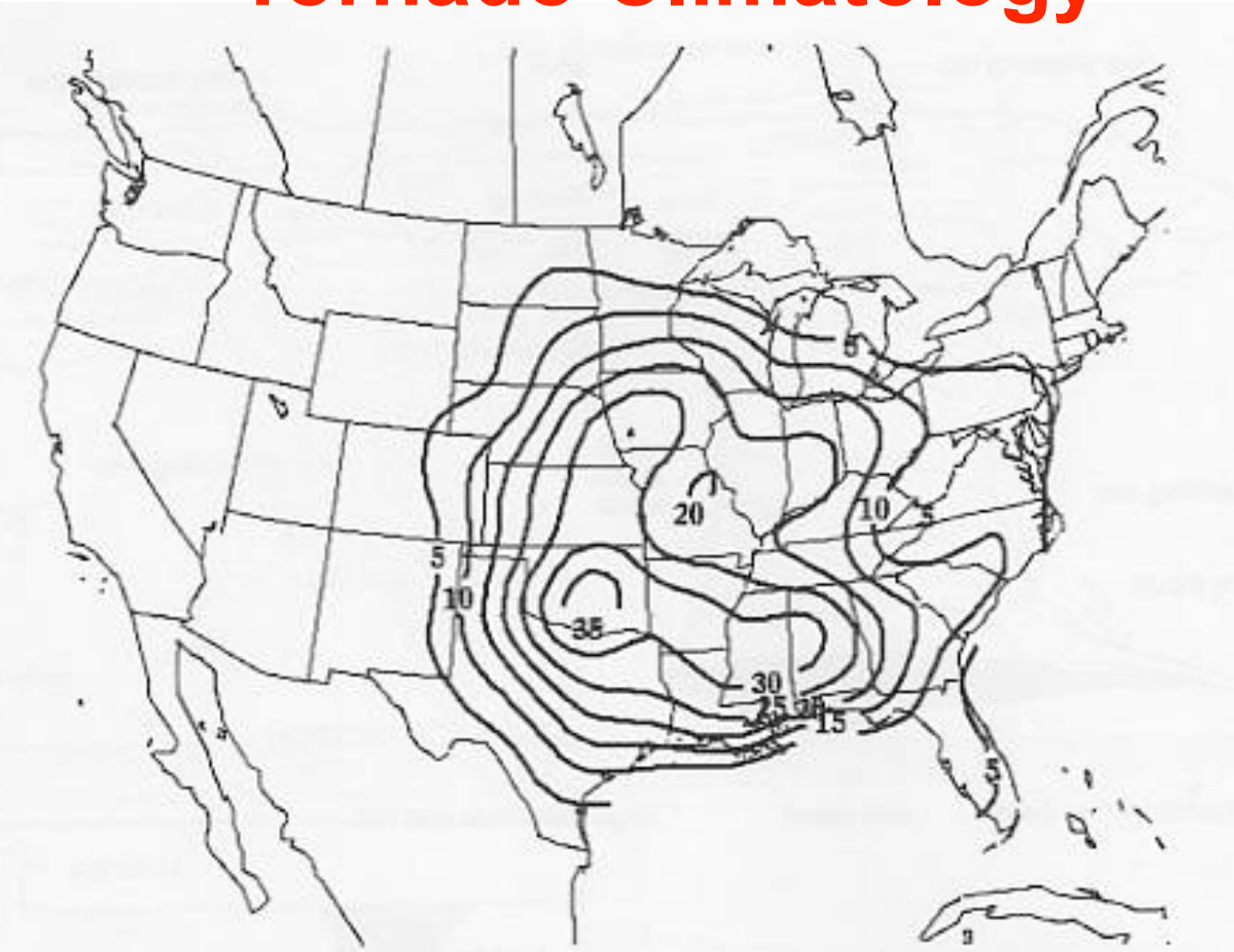

FIG. 5.5. Based on data from 1921 to 1995, the mean number of days per century of F2 intensity or greater tornado occurrence within 40km of a point in the United States (Concannon et al. 2000). Contour interval is 5 days, with minimum level equal to 5.

http://severewx.atmos.uiuc.edu/18/tornado.freq.html

Davies-Jones et al. 2001

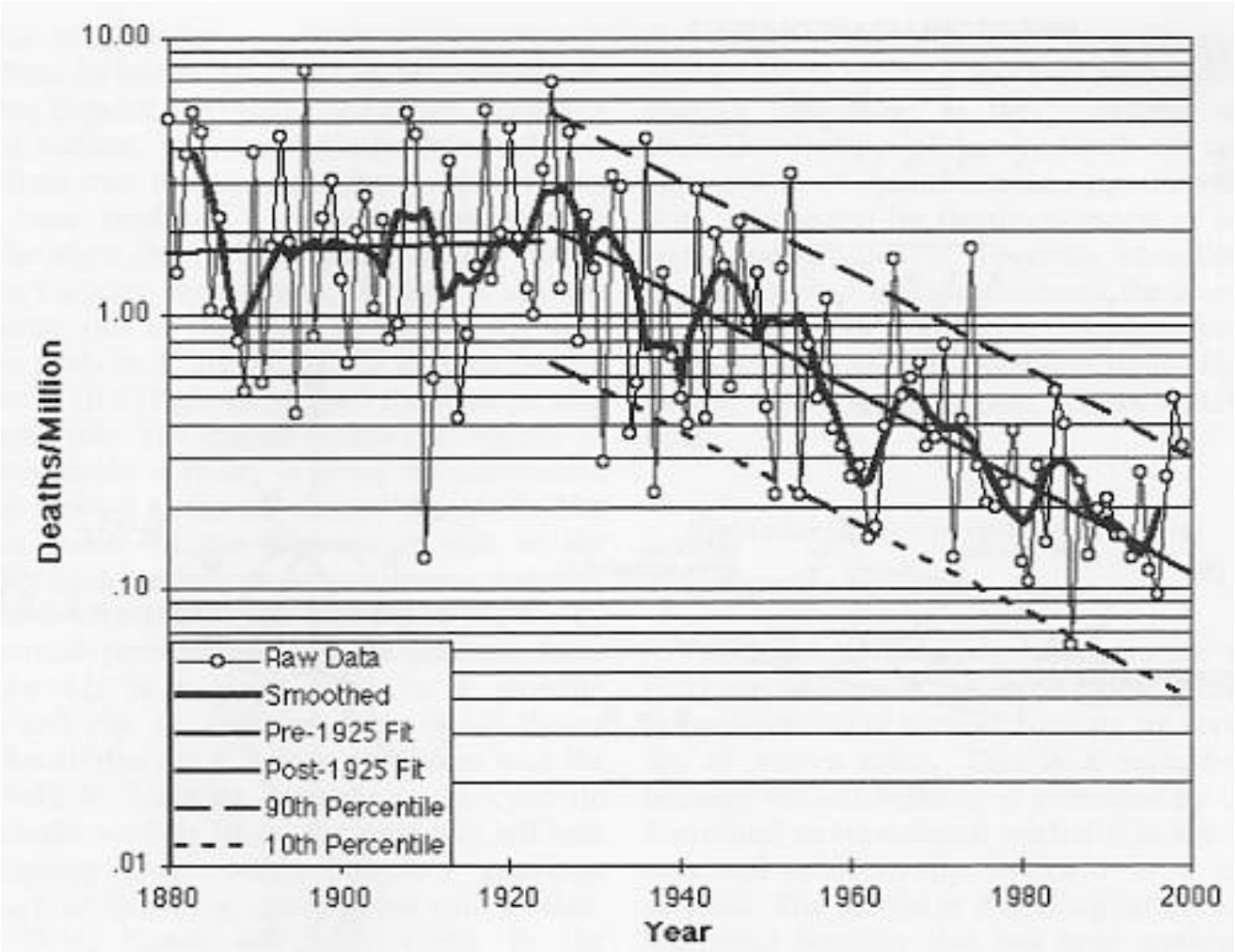

FIG. 5.6. Population-normalized annual death toll due to tornadoes in the United States (Doswell et al. 1999).

Davies-Jones et al. 2001

Doppler On Wheels (DOWs)

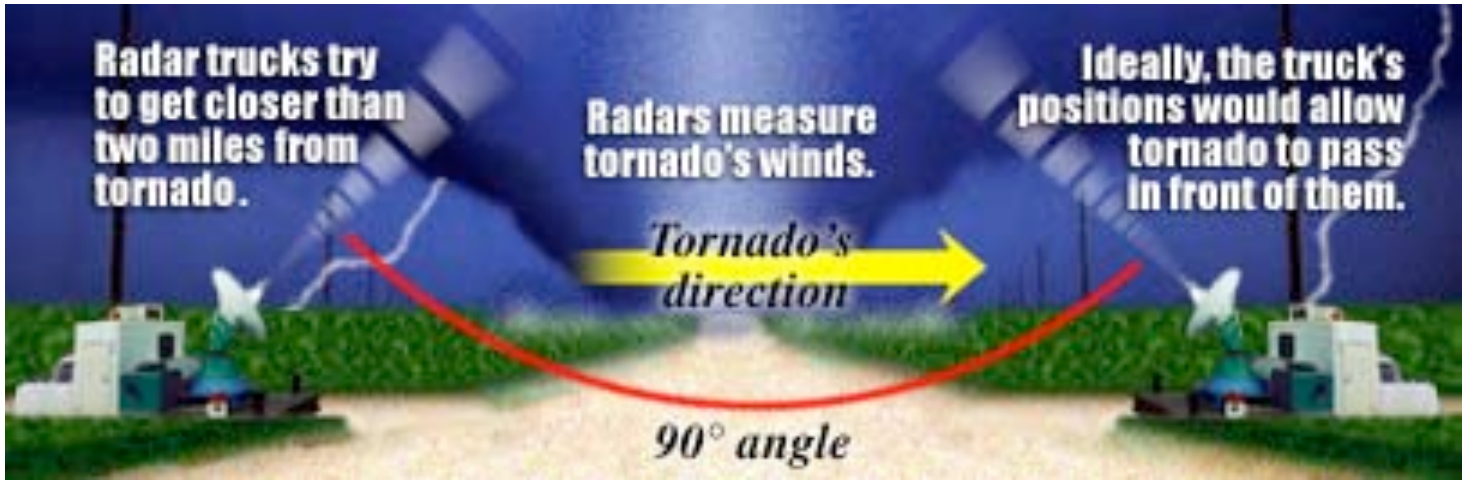

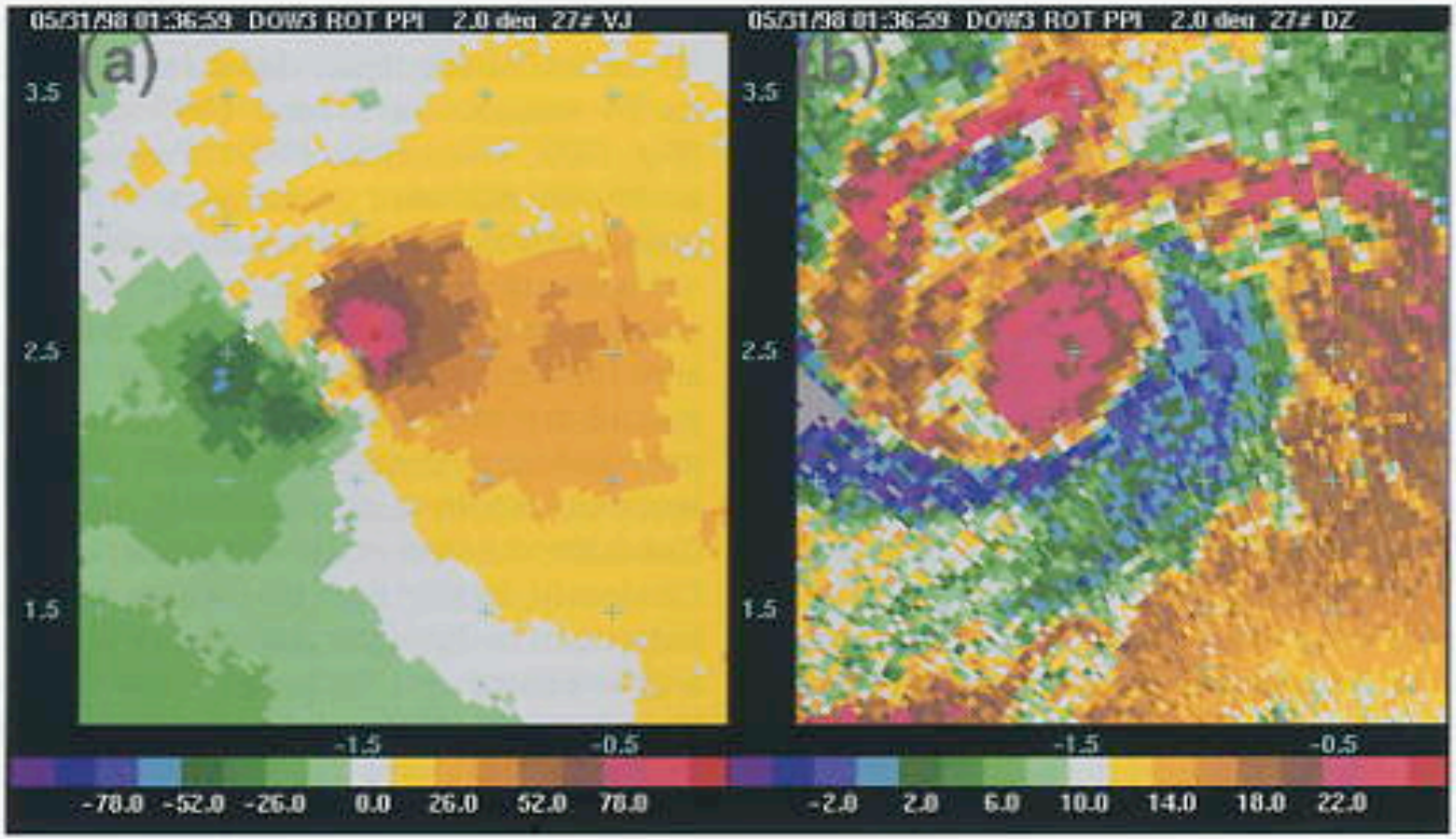

FIG. 5.27. Data collected by the Doppler on Wheels radar of an F-4 tornado near Spencer, South Dakota, on 31 May 1998. (a) Radar reflectivity factor and (b) Doppler velocity, at 0136:59 UTC. Courtesy of J. Wurman.

Davies-Jones et al. 2001

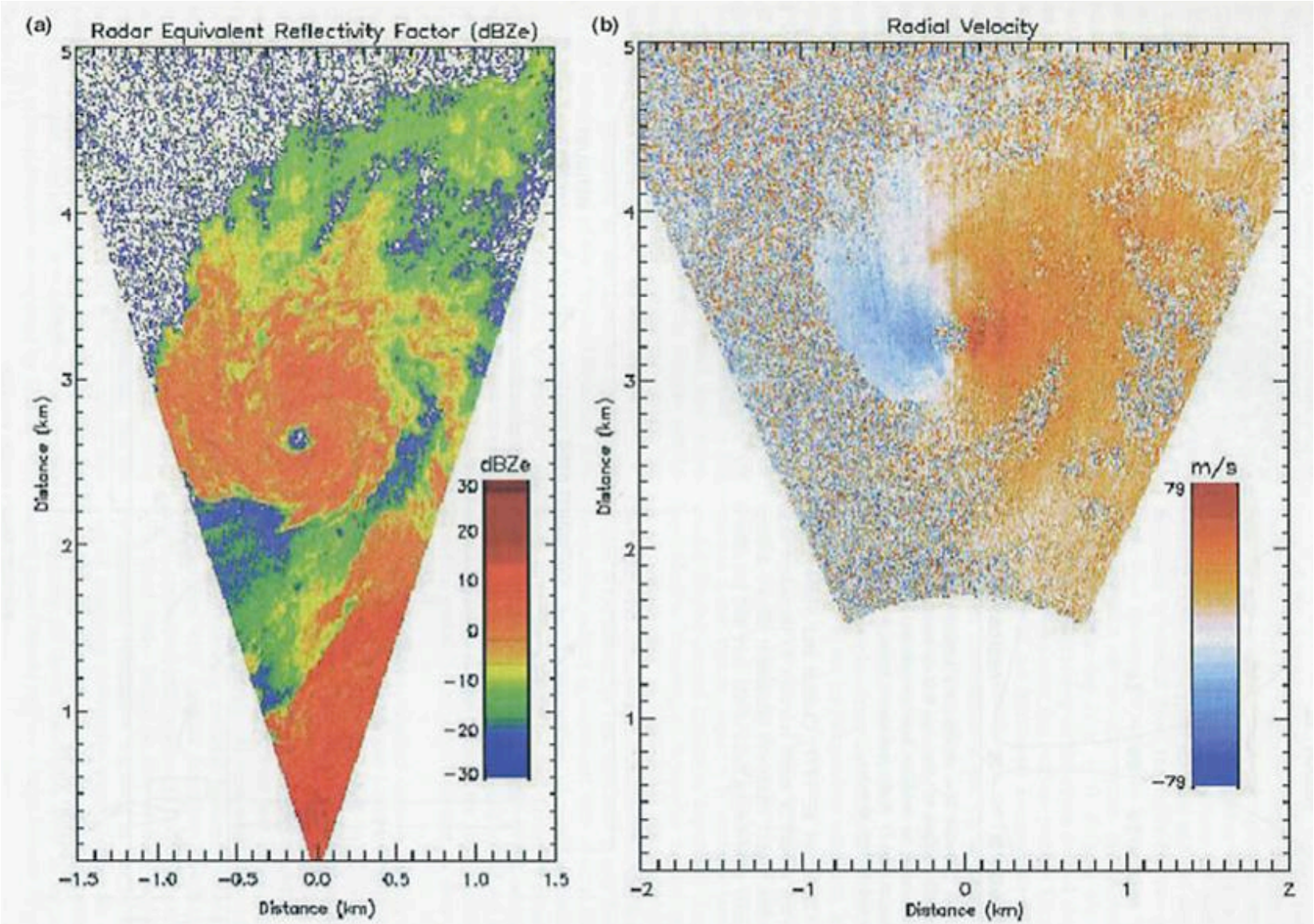

FIG. 5.23. Data collected by the University of Massachusetts, Amherst, 3-mm wavelength radar of an F-3 tornado near Verden, Oklahoma, on 3 May 1999. (a) Radar reflectivity factor, at 2254:57 UTC. (b) Doppler velocity, at 2255:53 UTC. Courtesy of A. Pazmany and H. Bluestein.

Davies-Jones et al. 2001

Non-Supercell Tornadoes

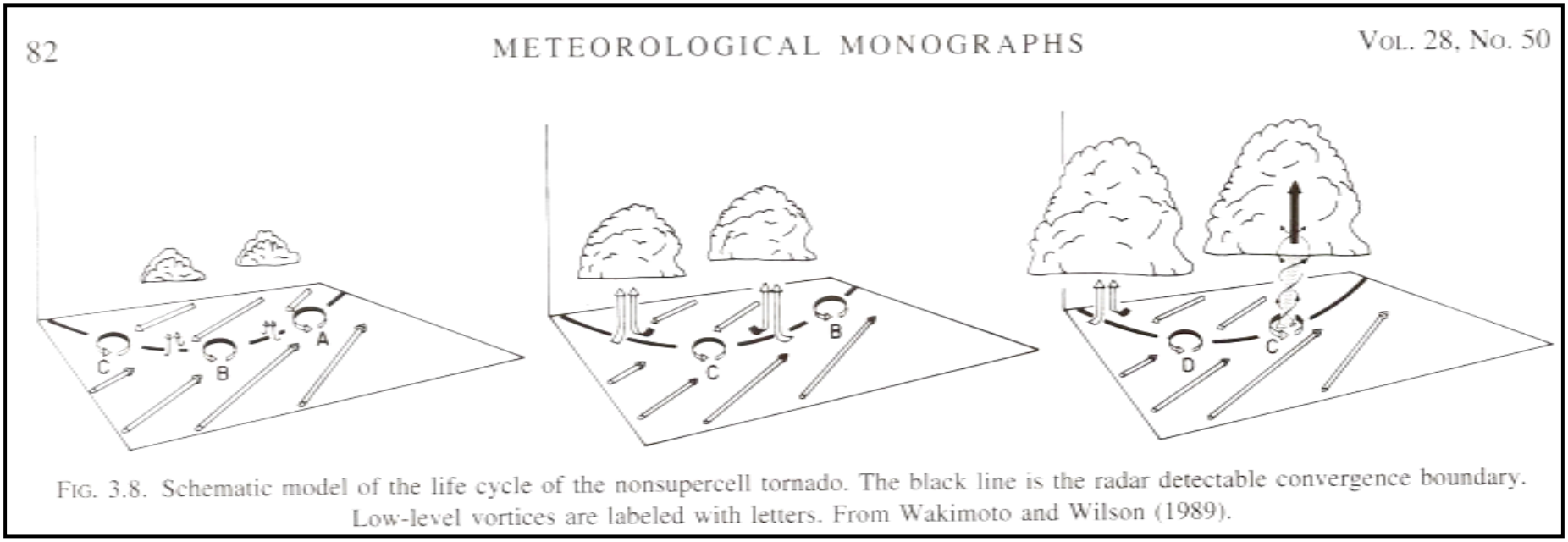

FIG. 3.8. Schematic model of the life cycle of the nonsupercell tornado. The black line is the radar detectable convergence boundary. Low-level vortices are labeled with letters. From Wakimoto and Wilson (1989).

Source: Johnson and Mapes (2001), AMS *Meteor. Monogr.,* No. 50

http://severewx.atmos.uiuc.edu/18/182-landspout/landspout-tr/landspouttr_wilhelmson-lee.mov

Hail Formation

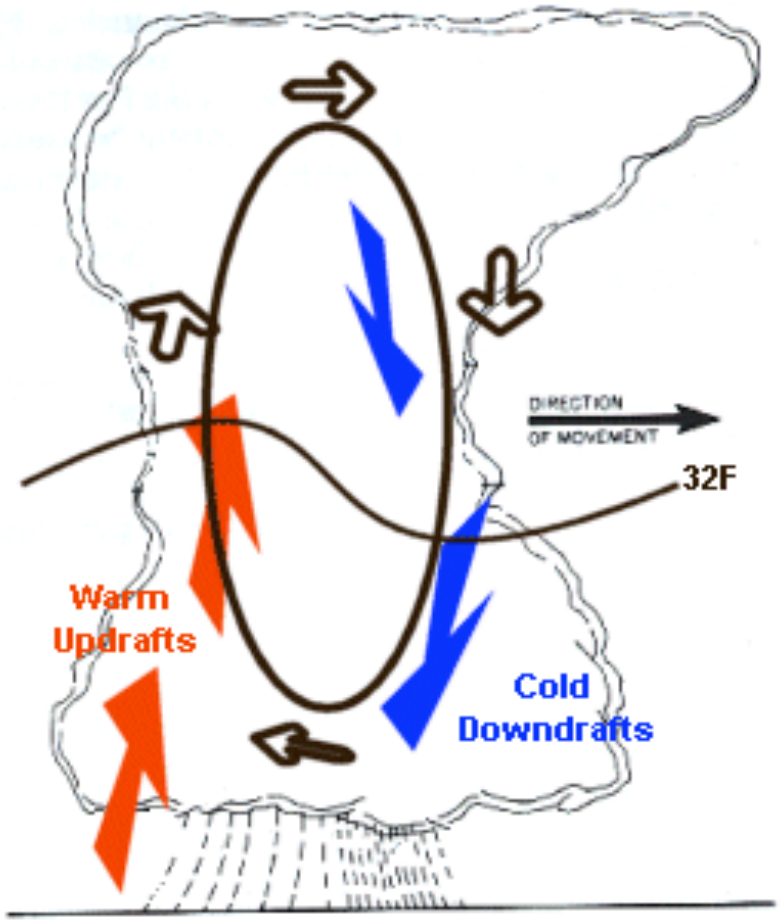

http://severewx.atmos.uiuc.edu/19/2.inch.hail.probs.html

22 June 2003
Aurora, NE

Largest hailstone ever recorded

18.75” Circumference
1.5 Lbs.

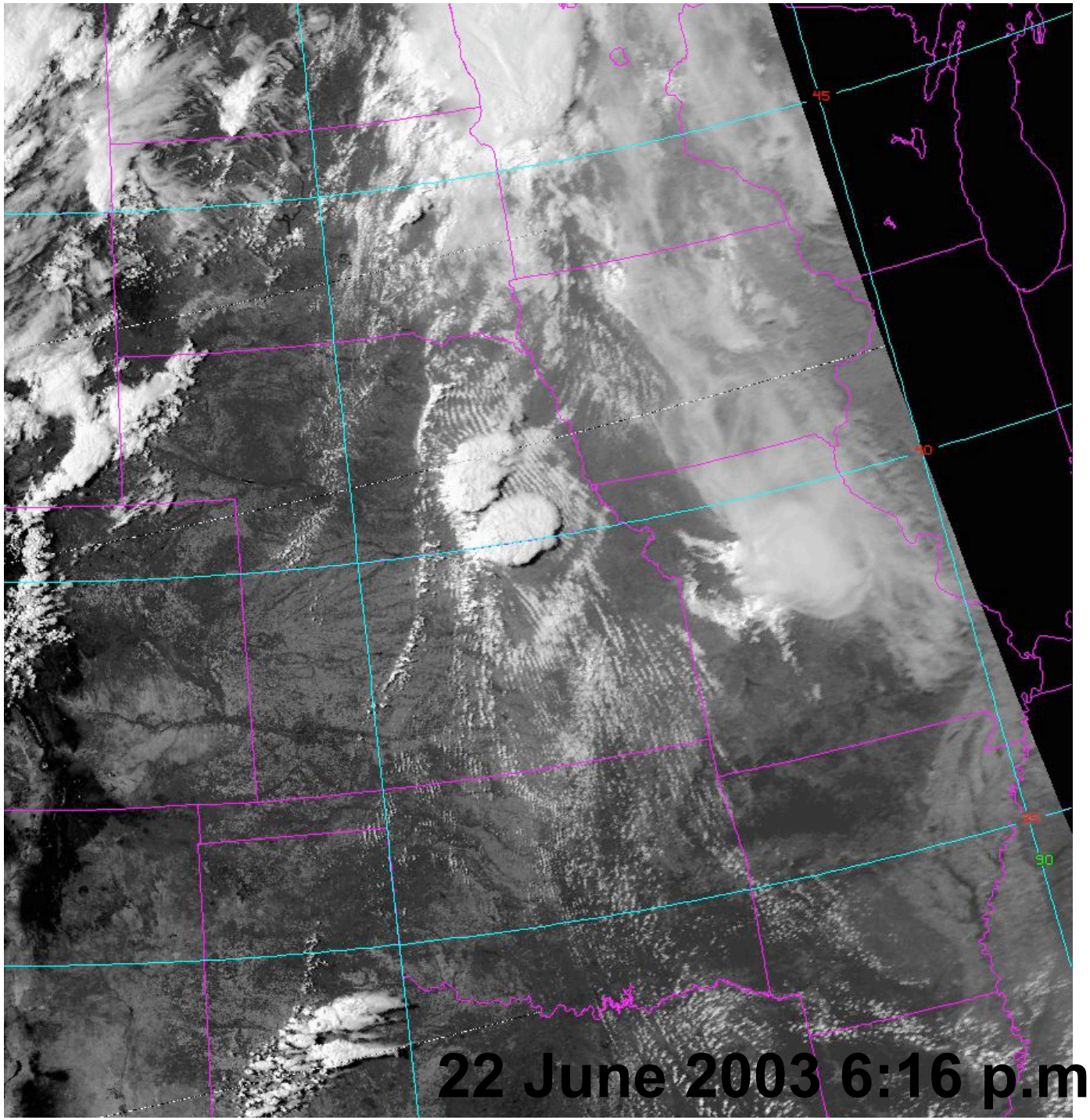
45
40
35
30
22 June 2003 6:16 p.m. CDT

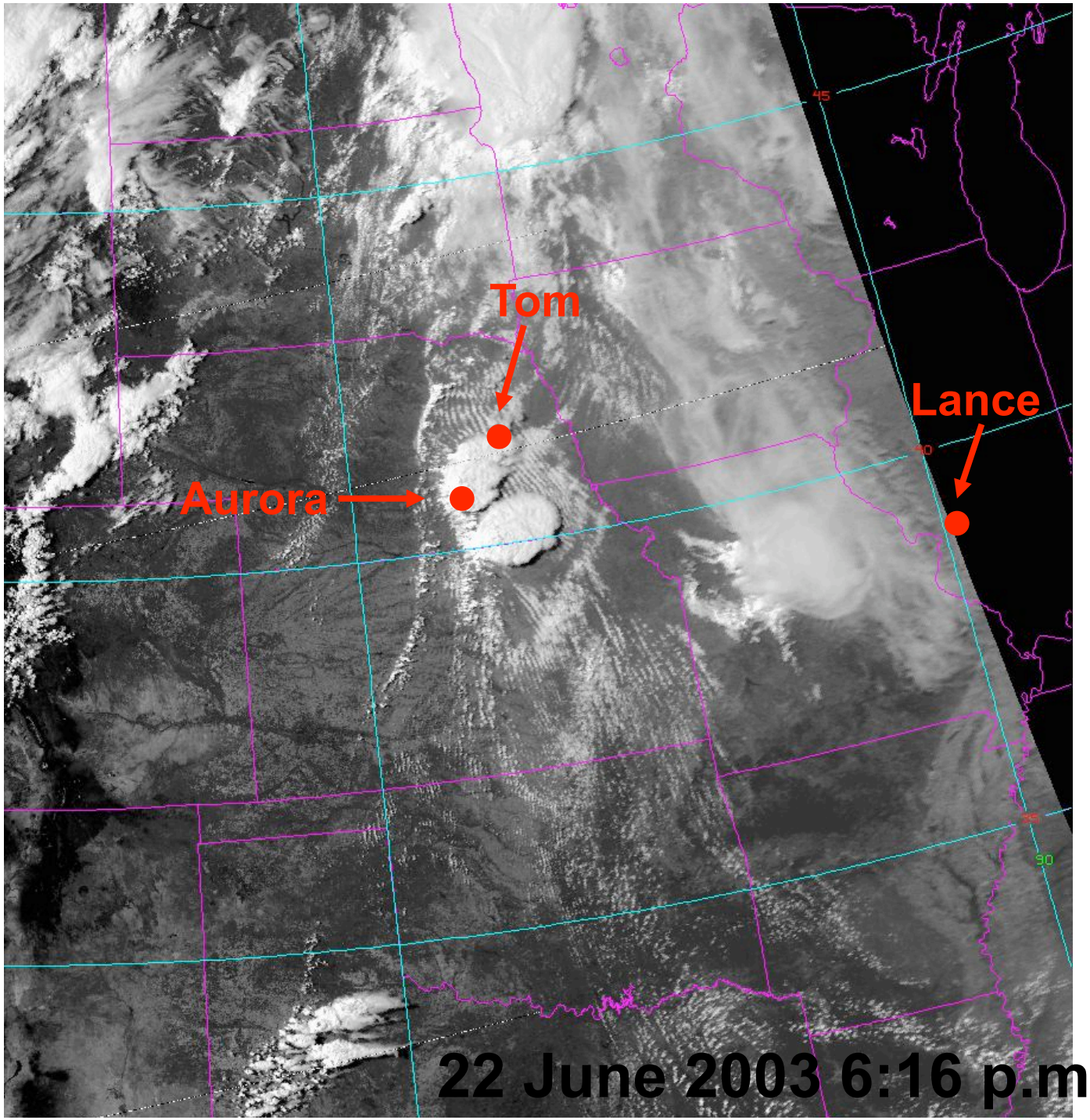
Tom
Lance
Aurora
22 June 2003 6:16 p.m. CDT

17.5” Circumference
2 Lbs.

3 September 1970
Coffeyville, KS

Heaviest hailstone ever recorded

Severe Weather Forecasting Example

18–19 October 2004

Wind Speed (knots) / MSLP (mb)

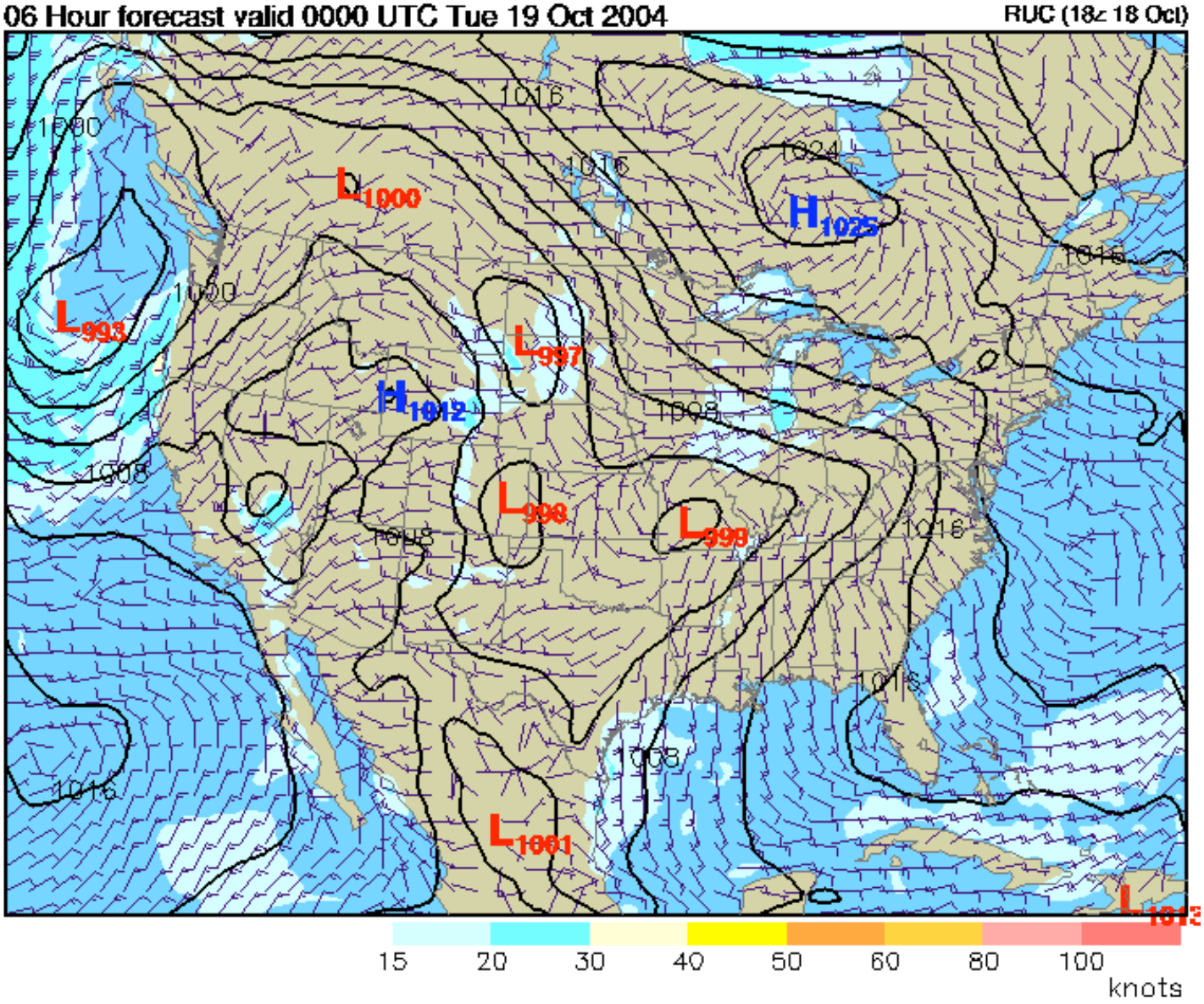

http://www.rap.ucar.edu/weather/

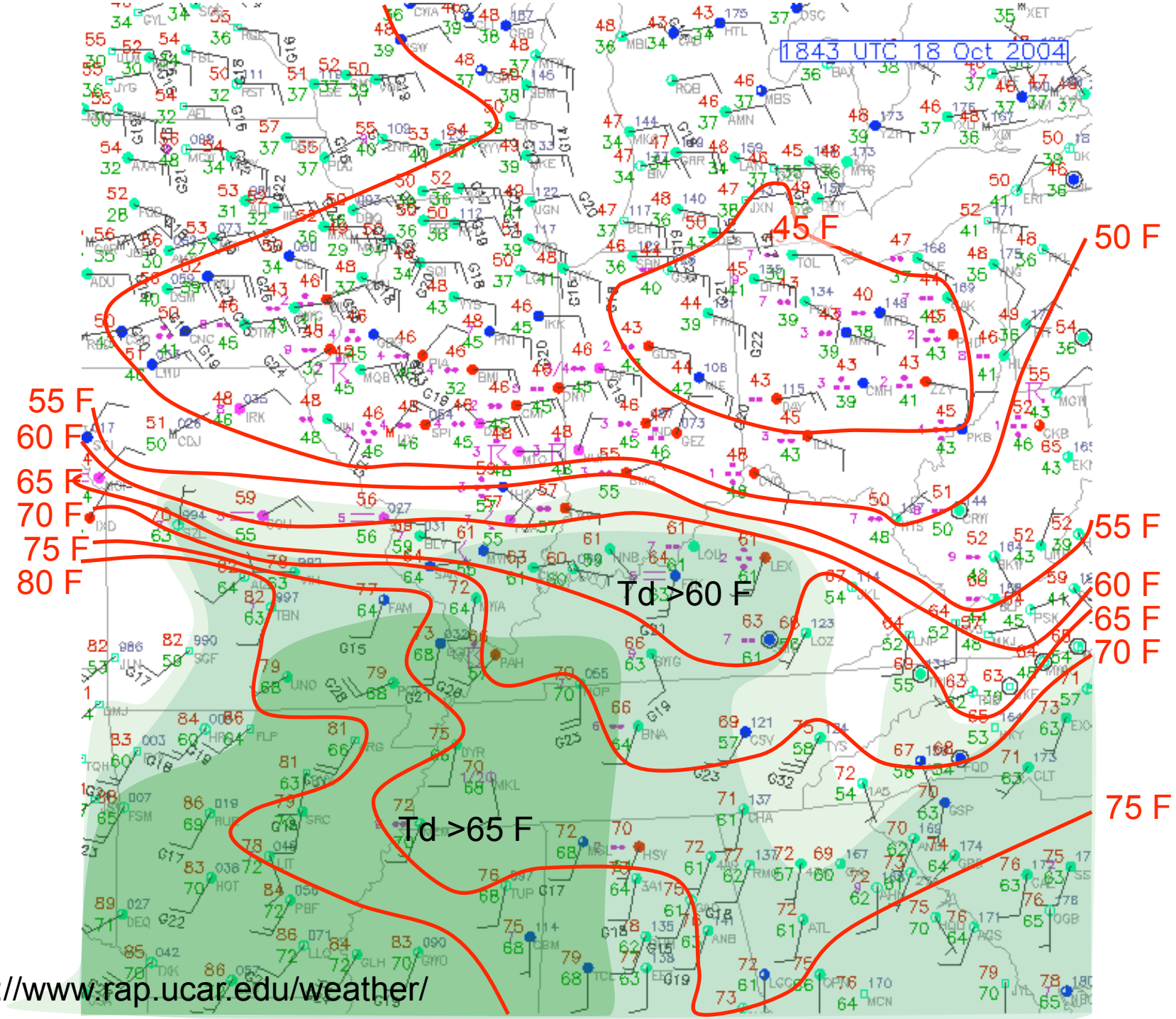
1843 UTC 18 Oct 2004
45 F
50 F
55 F
60 F
65 F
70 F
75 F
80 F
55 F
60 F
65 F
70 F
75 F
Td >60 F
Td >65 F
http://www.rap.ucar.edu/weather/

850 mb Heights (dm) / Isotachs (knots)

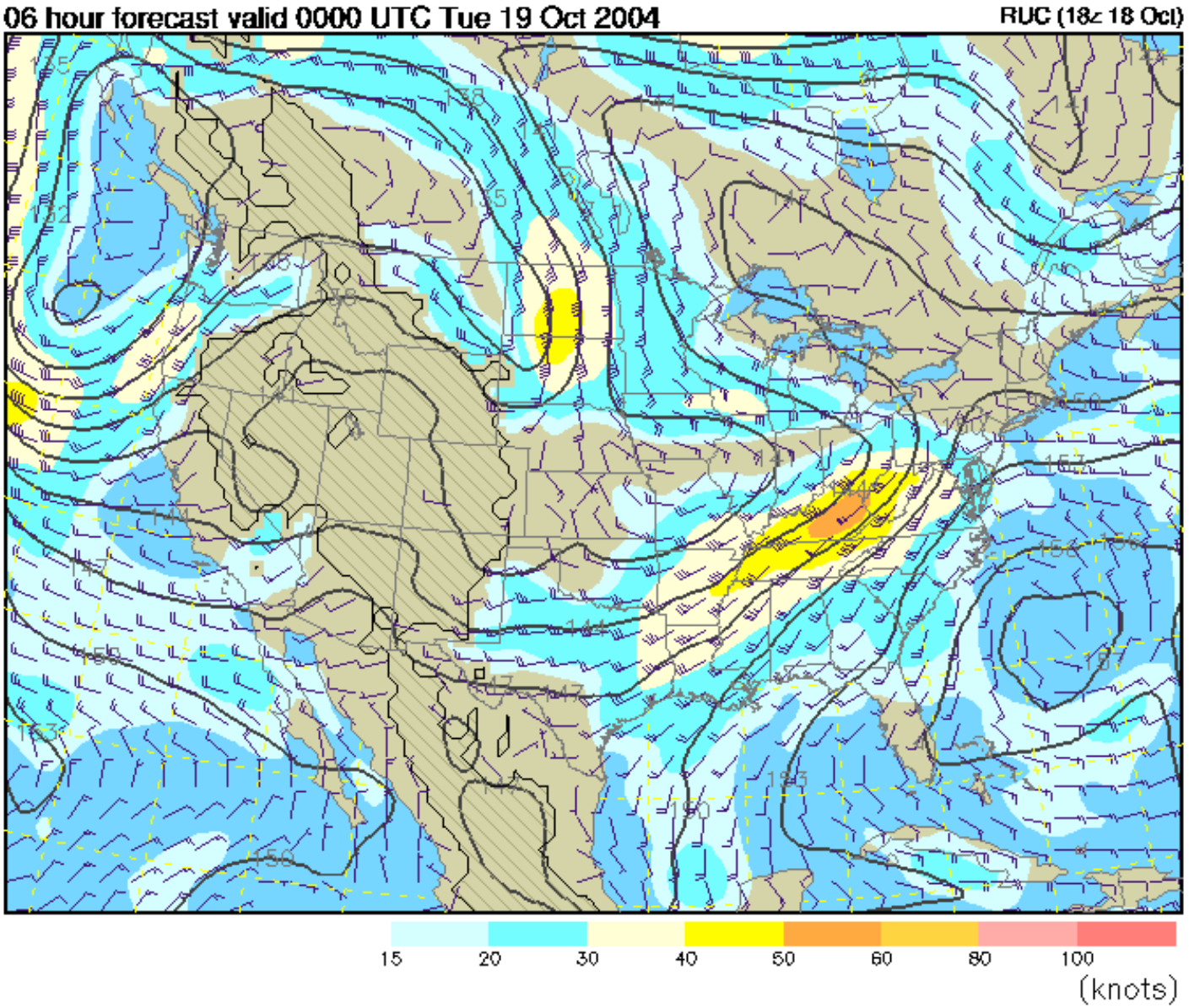

http://www.rap.ucar.edu/weather/

500 mb Heights (dm) / Isotachs (knots)

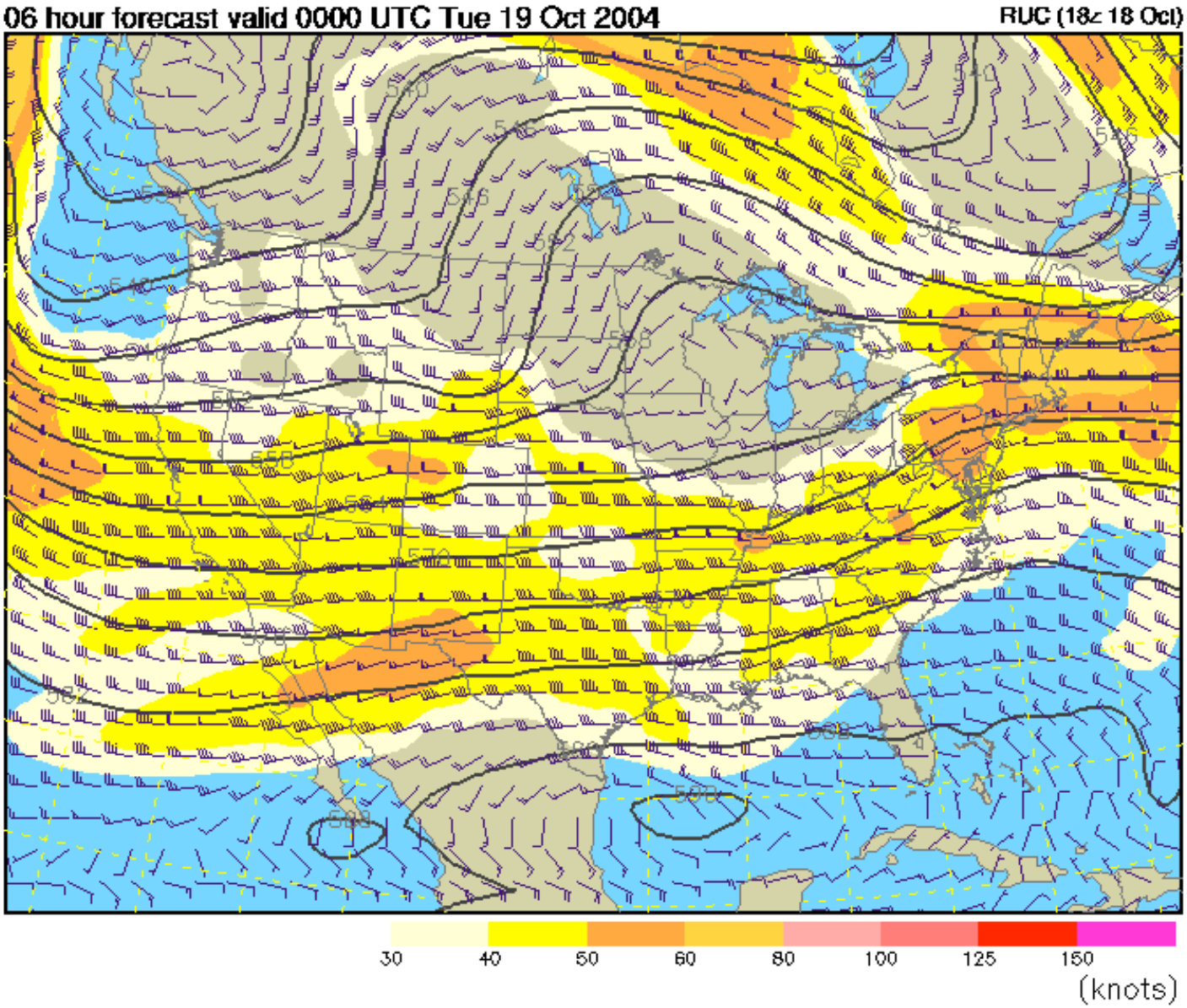

http://www.rap.ucar.edu/weather/

250 mb Heights (dm) / Isotachs (knots)

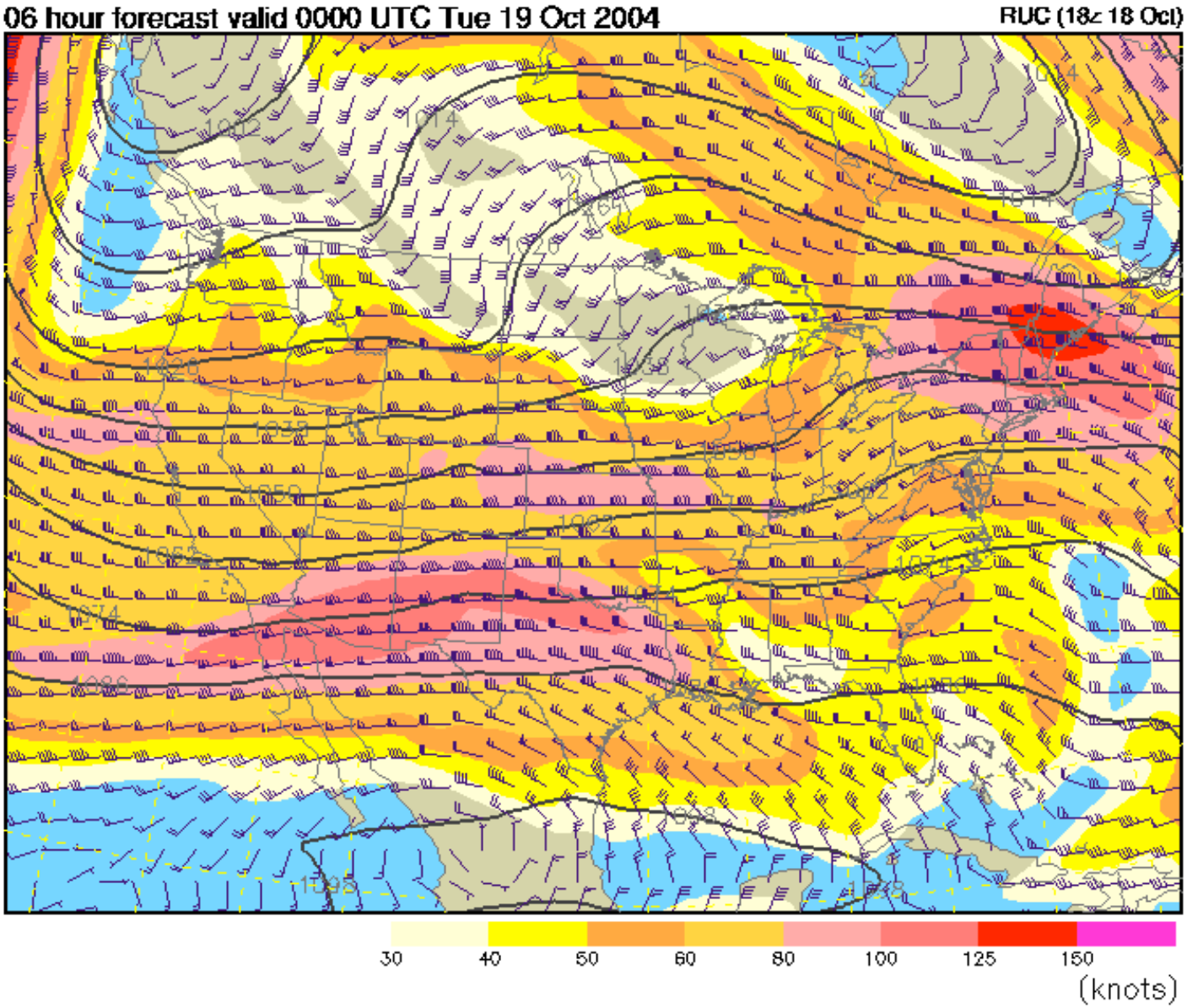

http://www.rap.ucar.edu/weather/

72340 LZK North Little Rock

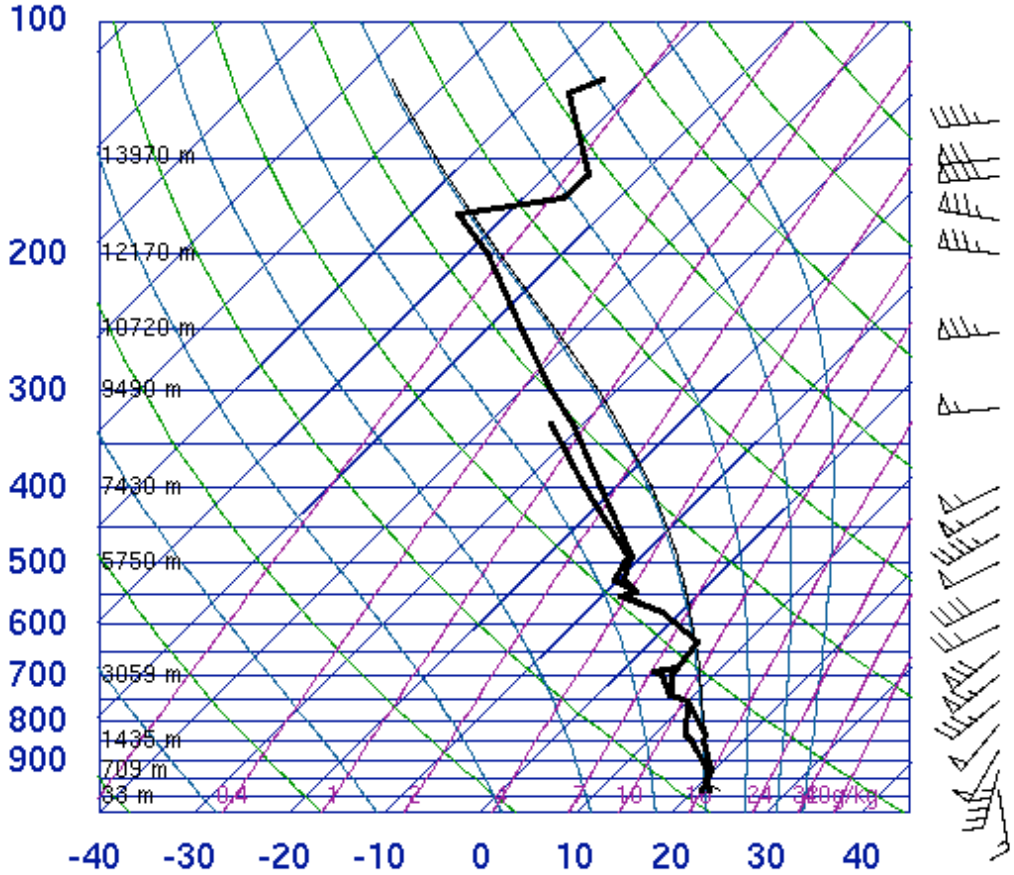

SLAT	34.73
SLON	-92.23
SELV	78.00
SHOW	-3.80
LIFT	-5.30
LFTV	-5.61
SWET	469.0
KINX	40.20
CTOT	25.30
VTOT	26.70
TOTL	52.00
CAPE	1546.
CAPV	1621.
CINS	-9.42
CINV	-7.99
EQLV	176.0
EQTV	176.0
LFCT	856.3
LFCV	872.4
BRCH	11.01
BRCV	11.53
LCLT	293.5
LCLP	956.3
MLTH	297.2
MLMR	16.00
THCK	5717.
PWAT	51.97

72340 LZK North Little Rock

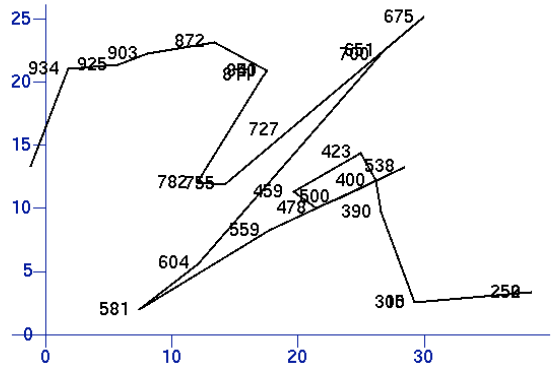

12Z 18 Oct 2004 University of Wyoming

12Z 18 Oct 2004 University of Wyoming

72340 LZK North Little Rock

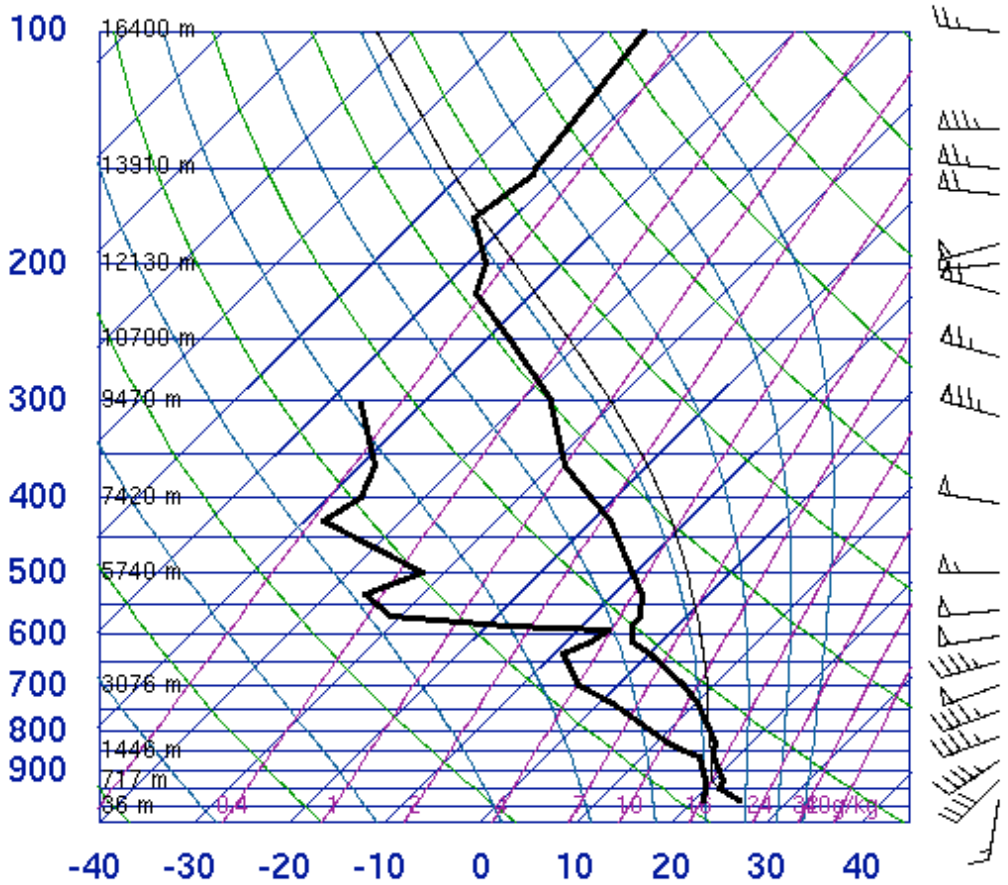

SLAT	34.73
SLON	-92.23
SELV	78.00
SHOW	-3.13
LIFT	-5.83
LFTV	-6.65
SWET	447.1
KINX	30.10
CTOT	24.10
VTOT	27.30
TOTL	51.40
CAPE	2377.
CAPV	2583.
CINS	-27.8
CINV	-16.9
EQLV	171.9
EQTV	171.9
LFCT	797.3
LFCV	855.6
BRCH	18.13
BRCV	19.70
LCLT	293.0
LCLP	929.2
MLTH	299.2
MLMR	16.02
THCK	5704.
PWAT	37.01

72340 LZK North Little Rock

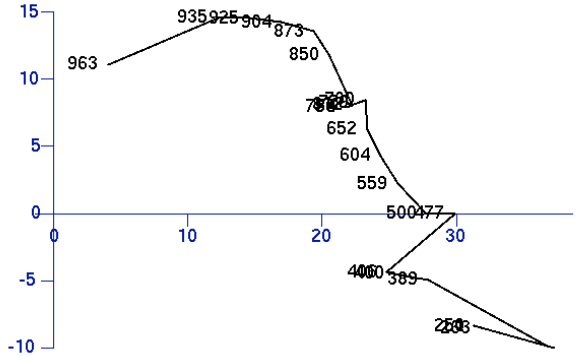

18Z 18 Oct 2004

University of Wyoming

18Z 18 Oct 2004

University of Wyoming

72340 LZK North Little Rock

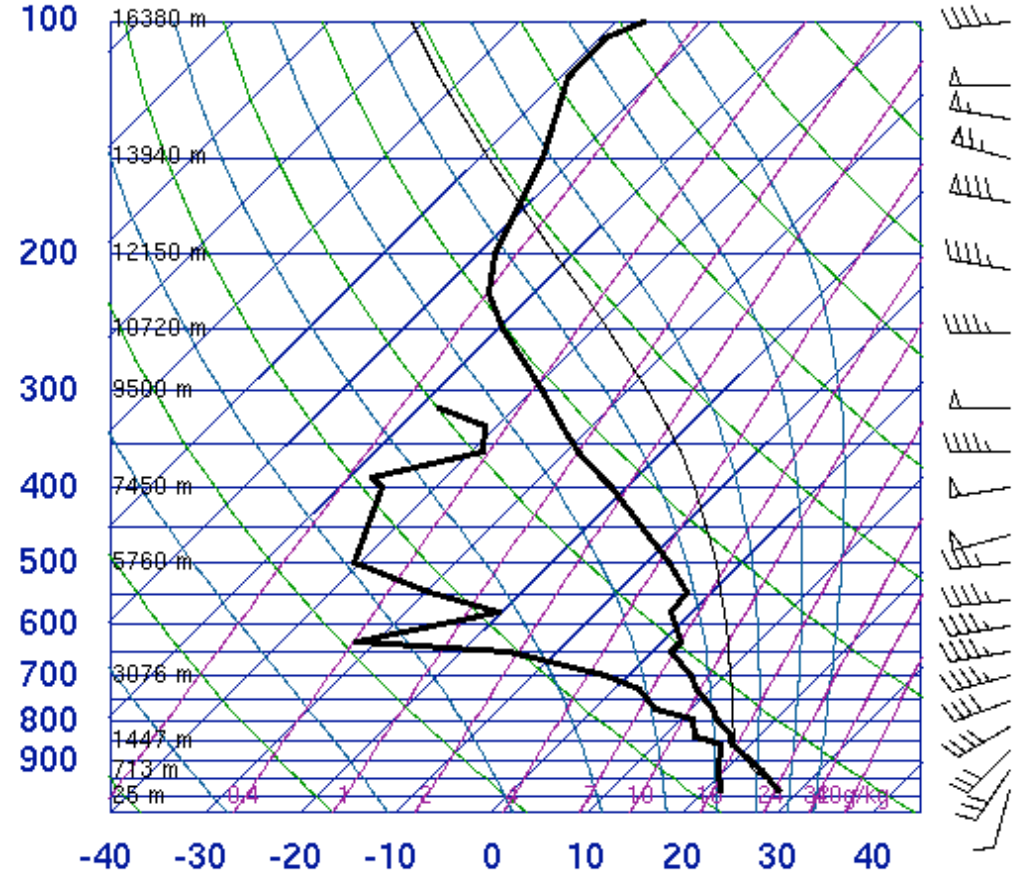

SLAT	34.73
SLON	-92.23
SELV	78.00
SHOW	-2.37
LIFT	-4.87
LFTV	-5.87
SWET	388.8
KINX	31.70
CTOT	23.10
VTOT	25.10
TOTL	48.20
CAPE	3220.
CAPV	3479.
CINS	-20.5
CINV	-15.7
EQLV	172.4
EQTV	172.4
LFCT	861.1
LFCV	866.3
BRCH	38.04
BRCV	41.09
LCLT	292.5
LCLP	886.9
MLTH	302.7
MLMR	16.30
THCK	5735.
PWAT	37.39

72340 LZK North Little Rock

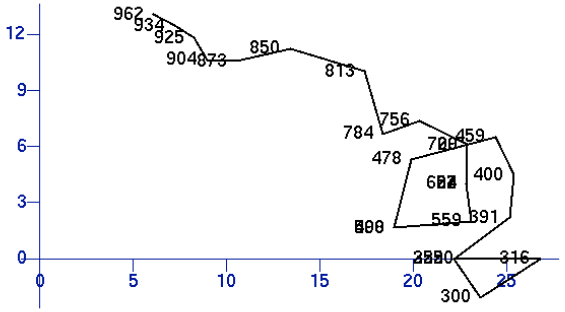

00Z 19 Oct 2004

University of Wyoming

00Z 19 Oct 2004

University of Wyoming

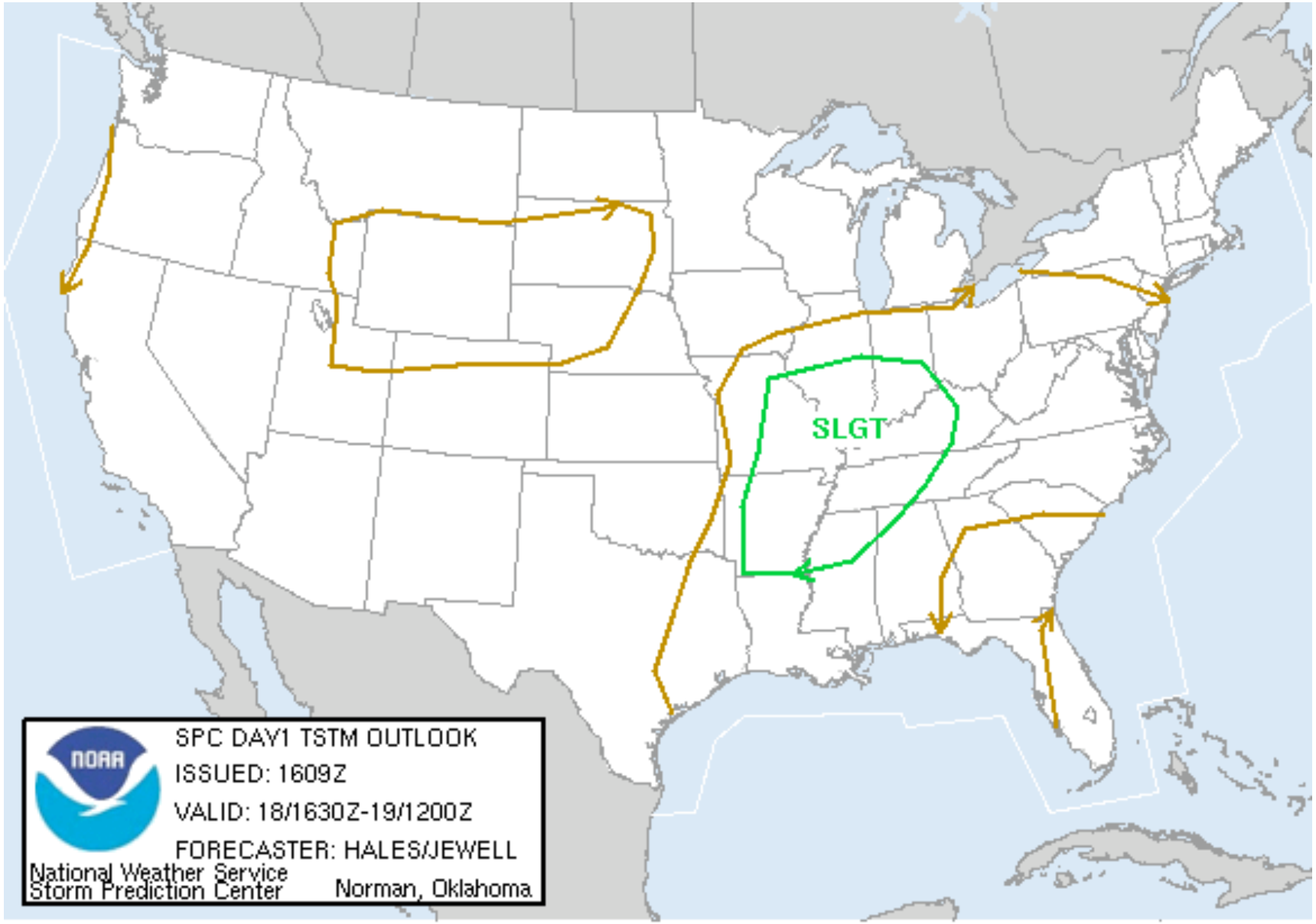

http://www.spc.noaa.gov

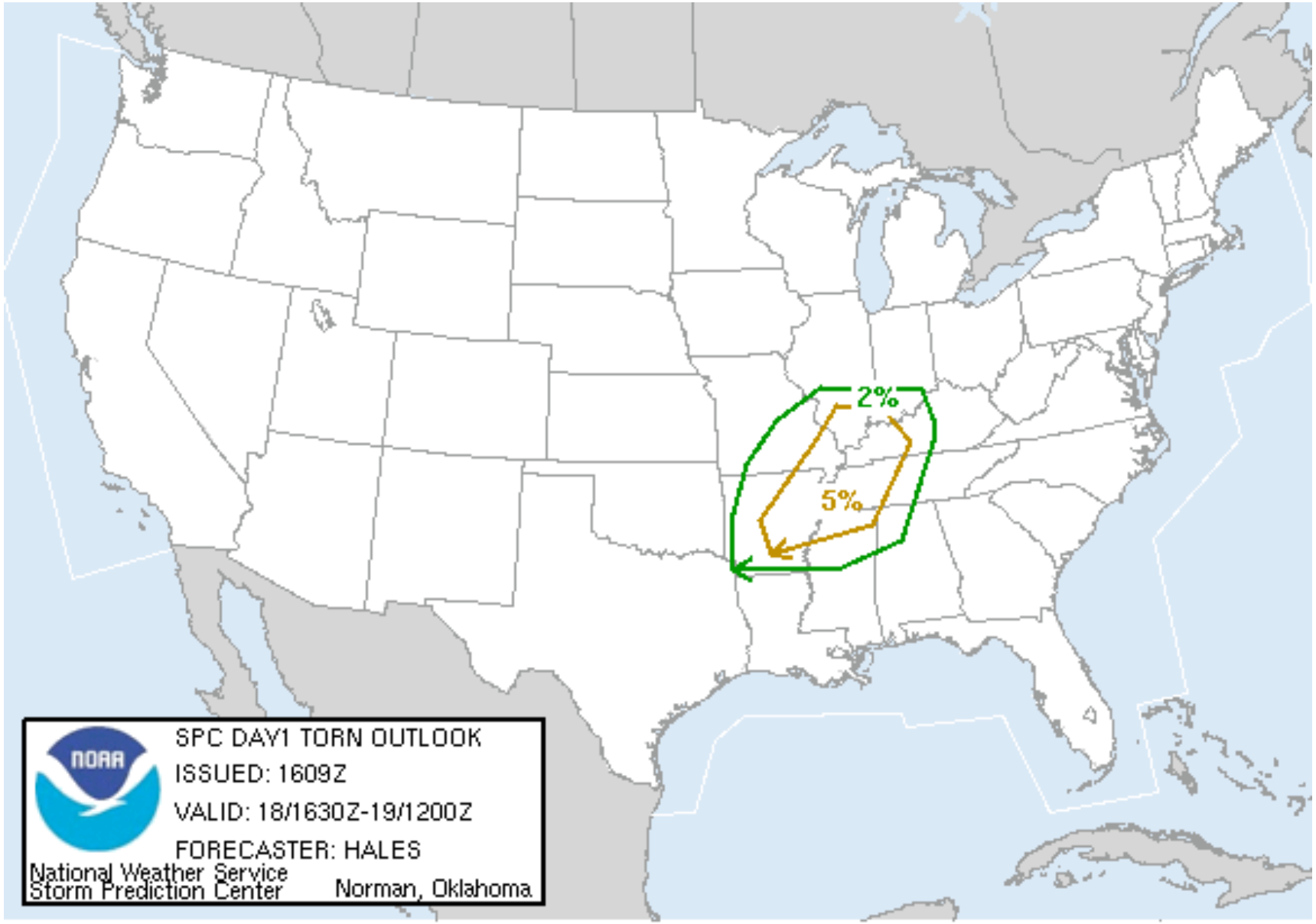

http://www.spc.noaa.gov

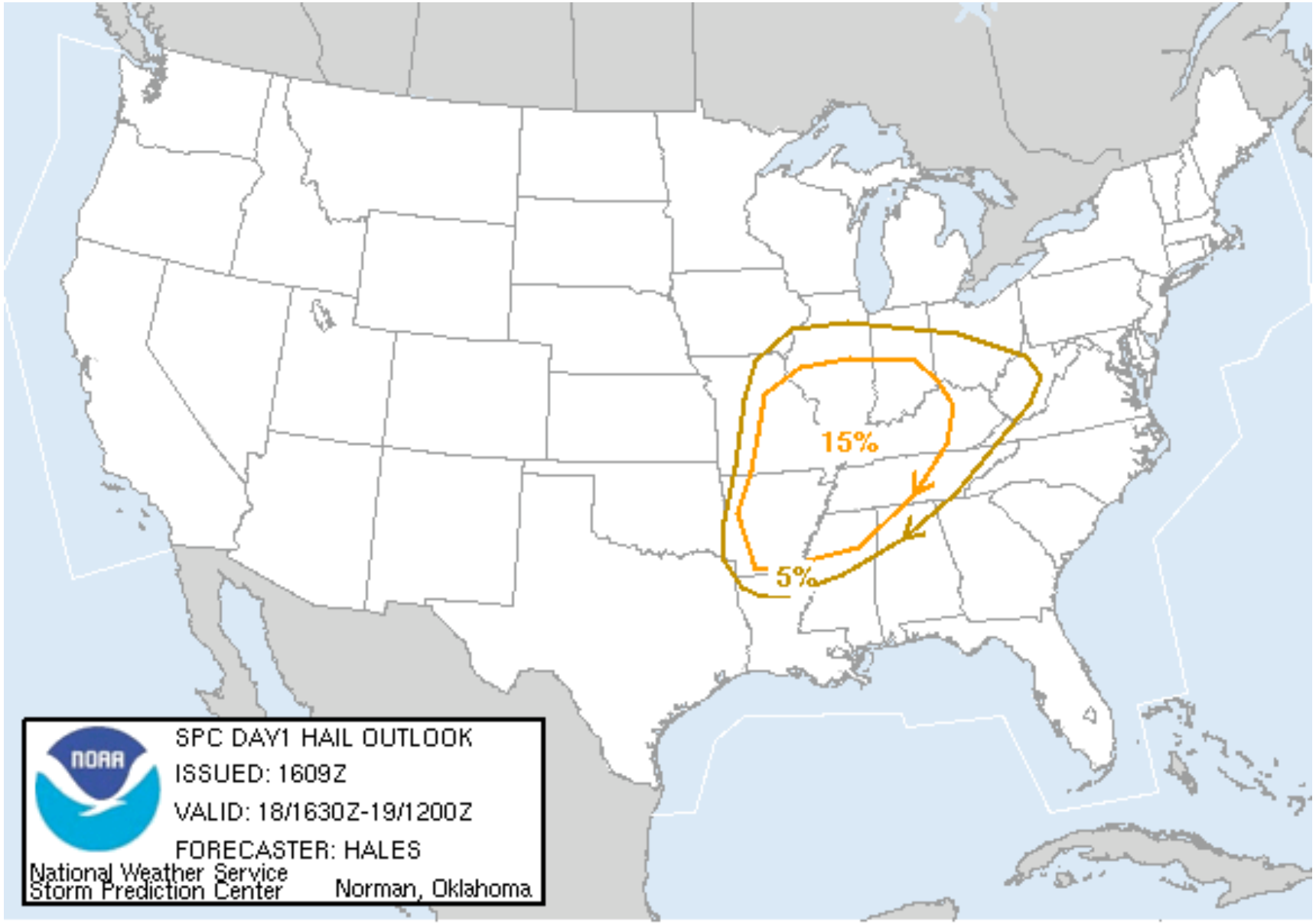

http://www.spc.noaa.gov

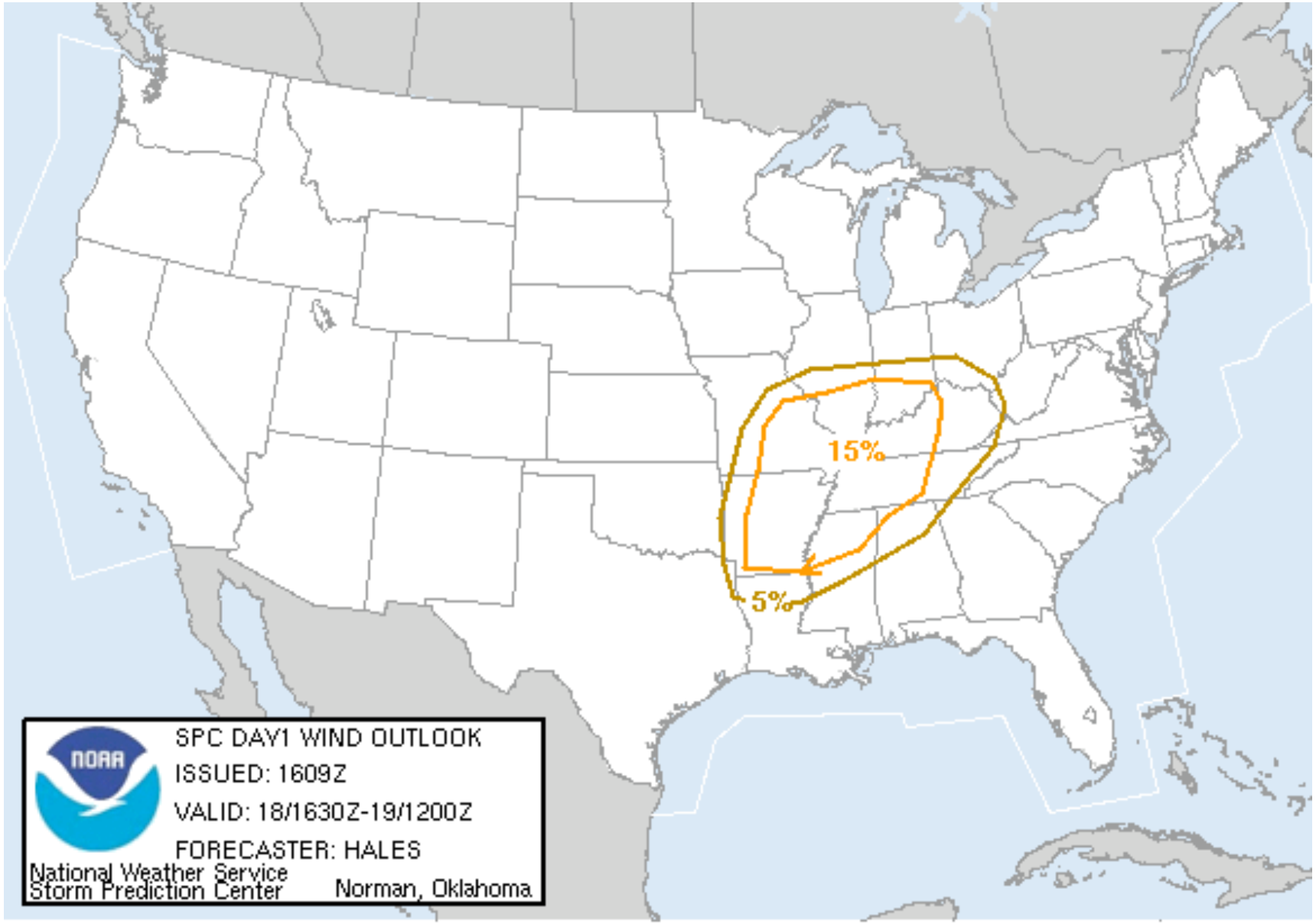

http://www.spc.noaa.gov

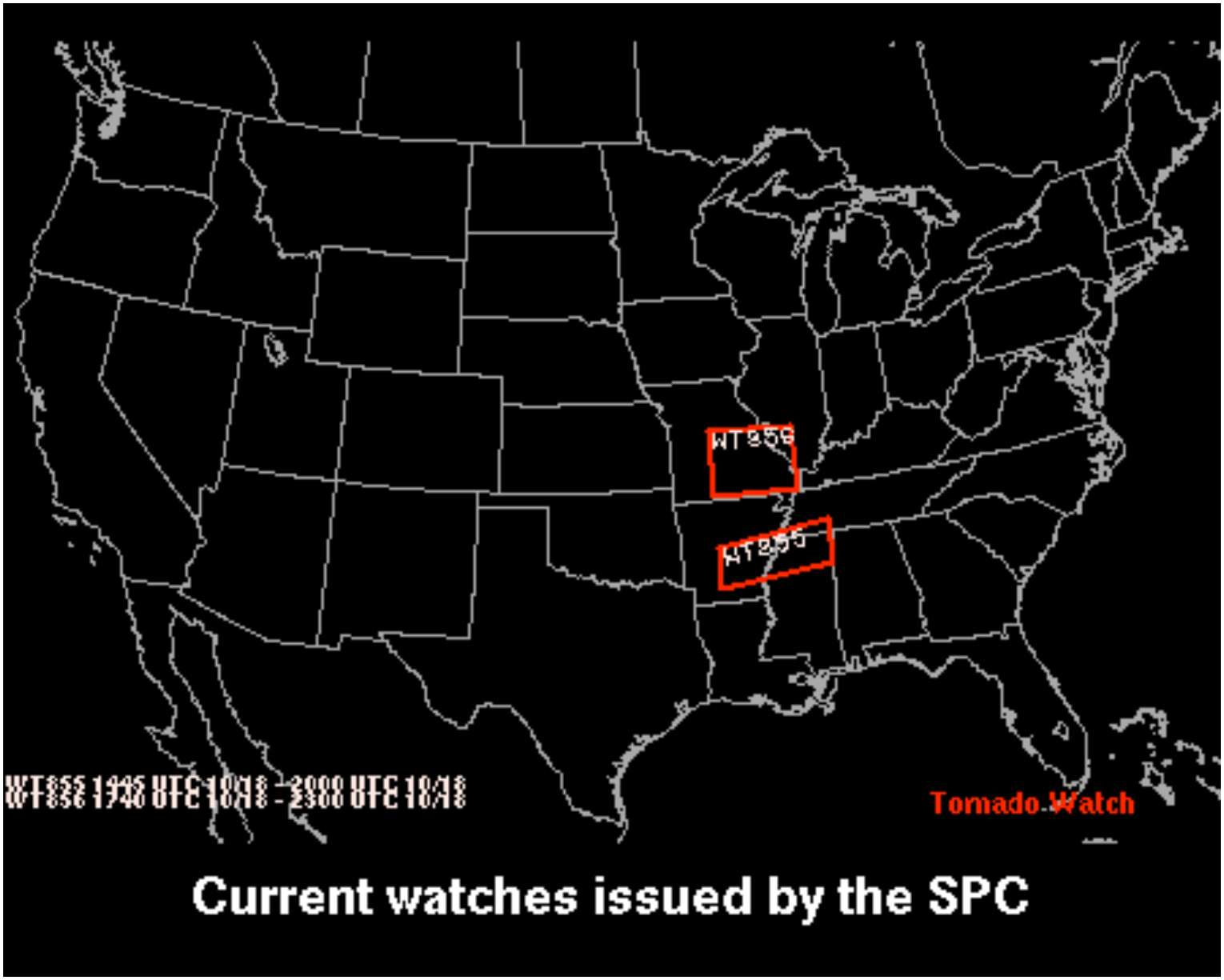

http://www.spc.noaa.gov

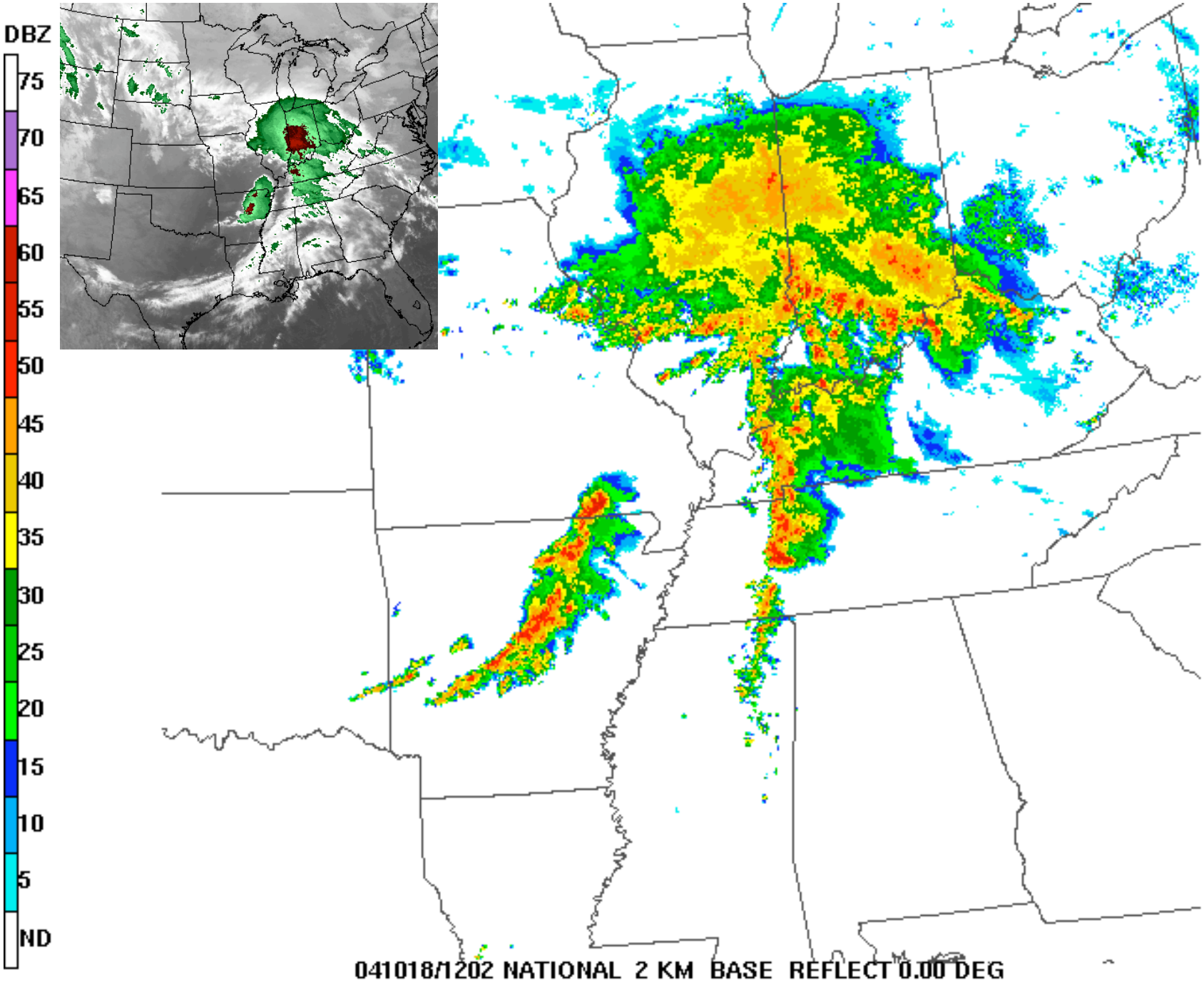
DBZ
75
70
65
60
55
50
45
40
35
30
25
20
15
10
5
ND
041018/1202 NATIONAL 2 KM BASE REFLECT 0.00 DEG

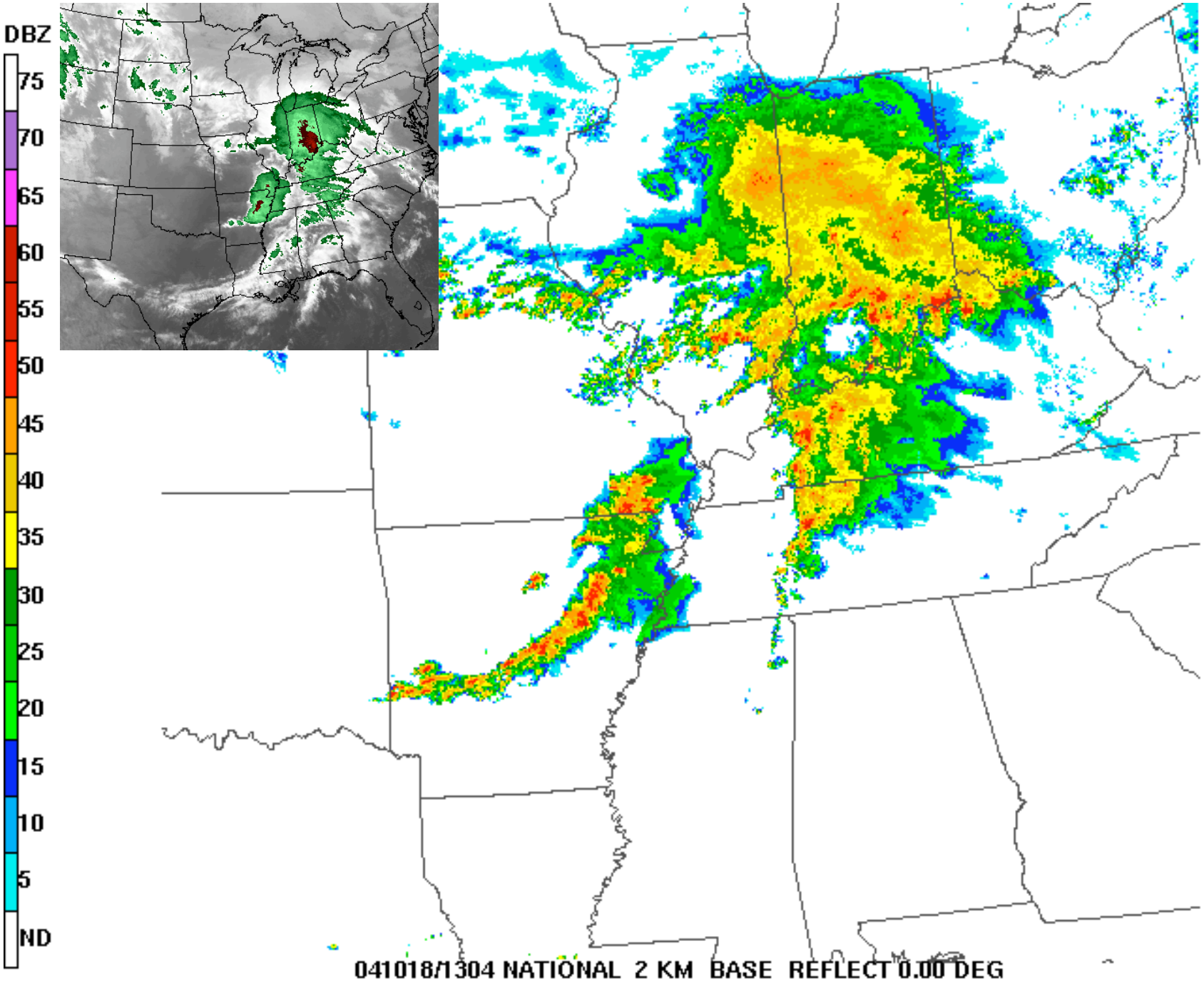
DBZ
75
70
65
60
55
50
45
40
35
30
25
20
15
10
5
ND
041018/1304 NATIONAL 2 KM BASE REFLECT 0.00 DEG

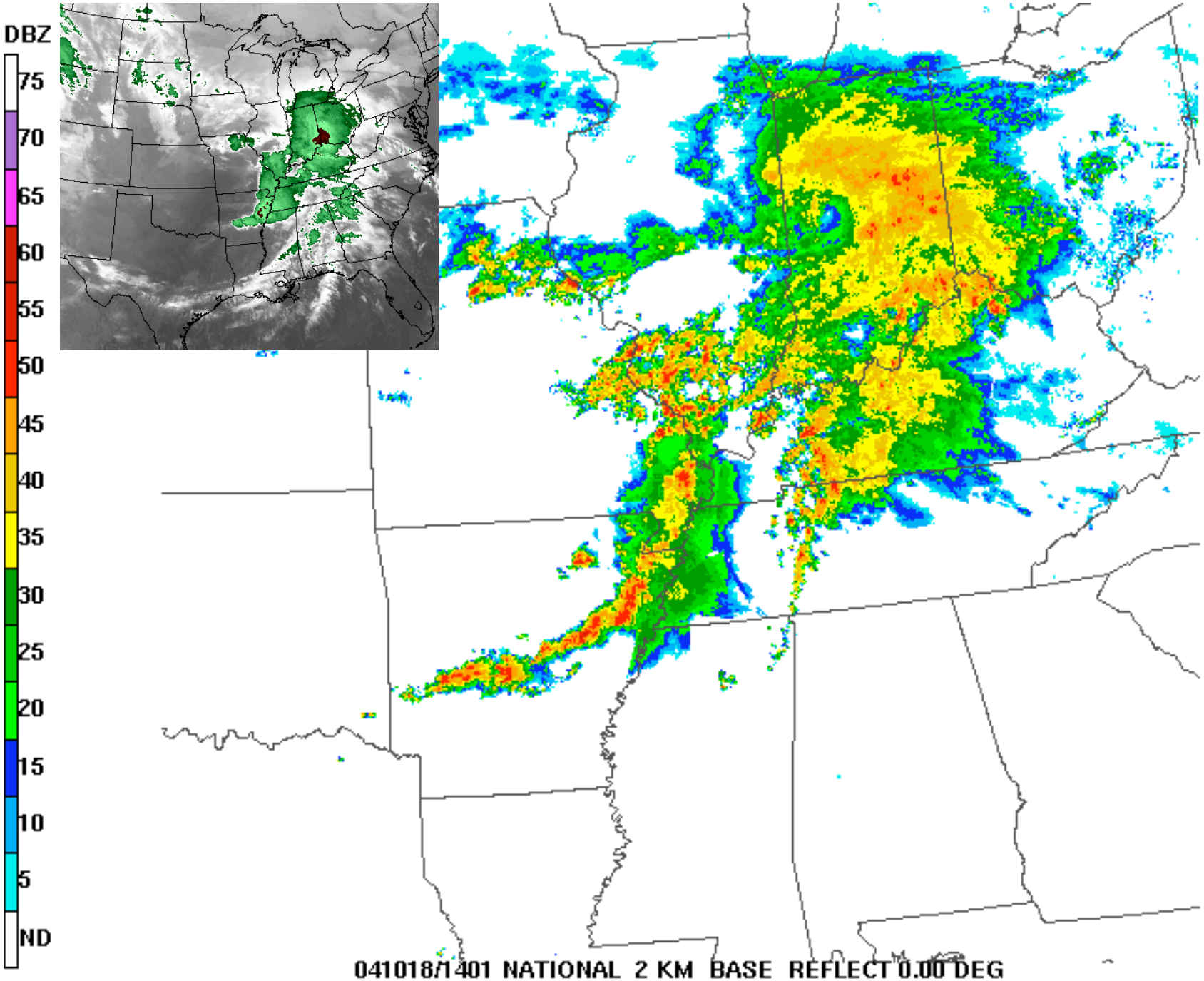
DBZ
75
70
65
60
55
50
45
40
35
30
25
20
15
10
5
ND
041018/1401 NATIONAL 2 KM BASE REFLECT 0.00 DEG

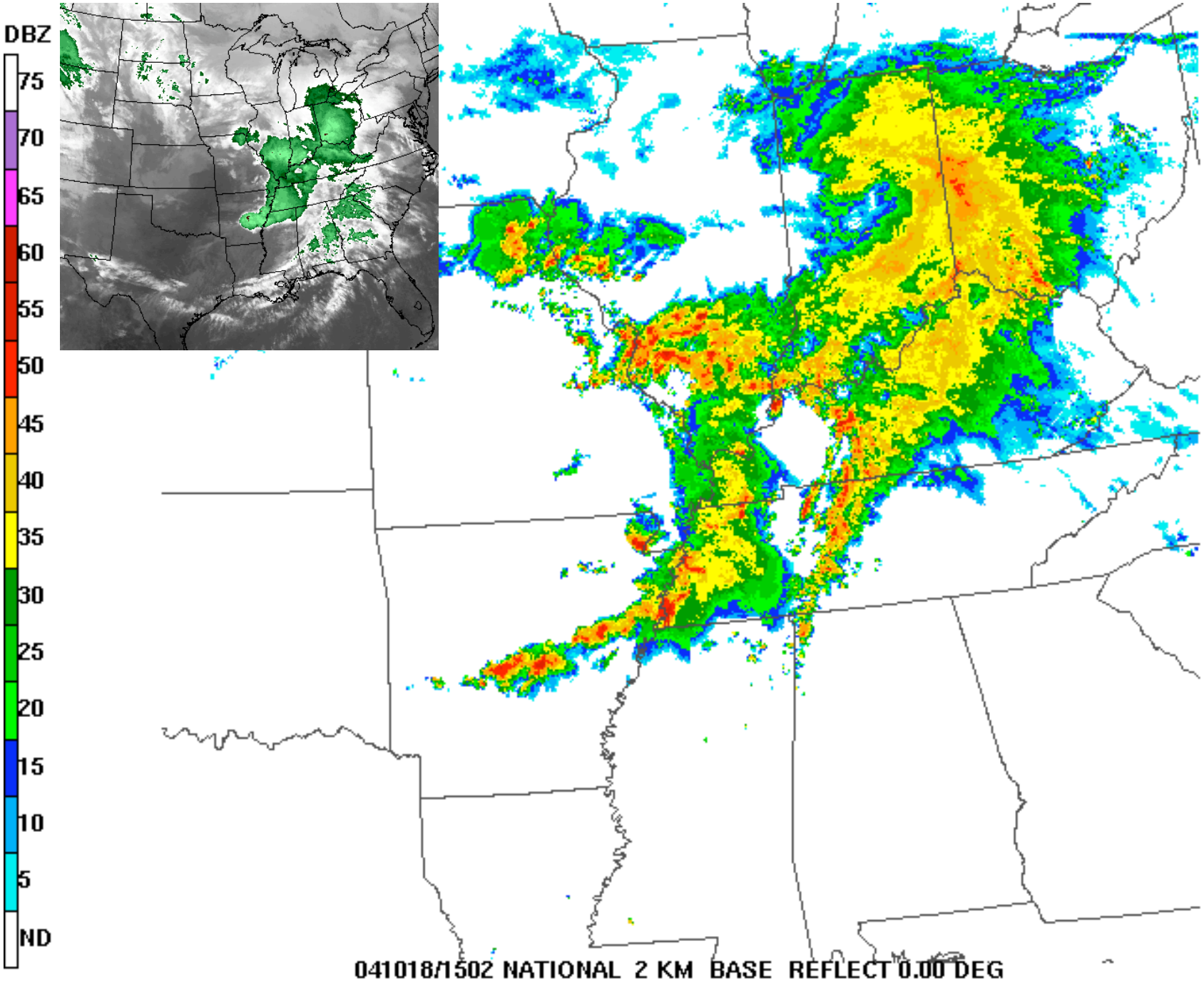
DBZ
75
70
65
60
55
50
45
40
35
30
25
20
15
10
5
ND
041018/1502 NATIONAL 2 KM BASE REFLECT 0.00 DEG

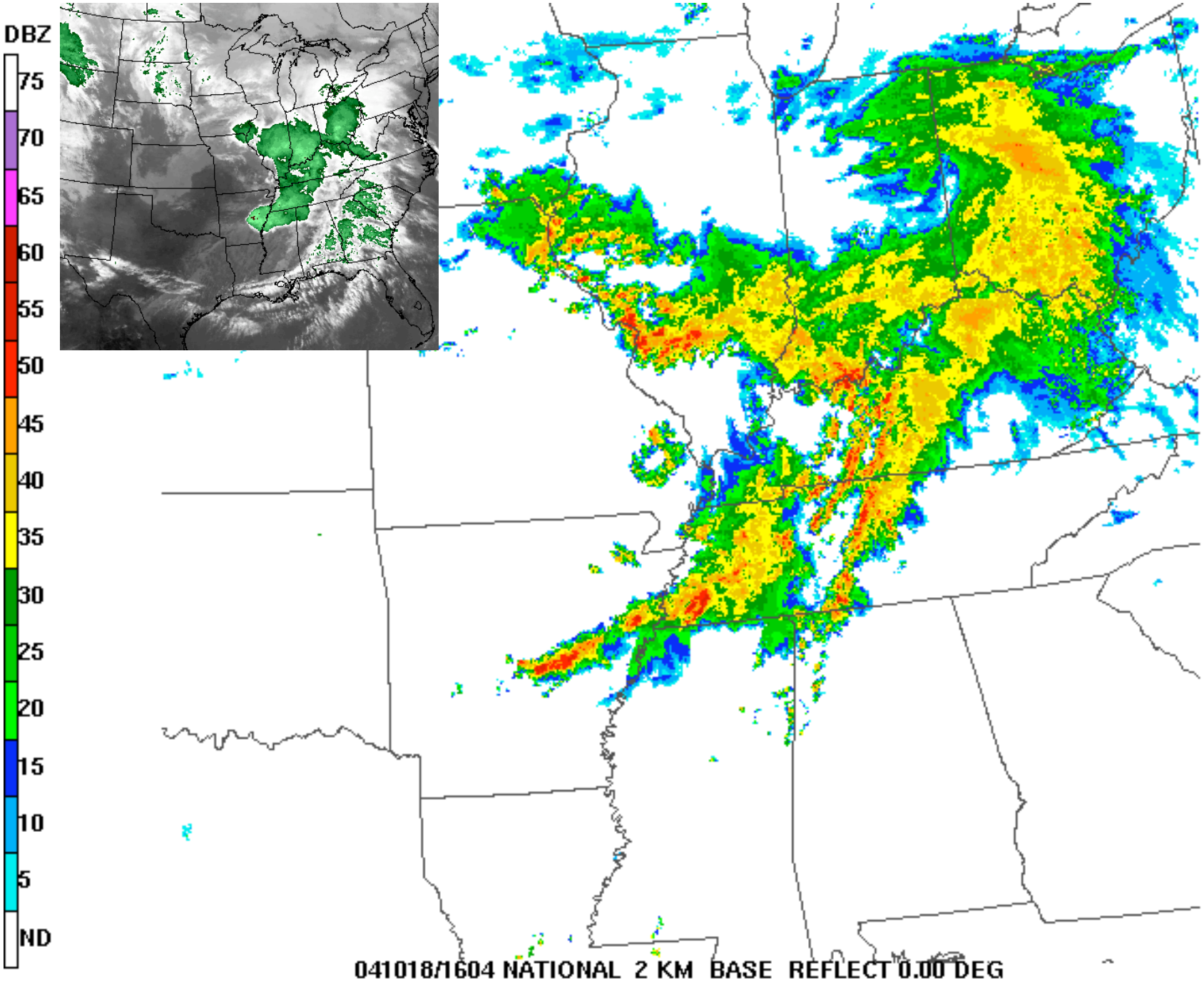
DBZ
75
70
65
60
55
50
45
40
35
30
25
20
15
10
5
ND
041018/1604 NATIONAL 2 KM BASE REFLECT 0.00 DEG

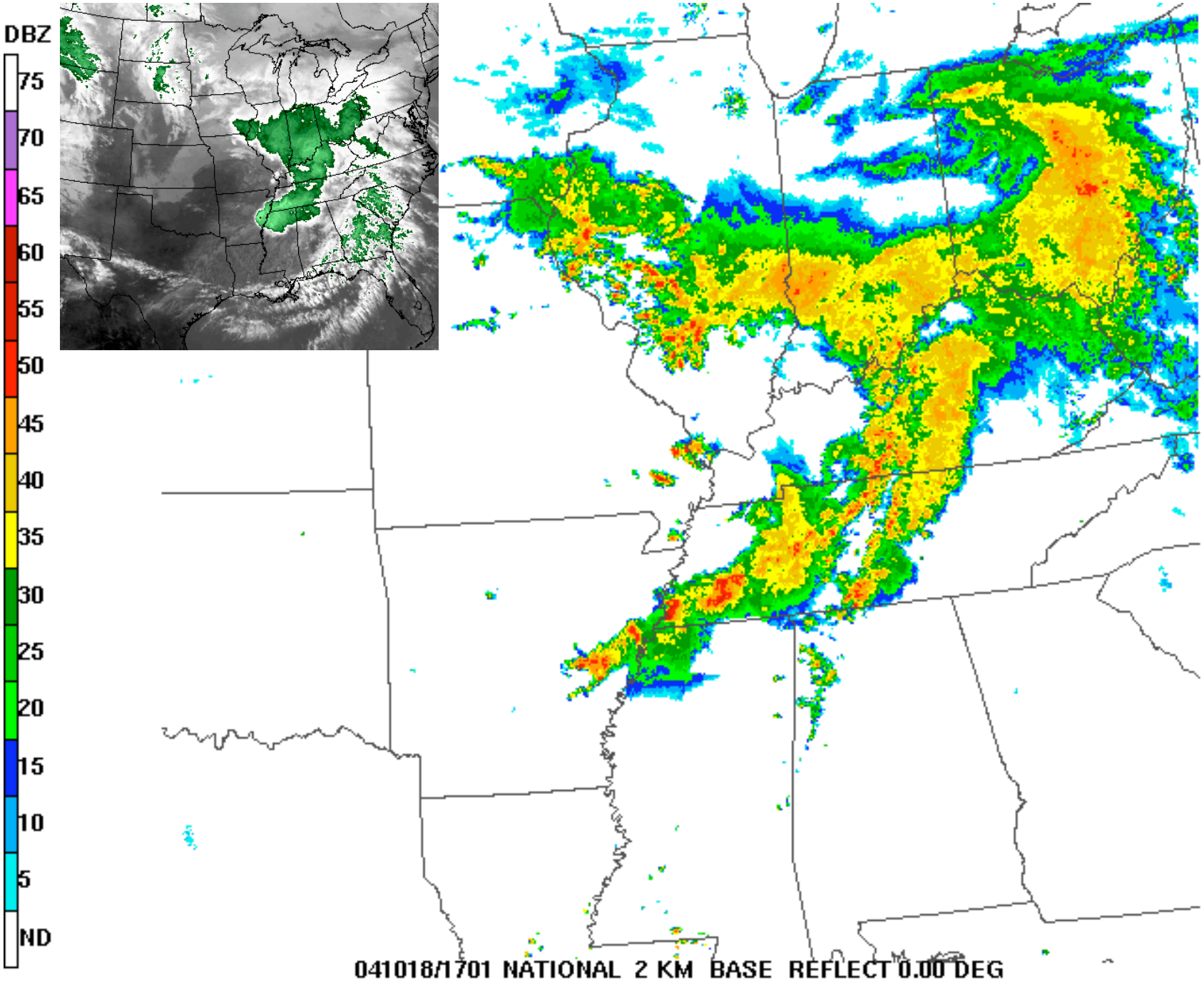
DBZ
75
70
65
60
55
50
45
40
35
30
25
20
15
10
5
ND
041018/1701 NATIONAL 2 KM BASE REFLECT 0.00 DEG

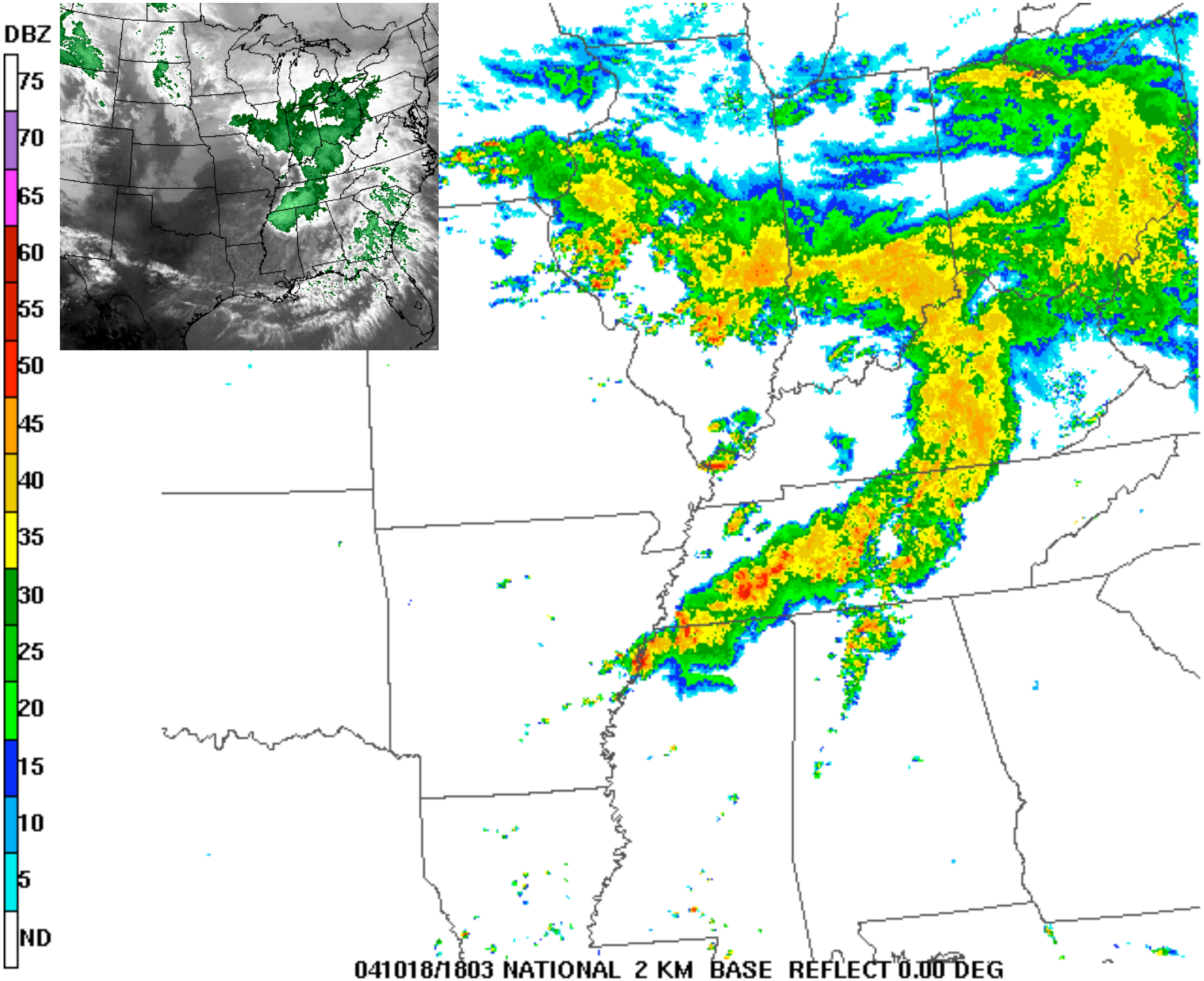
DBZ
75
70
65
60
55
50
45
40
35
30
25
20
15
10
5
ND
041018/1803 NATIONAL 2 KM BASE REFLECT 0.00 DEG

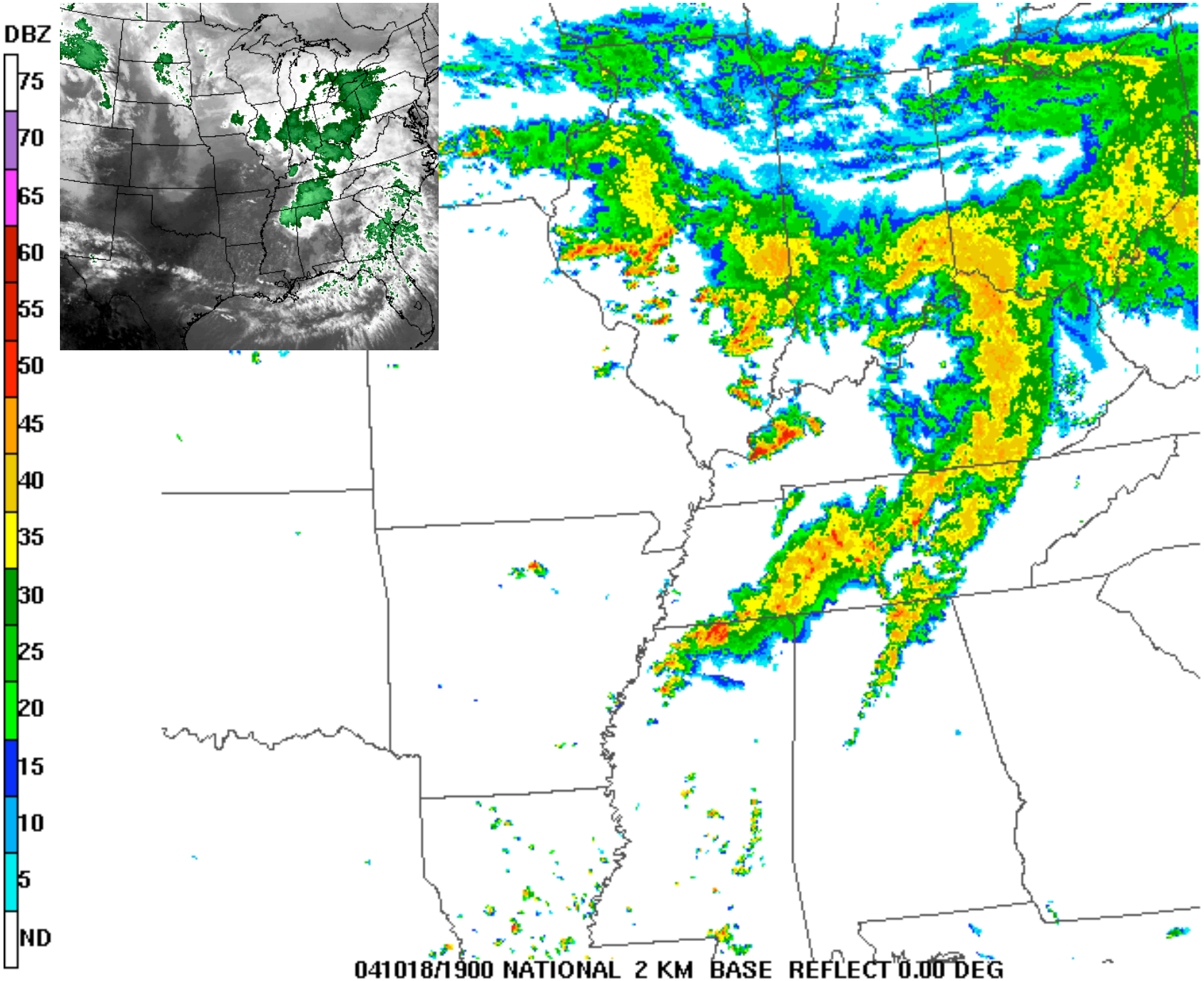
DBZ
75
70
65
60
55
50
45
40
35
30
25
20
15
10
5
ND
041018/1900 NATIONAL 2 KM BASE REFLECT 0.00 DEG

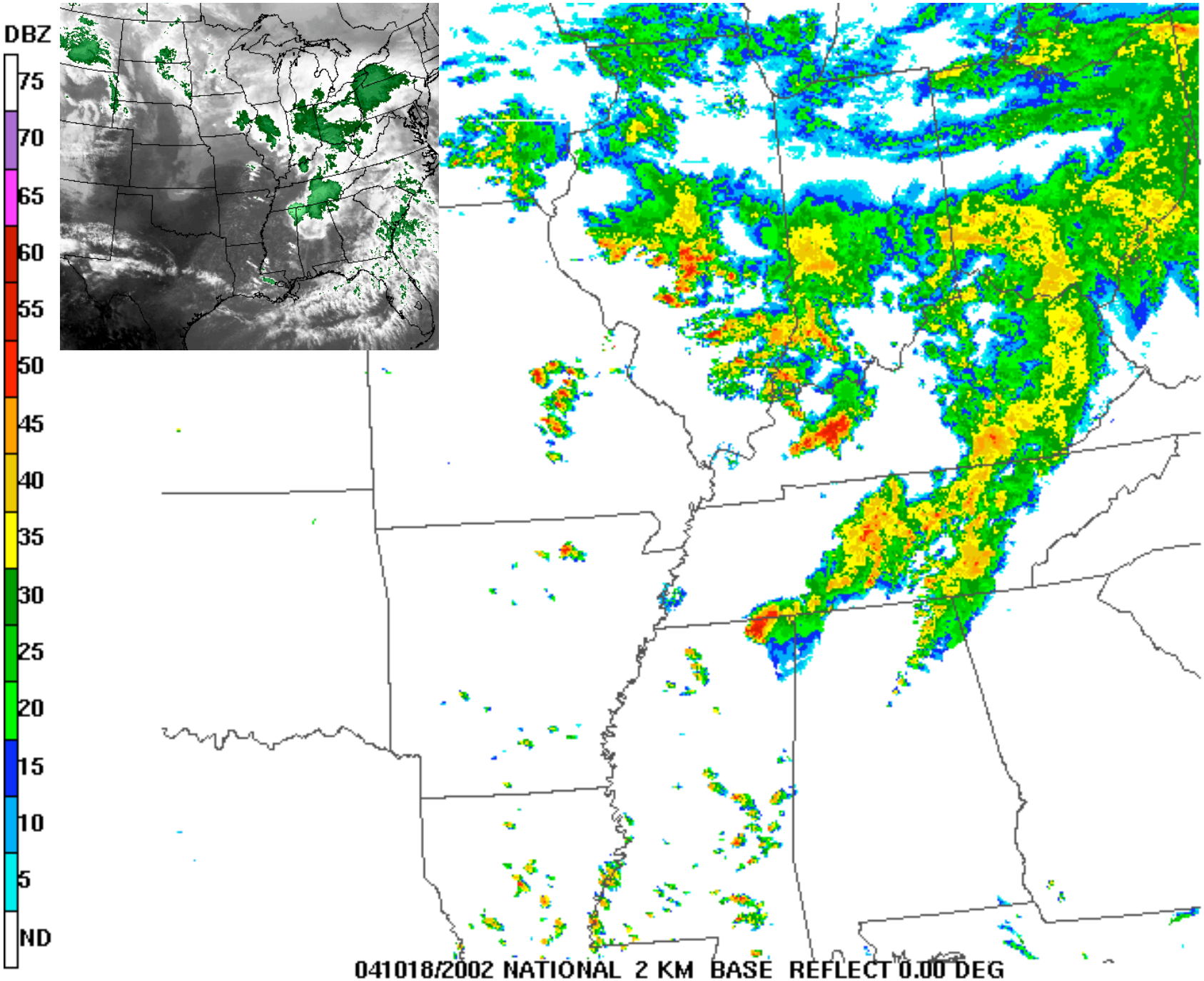
DBZ
75
70
65
60
55
50
45
40
35
30
25
20
15
10
5
ND
041018/2002 NATIONAL 2 KM BASE REFLECT 0.00 DEG

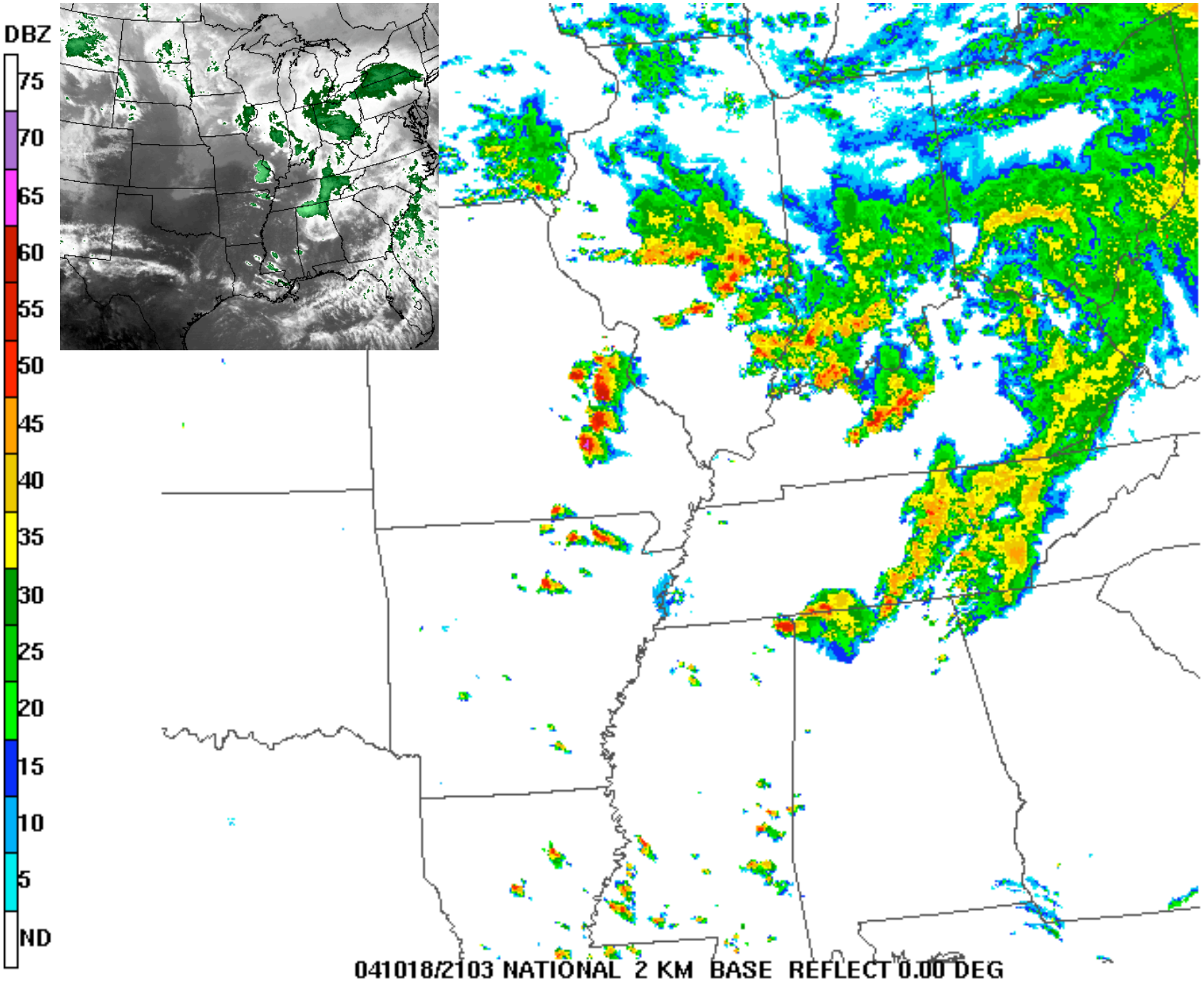
DBZ
75
70
65
60
55
50
45
40
35
30
25
20
15
10
5
ND
041018/2103 NATIONAL 2 KM BASE REFLECT 0.00 DEG

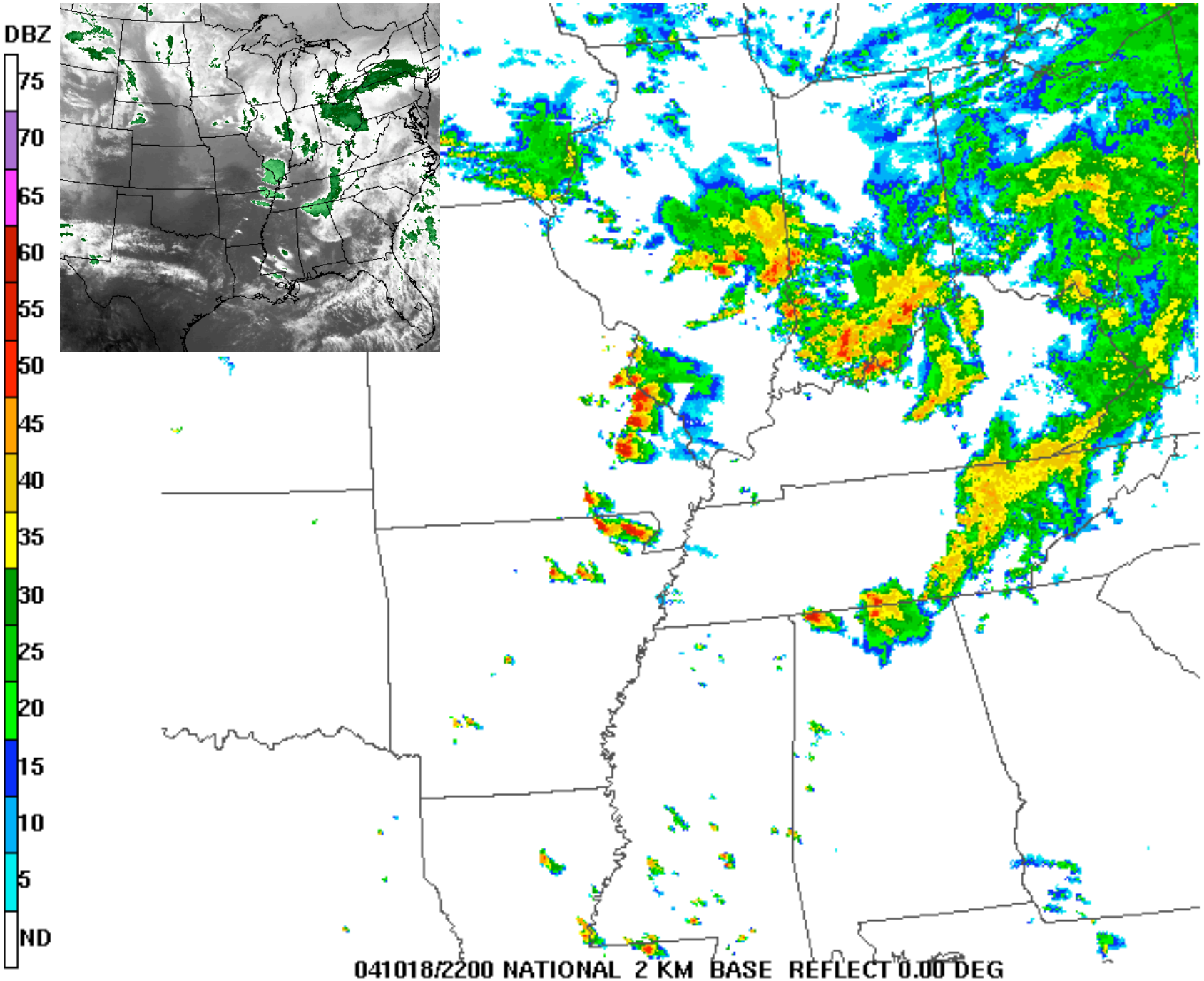
DBZ
75
70
65
60
55
50
45
40
35
30
25
20
15
10
5
ND
041018/2200 NATIONAL 2 KM BASE REFLECT 0.00 DEG

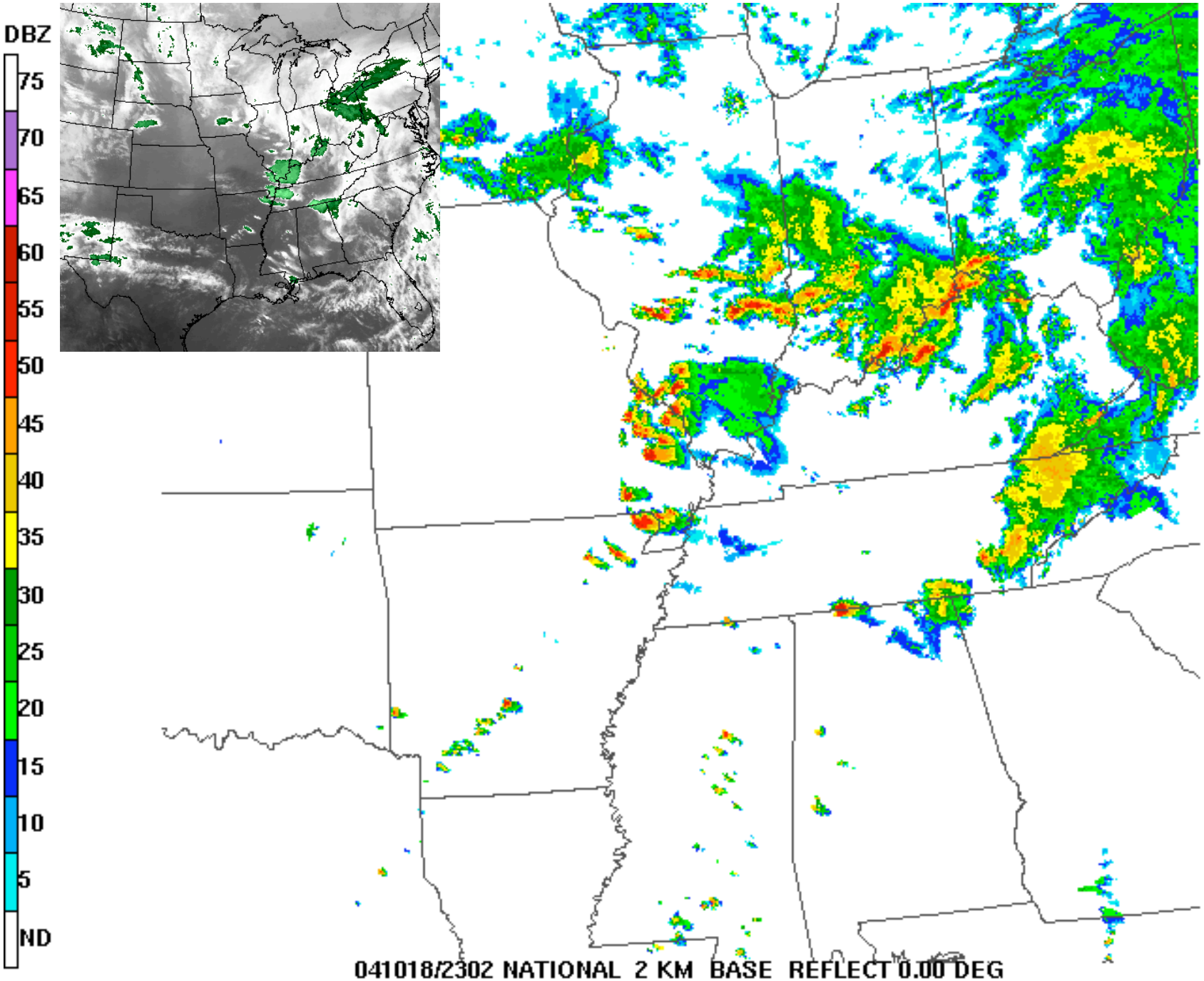
DBZ
75
70
65
60
55
50
45
40
35
30
25
20
15
10
5
ND
041018/2302 NATIONAL 2 KM BASE REFLECT 0.00 DEG

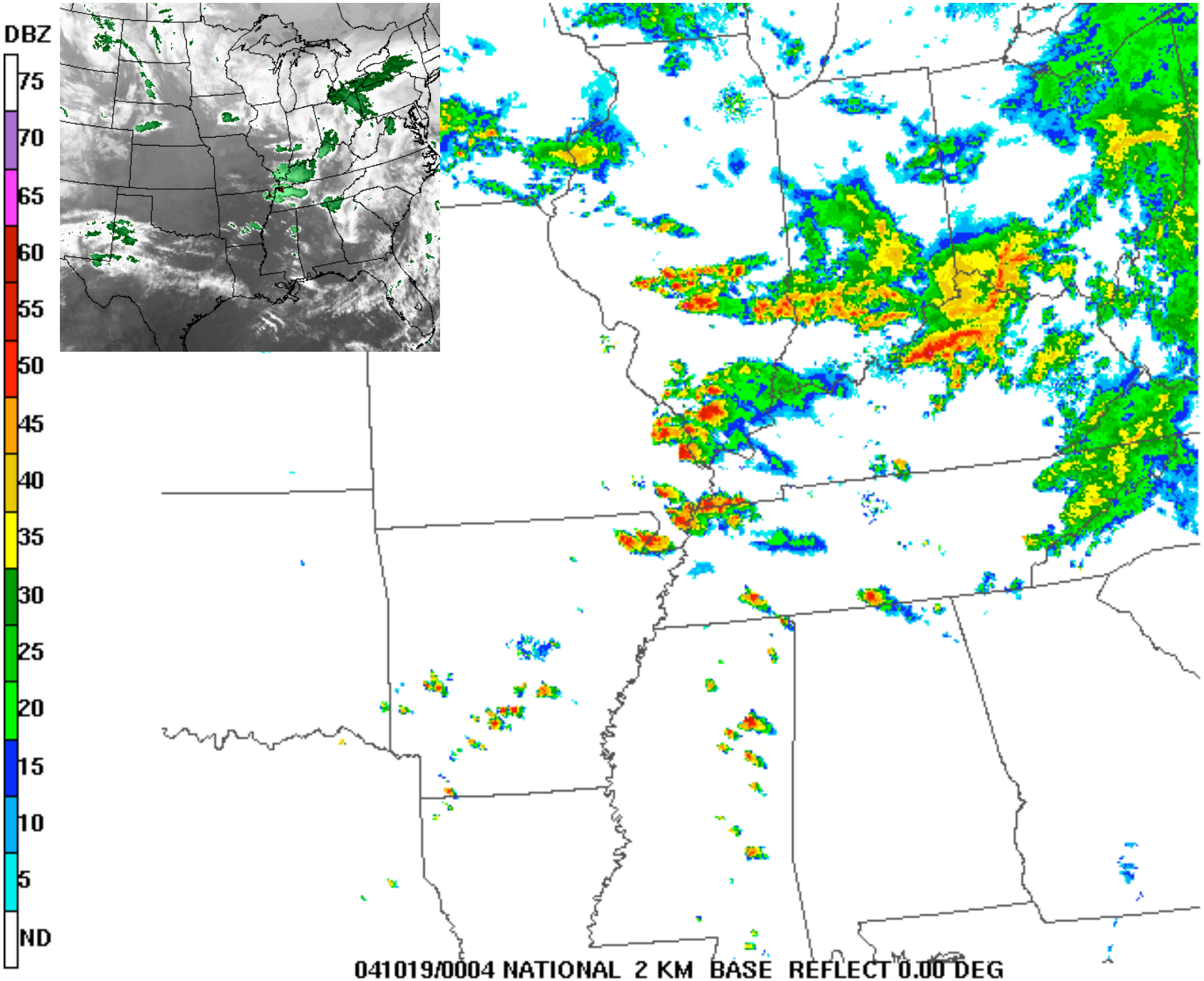
DBZ
75
70
65
60
55
50
45
40
35
30
25
20
15
10
5
ND
041019/0004 NATIONAL 2 KM BASE REFLECT 0.00 DEG

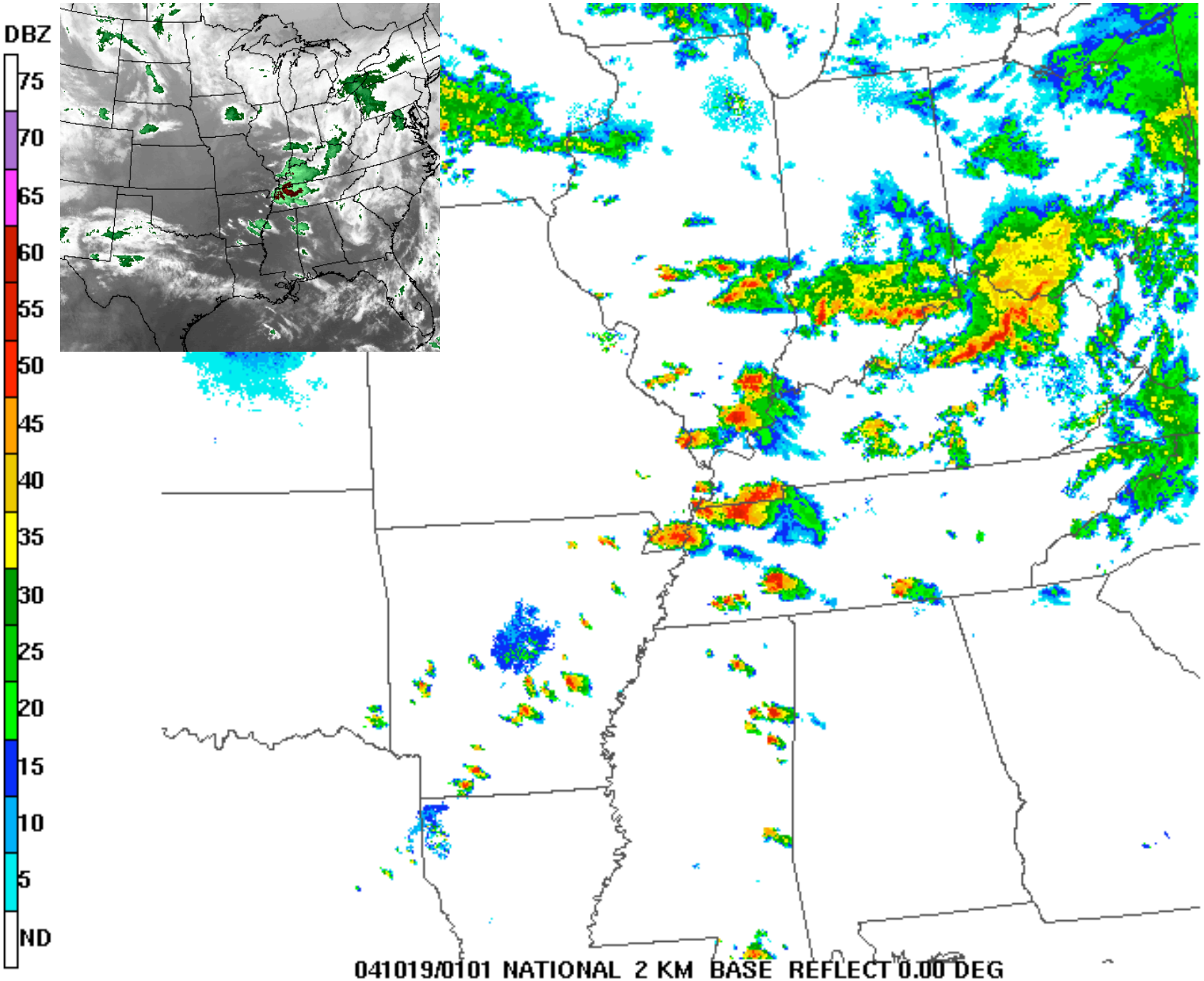
DBZ
75
70
65
60
55
50
45
40
35
30
25
20
15
10
5
ND
041019/0101 NATIONAL 2 KM BASE REFLECT 0.00 DEG

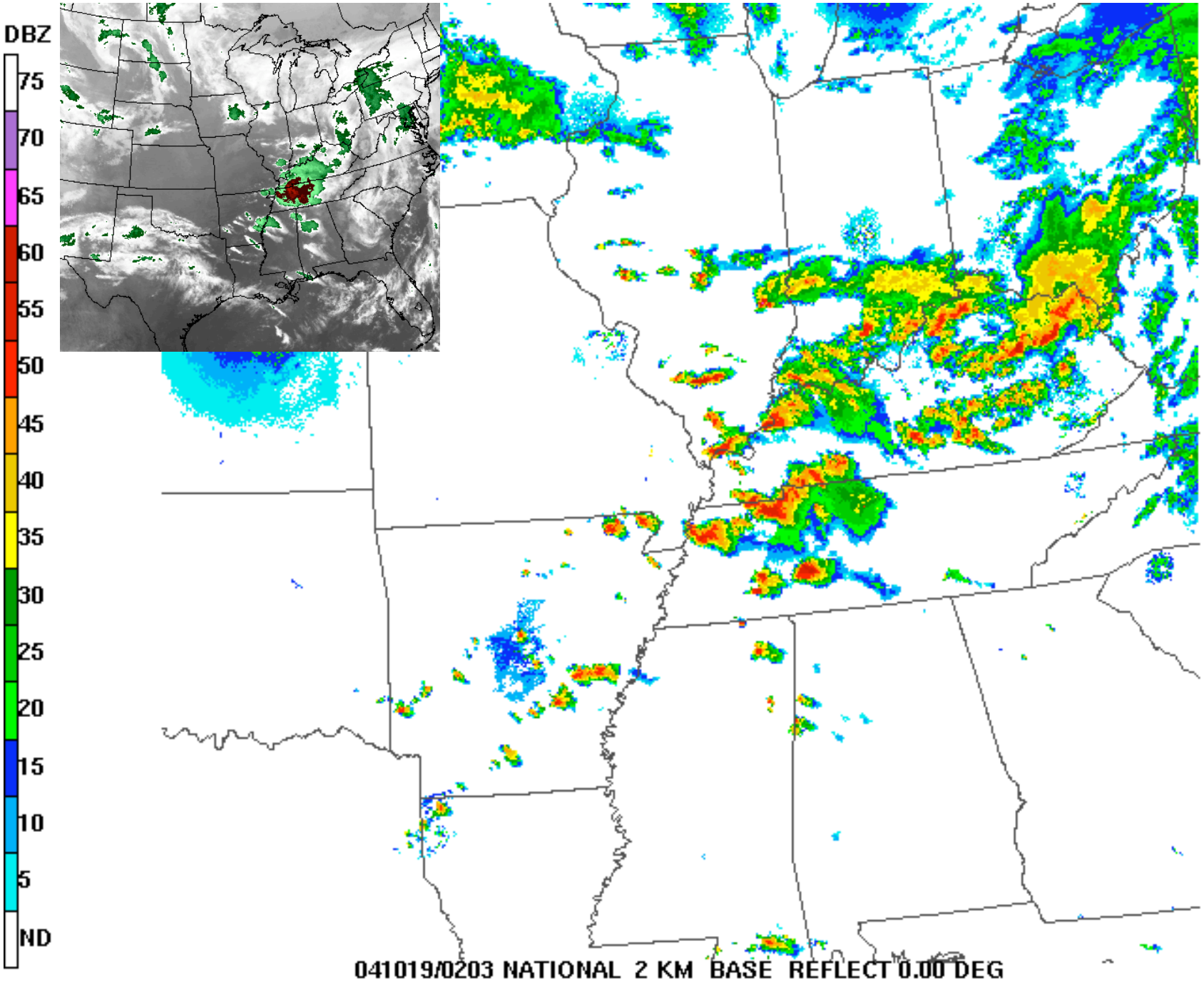
DBZ
75
70
65
60
55
50
45
40
35
30
25
20
15
10
5
ND
041019/0203 NATIONAL 2 KM BASE REFLECT 0.00 DEG

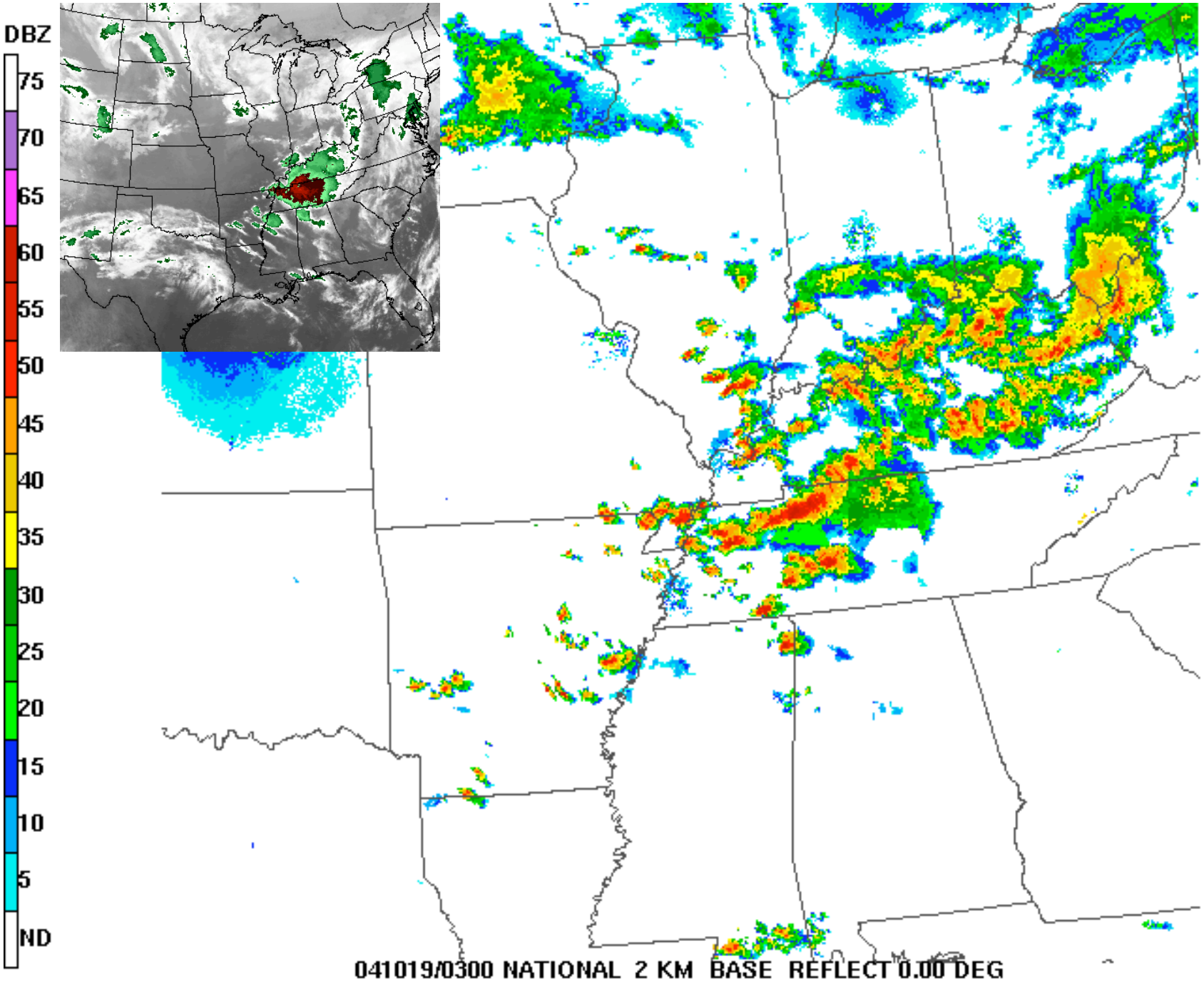
DBZ
75
70
65
60
55
50
45
40
35
30
25
20
15
10
5
ND
041019/0300 NATIONAL 2 KM BASE REFLECT 0.00 DEG

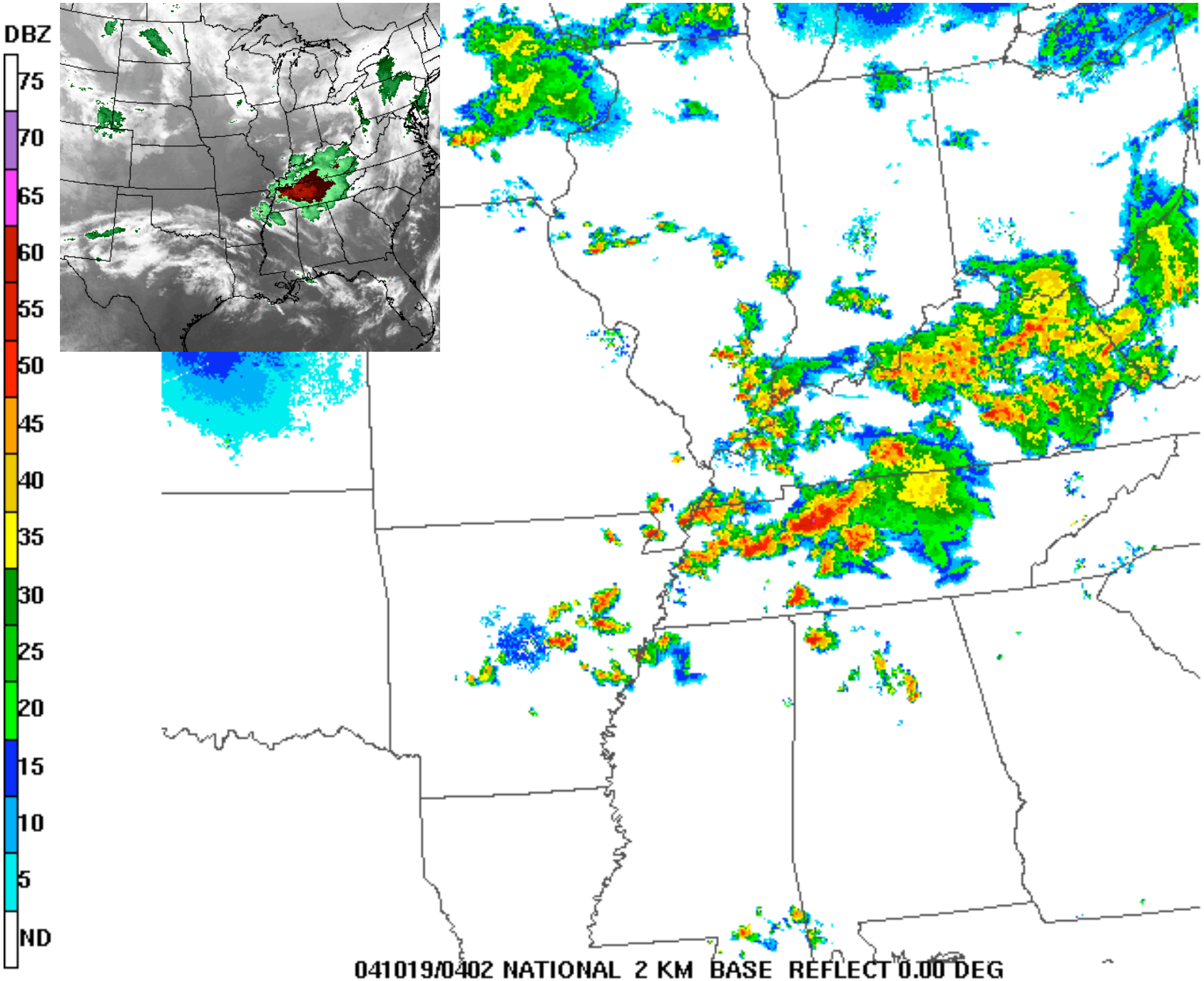
DBZ
75
70
65
60
55
50
45
40
35
30
25
20
15
10
5
ND
041019/0402 NATIONAL 2 KM BASE REFLECT 0.00 DEG

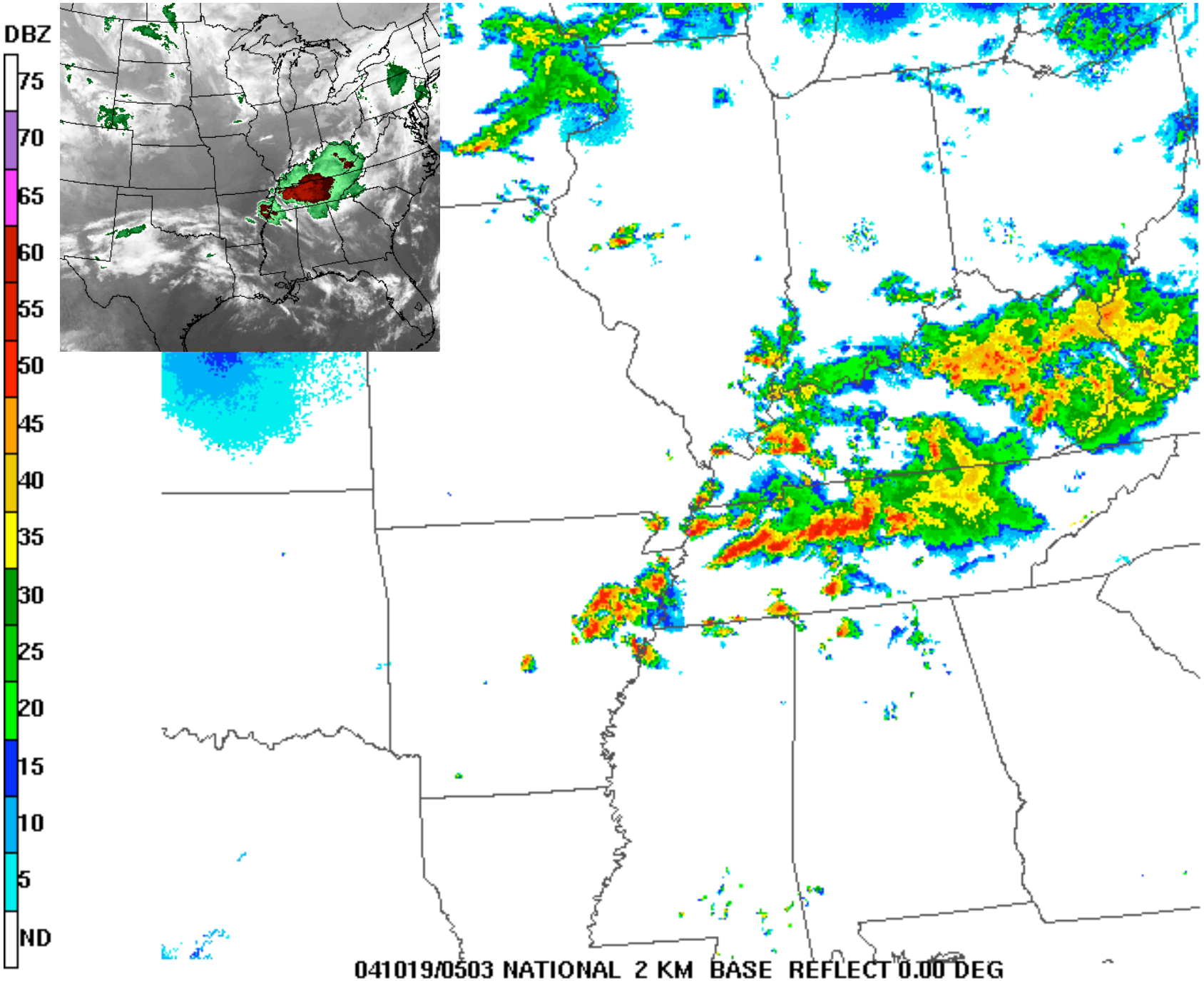
DBZ
75
70
65
60
55
50
45
40
35
30
25
20
15
10
5
ND
041019/0503 NATIONAL 2 KM BASE REFLECT 0.00 DEG

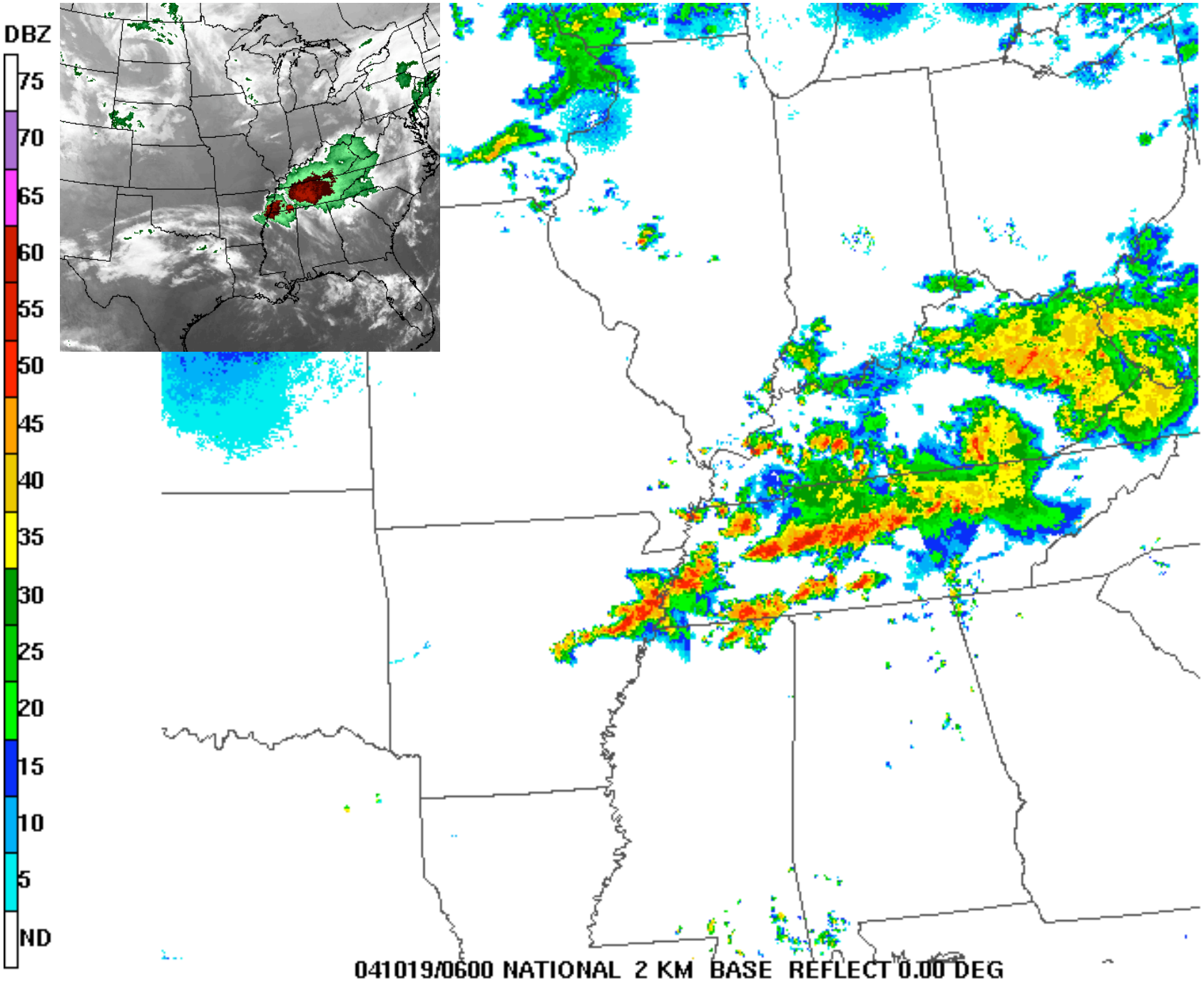
DBZ
75
70
65
60
55
50
45
40
35
30
25
20
15
10
5
ND
041019/0600 NATIONAL 2 KM BASE REFLECT 0.00 DEG

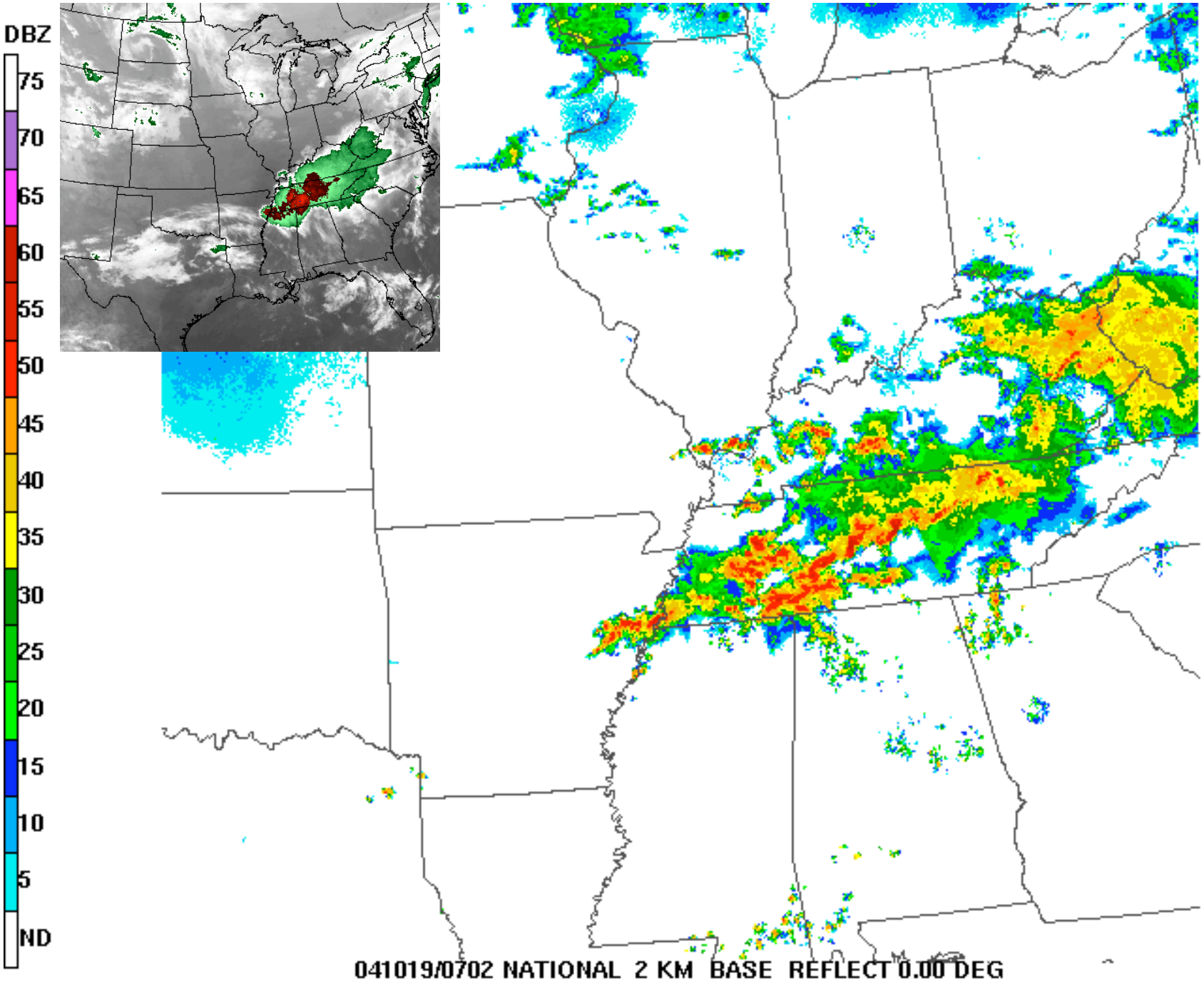
DBZ
75
70
65
60
55
50
45
40
35
30
25
20
15
10
5
ND
041019/0702 NATIONAL 2 KM BASE REFLECT 0.00 DEG

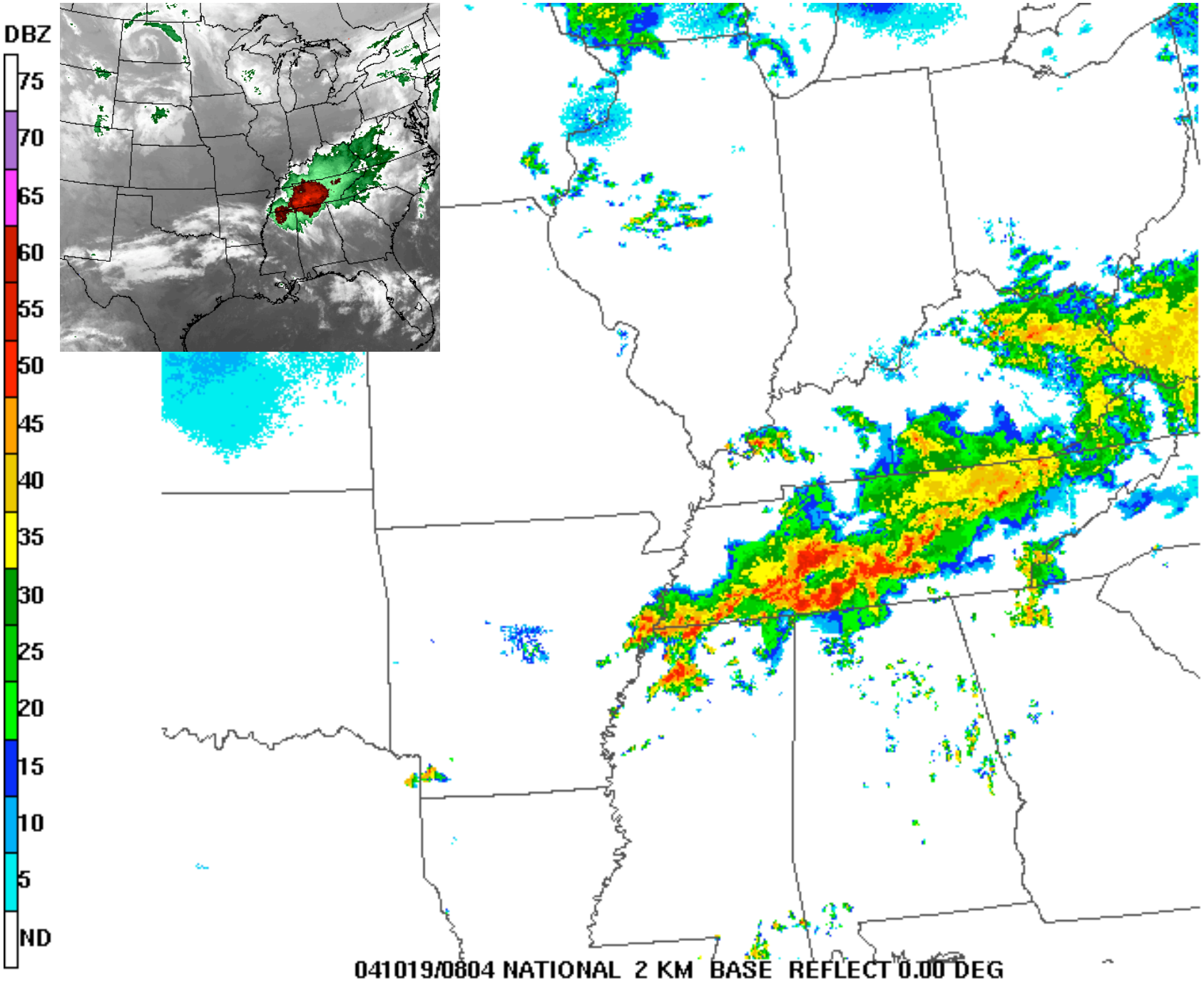
DBZ
75
70
65
60
55
50
45
40
35
30
25
20
15
10
5
ND
041019/0804 NATIONAL 2 KM BASE REFLECT 0.00 DEG

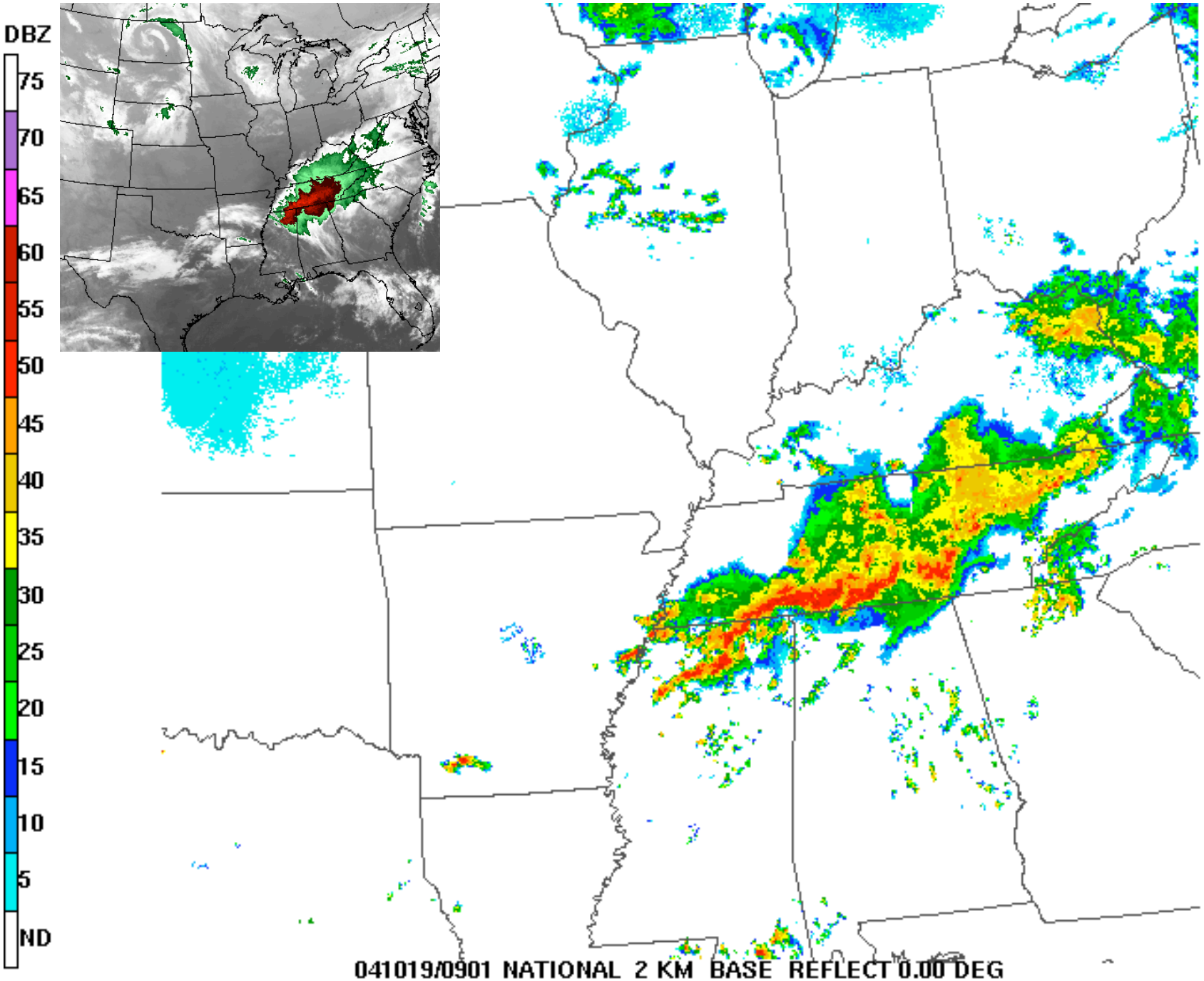
DBZ
75
70
65
60
55
50
45
40
35
30
25
20
15
10
5
ND
041019/0901 NATIONAL 2 KM BASE REFLECT 0.00 DEG

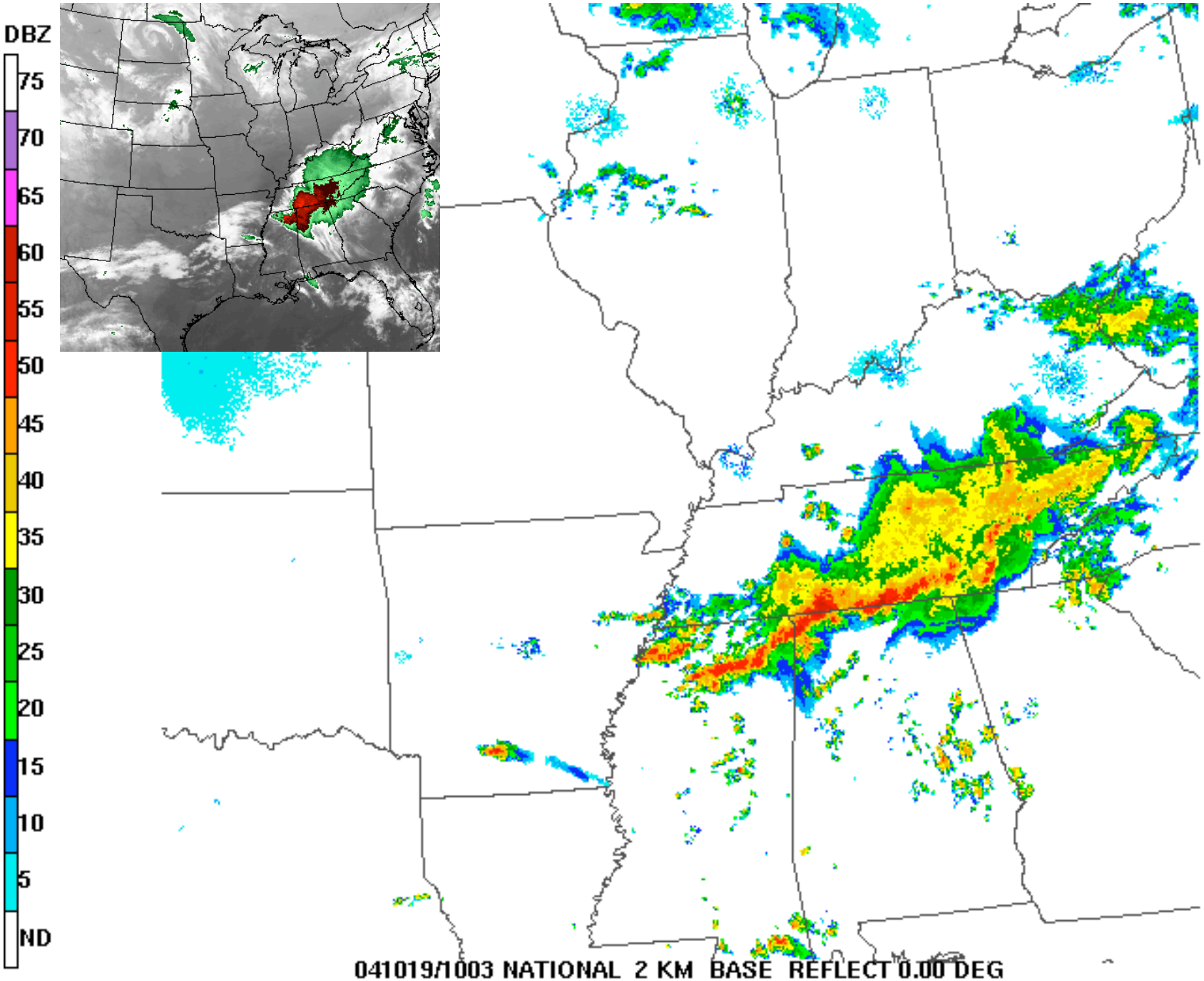
DBZ
75
70
65
60
55
50
45
40
35
30
25
20
15
10
5
ND
041019/1003 NATIONAL 2 KM BASE REFLECT 0.00 DEG

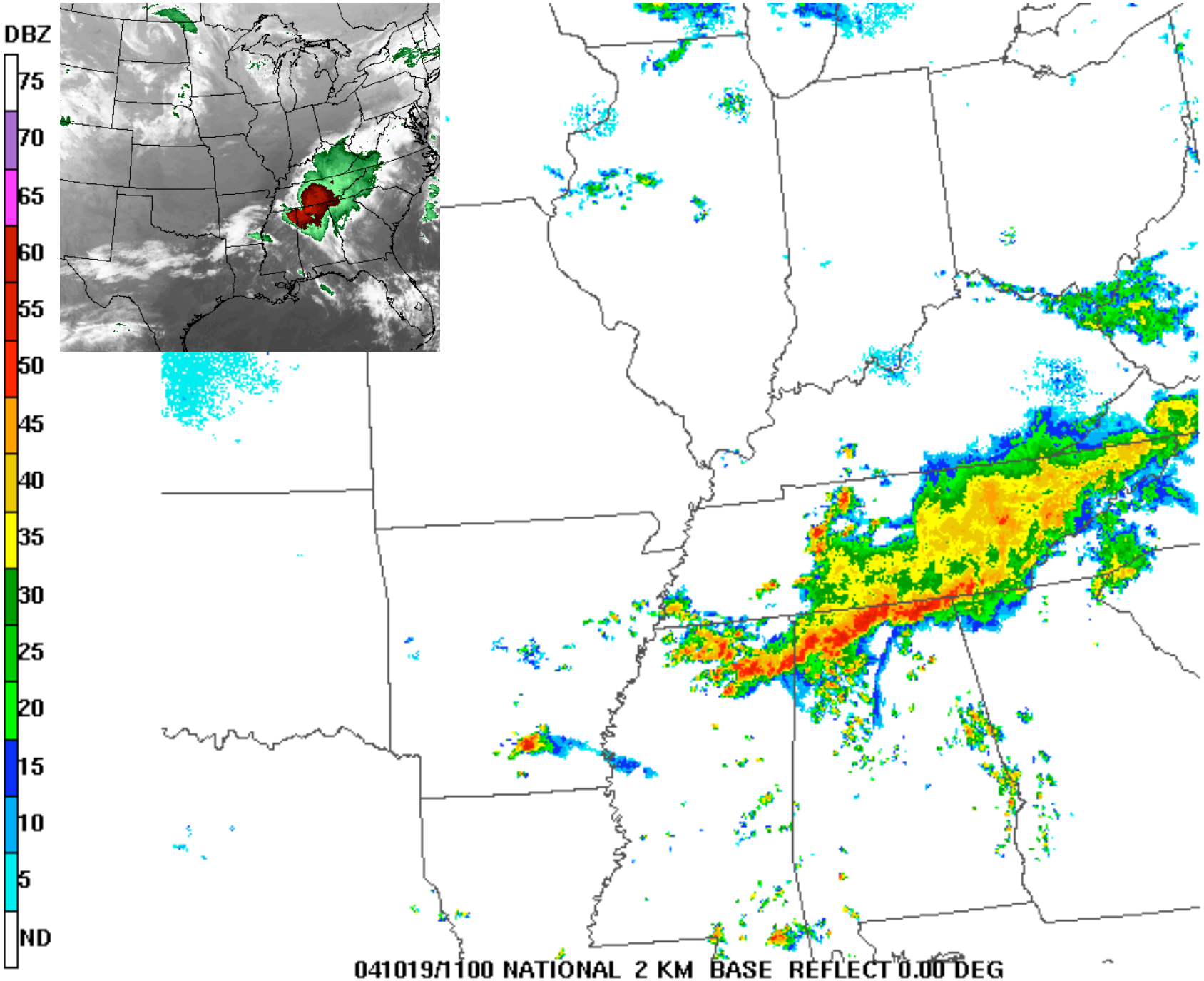
DBZ
75
70
65
60
55
50
45
40
35
30
25
20
15
10
5
ND
041019/1100 NATIONAL 2 KM BASE REFLECT 0.00 DEG

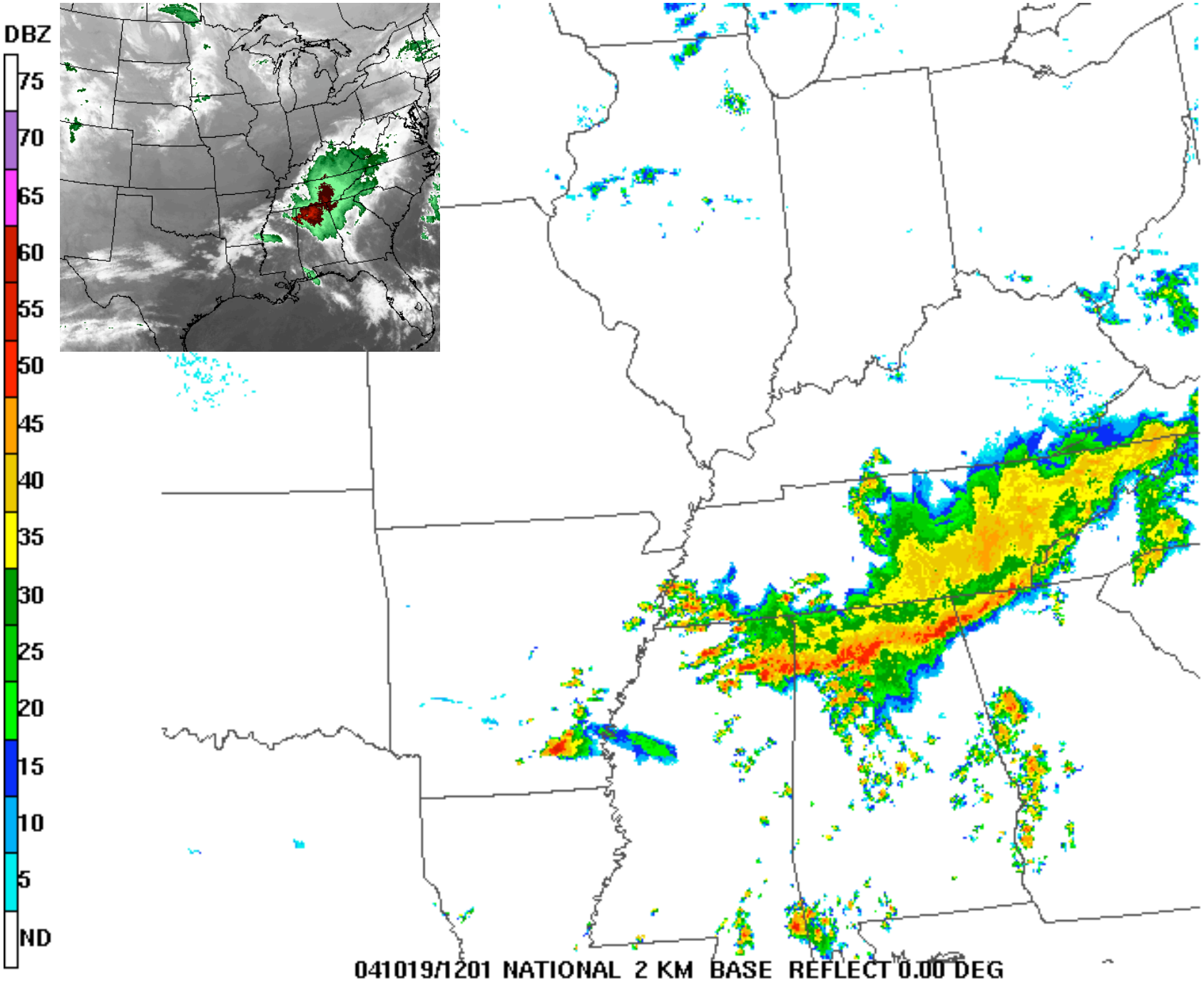
DBZ
75
70
65
60
55
50
45
40
35
30
25
20
15
10
5
ND
041019/1201 NATIONAL 2 KM BASE REFLECT 0.00 DEG

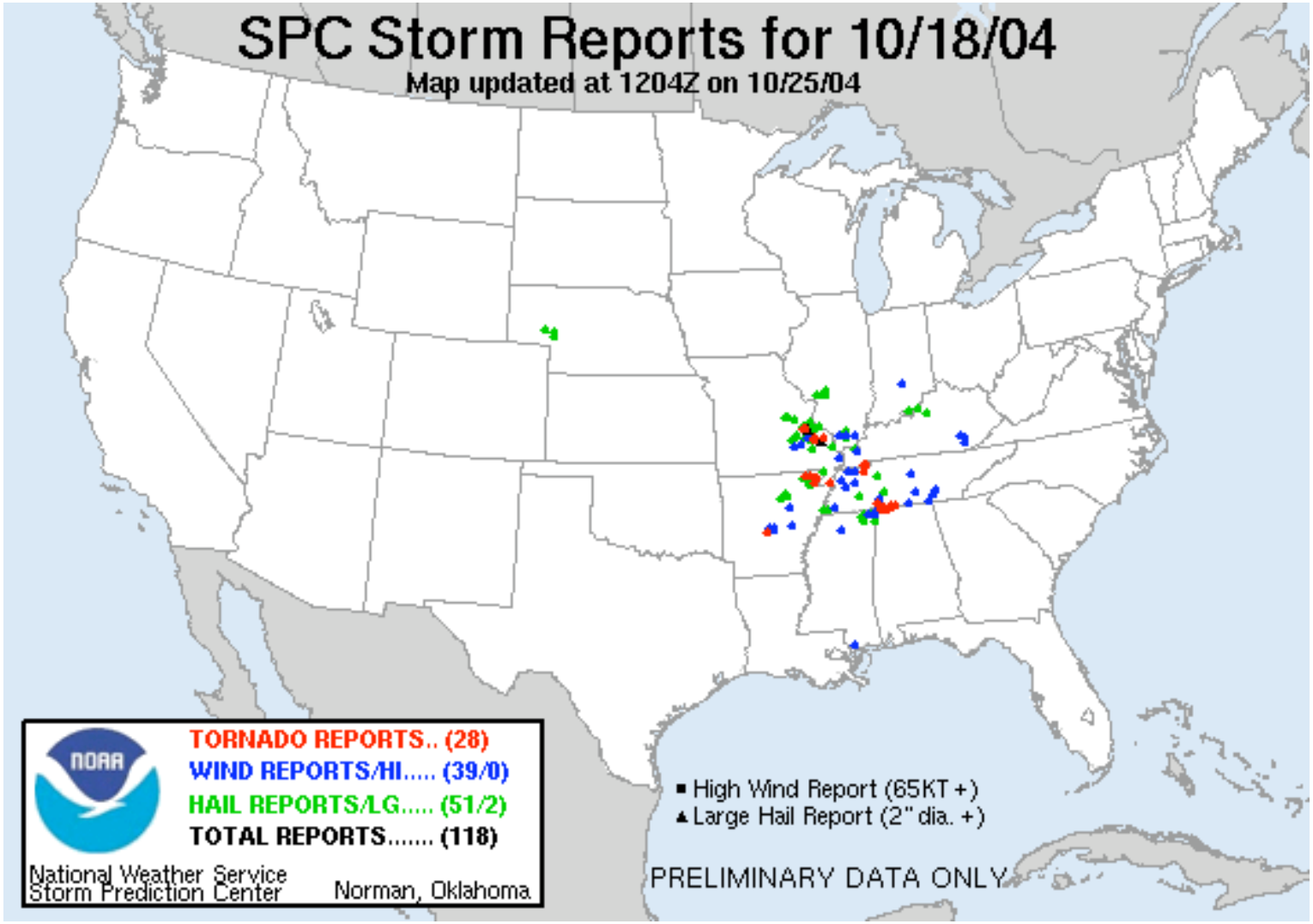

http://www.spc.noaa.gov

Sources and References

- Internet sources are indicated on the applicable figures.
- References:

Barnes, S. L., and C. W. Newton, 1983: Thunderstorms in the synoptic setting. *Thunderstorm Morphology and Dynamics,* E. Kessler, Ed., University of Oklahoma, 75–112.

Bluestein, H. B., 1993*: Observations and Theory of Weather Systems*. Vol. II: *Synoptic-Dynamic Meteorology in Midlatitudes*., Oxford University Press, 594 pp.

Coniglio, M. C., D. J. Stensrud, and M. B. Richman, 2004: An observational study of derecho-producing convective systems. *Wea. Forecasting,* **19,** 320–337.

Davies-Jones, R., R. J. Trapp, and H. B. Bluestein, 2001: Tornadoes and tornadic storms. *Severe Convective Storms*, *Meteor. Monogr*., No. 50, Amer. Meteor. Soc., 167–221.

Fritsch, J. M., and G. S. Forbes, 2001: Mesoscale convective systems. *Severe Convective Storms, Meteor. Monogr*., No. 50, Amer. Meteor. Soc., 323–357.

Johns, R. H., and W. D. Hirt, 1987: Derechos: Widespread convectively induced windstorms. *Wea. Forecasting,* **2,** 32–49**.**

Johnson, R. H., and B. E. Mapes, 2001: Mesoscale processes and severe convective weather. *Severe Convective Storms, Meteor. Monogr.,* No. 50, Amer. Meteor. Soc., 71–122.

Lemon, L. R., and C. A. Doswell, III, 1979: Severe thunderstorm evolution and mesocyclone structure as related to tornadogenesis. *Mon. Wea. Rev*., **107**, 1184–1197.

Moller, A. R., 2001: Severe local storms forecasting. *Severe Convective Storms, Meteor. Monogr*., No. 50, Amer. Meteor. Soc., 433–480.

Wakimoto, R. M., 2001: Convectively driven high wind events. *Severe Convective Storms, Meteor. Monogr*., No. 50, Amer. Meteor. Soc., 255–298.

Weisman, M. L., 1993: The genesis of severe, long-lived bow echoes. *J. Atmos. Sci.,* **50,** 645–670